

UNCONDITIONAL DENSITY BOUNDS FOR QUADRATIC NORM-FORM ENERGIES VIA LORENTZIAN SPECTRAL WEIGHTS PERSISTENT HEURISTICS: MINI MONOGRAPH I

PETER SHILLER

ABSTRACT. For a real quadratic field $\mathbb{Q}(\sqrt{d})$, we study the norm-form energy $N = S_\zeta^2 - d \cdot S_L^2$, where S_ζ and S_L are Lorentzian-weighted zero sums with $w(\rho) = 2/(\frac{1}{4} + \gamma^2)$. We prove three main results. (1) *Spacelike spectral data*: $N < 0$ unconditionally for all squarefree $d > 1$, as a consequence of a low-lying zero dominance theorem proved via explicit zero-counting. (2) *Effective density bound*: at each verified truncation level M , $\text{dens}\{N > 0\} \leq 2\|f_{S_L^{(M)}}\|_\infty \cdot (W_1(\zeta)/\sqrt{d} + \epsilon_M)$, established unconditionally via Jacobi–Anger resonance analysis. At fixed M the bound is nontrivial only for sufficiently large d ; the $O(1/\sqrt{d})$ rate requires M to grow with d , which in turn requires a uniform density bound that we establish under a computationally verified finite-rank condition on the resonance lattice. (3) *Exact asymptotic*: under the computationally verified hypothesis that the infinite resonance lattice Λ_∞ has finite rank (verified for $M \leq 20$, where rank = 0), the sharp asymptotic $\text{dens}\{N > 0\} = C(d)/\sqrt{d} + o(1/\sqrt{d})$ holds. For $d = 5$, $C(5) = 2f_{S_L}(0) \cdot \mathbb{E}[|S_\zeta|] = 0.1191$; the constant depends on d through the zeros of $L(s, \chi_d)$, and $C(d) = O(1/\log d)$ as $d \rightarrow \infty$.

Appendix F tabulates the first 1000 zeros at 70 decimal places for $L(s, \chi_2)$, $L(s, \chi_3)$, $L(s, \chi_5)$, $L(s, \chi_6)$, $L(s, \chi_7)$, $L(s, \chi_{10})$, $L(s, \chi_{11})$, and $L(s, \chi_{13})$, all rigorously certified by ARB interval arithmetic.

CONTENTS

1. Introduction	3
1.1. Main results	3
1.2. Logical structure and the GSH barrier	4
1.3. Series context	4
1.4. Organization	4
1.5. Conventions	5
2. The Lorentzian Energy Functional	6
2.1. The Lorentzian weight	6
2.2. Weighted zero sums	7
2.3. The norm-form energy	7
2.4. Eigenspace interpretation	8
2.5. Per-prime sign structure	8
3. Negativity and Spacelike Theorems	8
3.1. Low-lying zero dominance	8

Date: March 1, 2026.

2020 Mathematics Subject Classification. Primary 11M06; Secondary 11M26, 11R42, 42A75.

Key words and phrases. Dirichlet L -functions, quadratic norm form, density bounds, Lorentzian spectral weights, Jacobi–Anger decomposition, Jessen–Wintner theorem, Besicovitch almost periodic functions.

3.2.	The spacelike corollary	10
3.3.	The negativity theorem for general characters	10
3.4.	Unconditional first-zero bound	10
3.5.	Robustness	11
4.	Cesàro Density Bounds via Almost Periodic Spectral Sums	11
4.1.	Shifted zero sums	11
4.2.	The Grand Simplicity Hypothesis	11
4.3.	Parseval identity	12
4.4.	Cesàro spacelike theorem	12
4.5.	Covariance identity	16
4.6.	Density of positive excursions	16
4.7.	Unconditional density vanishing in the Euler product regime	18
5.	Besicovitch Norms of Spectral Sums	19
6.	Finite Density Bounds via Jacobi–Anger Decomposition	20
6.1.	The Jacobi–Anger decomposition	21
6.2.	Resonance certification for $M = 20$	21
6.3.	Bessel decay estimates	22
6.4.	Lattice counting	23
6.5.	Unconditional finiteness at finite M	24
7.	Telescoping Extension to Infinite Spectral Sums	25
7.1.	Monotonicity of the main term	25
7.2.	The self-referential telescoping bound	26
7.3.	The major-arc/minor-arc decomposition	28
7.4.	A level-crossing bound	30
8.	Cross-Function Energy Bounds and the Effective Density Theorem	30
8.1.	Orthogonality	31
8.2.	The energy bound	31
8.3.	The containment lemma and density bound	31
9.	Exact Density Formula under Verified Resonance Absence	34
9.1.	Verified resonance absence	34
9.2.	The exact density formula	35
10.	Numerical Verification	37
10.1.	Density verification	37
10.2.	Telescoping convergence	38
11.	Conclusion	38
12.	The Null Crossing and Spectral Phase Transition	39
12.1.	The norm form on the real axis	39
12.2.	The unique null crossing	39
12.3.	Integer crossing obstruction	40
13.	Connections and Open Problems	41
13.1.	Relation to Katz–Sarnak statistics	41
13.2.	Extensions to higher degree	42
13.3.	Further questions	42
13.4.	Weight robustness	43
	Acknowledgments	45
	Appendix A. Computational Methods and Numerical Verification	45

Appendix B. Zeros of $L(s, \chi_5)$ to 70 Decimal Places (Conductor 5, $d = 5$)	51
Appendix C. Quadratic L -Function Zeros to 20 Decimal Places (Seven Discriminants)	56
Appendix D. Riemann Zeta Zeros (20 Decimal Places)	58
Appendix E. ARB Certification of Zero Data	59
Appendix F. Tables of Zeros of Quadratic Dirichlet L -Functions of Small Conductor	59
References	60

1. INTRODUCTION

Let $d > 1$ be squarefree and let χ_d denote the Kronecker symbol of the fundamental discriminant Δ_K of $K = \mathbb{Q}(\sqrt{d})$. The Dedekind zeta function factors as

$$\zeta_K(s) = \zeta(s) \cdot L(s, \chi_d), \tag{1}$$

coupling the zeros of the Riemann zeta function to those of the quadratic Dirichlet L -function. We ask whether this coupling can be detected spectrally, by weighting zeros so that low-lying ones dominate. The answer is yes: the resulting quadratic form on weighted zero sums is always negative (the L -function zeros win), and the set where it becomes positive has density $O(1/\sqrt{d})$. Both statements hold unconditionally in the Euler-product formulation; on the zero side, they hold at any verified truncation level and extend to the full series under a computationally verified finite-rank condition (rank = 0 for the first 20 zeros).

For a zero $\rho = \frac{1}{2} + i\gamma$ on the critical line, define the Lorentzian weight

$$w(\rho) = \frac{2}{\frac{1}{4} + \gamma^2}. \tag{2}$$

This weight emphasizes low-lying zeros: a zero at height $\gamma = 1$ contributes weight 1.6, while a zero at height $\gamma = 14$ contributes weight 0.01. Define the weighted zero sums

$$S_\zeta = \sum_{\zeta(\rho)=0} w(\rho), \quad S_L = \sum_{L(\rho, \chi_d)=0} w(\rho), \tag{3}$$

and the norm-form energy

$$N = S_\zeta^2 - d \cdot S_L^2. \tag{4}$$

The signature $(1, 1)$ of this quadratic form reflects the Galois structure of K/\mathbb{Q} : the trivial eigenspace contributes positively, the sign eigenspace negatively.

1.1. Main results. We prove unconditionally that:

- (1) **Spacelike spectral data** (Corollary 3.5): $N = S_\zeta^2 - d \cdot S_L^2 < 0$ for all squarefree $d > 1$. This follows from the low-lying zero dominance theorem (Theorem 3.1: $S_L > S_\zeta^*$) via explicit zero-counting, and extends to Cesàro averages (Theorem 4.10: $\langle N \rangle_T < 0$ for all $T > 0$).
- (2) **Effective density bound** (Theorem 8.5): $\text{dens}\{N > 0\} \leq 2 \|f_{S_L^{(M)}}\|_\infty \cdot (W_1(\zeta)/\sqrt{d} + \epsilon_M)$ unconditionally at any verified truncation level M .
- (3) **Density rate and exact asymptotic** (Corollary 8.8, Theorem 9.4): $\text{dens}\{N > 0\} = O(1/\sqrt{d})$, sharpened to $\text{dens}\{N > 0\} = C(d)/\sqrt{d} + o(1/\sqrt{d})$, under the hypothesis that the infinite resonance lattice Λ_∞ has finite rank $d_\infty < \infty$ (verified $d_\infty = 0$ for $M \leq 20$). For $d = 5$, $C(5) = 0.1191$; the constant $C(d) = O(1/\log d)$ as $d \rightarrow \infty$.

These results do not assume the Riemann Hypothesis for either function. The spacelike property is robust to the choice of weight function (see Section 13.4). As a byproduct of the low-lying zero dominance proof, we obtain a universal first-zero bound $\gamma'_1(d) < 14.13$ for all fundamental discriminants (Proposition 3.9).

1.2. Logical structure and the GSH barrier. The progression of results reveals the fundamental role of \mathbb{Q} -linear independence:

Result	Assumes	Bound	Method
Thm 4.17: Density vanishing	Hypothesis 4.4(ii)	$O(1/\sqrt{d})$	Jessen–Wintner
Thm 4.19: Euler product density	nothing	$O(1/\sqrt{d})$	\mathbb{Q} -indep. of $\log p$
<i>The barrier: zero ordinates lack unconditional \mathbb{Q}-independence</i>			
Thm 6.9: Unconditional finiteness	nothing	$f_{S_L^{(M)}}(0) < \infty$	Jacobi–Anger + Bessel
Thm 8.5: Effective bound	nothing	$2\ f\ _\infty(W_1/\sqrt{d} + \epsilon_M)$	Containment + stability
Cor. 8.8: Density rate	$d_\infty < \infty$	$O(1/\sqrt{d})$	$M(d) +$ uniform bound
Thm 7.7: Limiting density	Verified ($M = 20$)	$f_{S_L}(0) < \infty$	DCT + resonance absence
Thm 9.4: Exact formula	Verified ($M = 20$)	C/\sqrt{d}	Marginal densities

The key insight is that the Jessen–Wintner approach requires \mathbb{Q} -linear independence to identify the Cesàro distribution with a product of independent random variables. On the Euler product side, this independence follows from unique factorization. On the zero side, it is precisely the Grand Simplicity Hypothesis. The unconditional effective bound bypasses this barrier at a fixed truncation level via the stability lemma; the $O(1/\sqrt{d})$ rate requires the truncation level to grow with d , which in turn requires a uniform bound on the density $\|f_{S_L^{(M)}}\|_\infty$. Under verified resonance absence ($d_\infty = 0$), this uniform bound holds because the unsigned Bessel integral is monotone decreasing in M ; more generally, it suffices that the infinite resonance lattice Λ_∞ has finite rank $d_\infty < \infty$.

1.3. Series context. This paper is the first in the series *Persistent Heuristics*. The Lorentzian weight arises from a spectral interpretation of the Weil explicit formula that emphasizes low-lying zeros over high zeros. While this emphasis might initially appear restrictive, it reveals genuine invariants: the spacelike property holds for any weight satisfying mild decay conditions (Section 13.4), and the density bounds depend on the weight only through computable constants.

1.4. Organization. Section 2 defines the Lorentzian weight and establishes its properties. Section 3 proves the low-lying zero dominance and spacelike theorems. Section 4 extends the negativity to Cesàro averages and establishes conditional density bounds under GSH, revealing the \mathbb{Q} -independence barrier. Sections 6 and 7 establish per-function density bounds via Jacobi–Anger analysis and finite truncation. Section 8 combines these with a stability argument to prove the effective density bound, and Section 9 derives the exact formula under verified resonance absence. Section 12 analyzes the unique null crossing on the real

axis. Section 13 discusses connections and open problems. Appendix A provides numerical verification.

Remark 1.1 (Purpose of Appendix F). The proofs in this paper require only the zero data in Appendices B–E: the first 200 zeros of $L(s, \chi_5)$ at 70-digit precision, the first 20 zeros of $L(s, \chi_d)$ at 20-digit precision for $d \in \{2, 3, 6, 7, 10, 11, 13\}$, and the first 60 zeros of $\zeta(s)$. In the course of this work, however, we computed and certified the first 1,000 zeros of $L(s, \chi_d)$ at 70 decimal places for all eight discriminants (8000 zeros in total); these extended tables are collected in the companion document Appendix F and are freely available as ancillary data files. To the best of our knowledge, no publicly available repository provides bulk high-precision zero ordinates for individual Dirichlet L -functions: the LMFDB [9] stores approximately 25 zeros per character at 30-digit precision (computed by Platt [13]), and the dataset of O’Bryant and Reznitzer [14] provides zeros for all primitive characters of conductor up to 934 at 12-digit precision. We hope the present tables serve as a useful reference for researchers requiring certified zero data for quadratic L -functions.

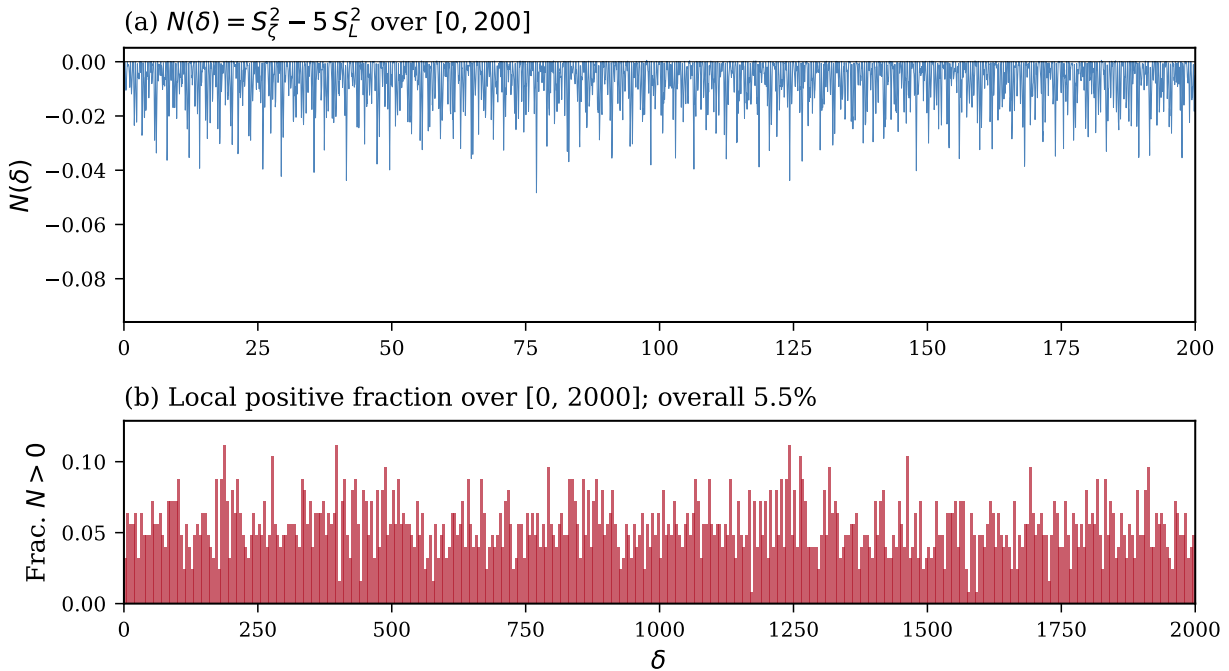


FIGURE 1. The norm form $N(\delta) = S_\zeta(\delta)^2 - 5 S_L(\delta)^2$ for $d = 5$, computed using the first 100 zeros of each function with Lorentzian weights $w(\gamma) = 2/(\frac{1}{4} + \gamma^2)$. Panel (a): the oscillating signal over $[0, 200]$, showing that N is overwhelmingly negative. Panel (b): the local fraction of δ -values where $N > 0$, computed in sliding windows across $[0, 2000]$; the measure of the set where $N > 0$ is approximately 5.5% over $[0, 2000]$, consistent with the predicted $O(1/\sqrt{d})$ density.

1.5. **Conventions.** Sums over zeros \sum_ρ run over the upper half-plane $\gamma > 0$, with each term representing a conjugate pair $\rho, \bar{\rho}$. The zero-counting function $N(T)$ counts zeros with $0 < \gamma \leq T$. The Fourier transform convention is $\hat{f}(\xi) = \int_{-\infty}^{\infty} f(x) e^{-2\pi i x \xi} dx$.

Throughout, γ_k denotes the k -th positive ordinate of $\zeta(s)$ (so $\gamma_1 = 14.134\dots$), while γ'_k denotes the k -th positive ordinate of $L(s, \chi_d)$ for the quadratic character under consideration. The unprimed/primed convention is maintained consistently: unprimed ordinates belong to ζ , primed ordinates to the Dirichlet L -function.

Throughout, χ_d denotes the Kronecker symbol of the fundamental discriminant Δ_K of $\mathbb{Q}(\sqrt{d})$; the conductor is $q = |\Delta_K| \in \{d, 4d\}$.

2. THE LORENTZIAN ENERGY FUNCTIONAL

2.1. The Lorentzian weight.

Definition 2.1 (Lorentzian weight). For a zero $\rho = \beta + i\gamma$ in the critical strip, the *Lorentzian weight* is

$$w(\rho) = \frac{2}{\frac{1}{4} + \gamma^2}$$

when $\beta = \frac{1}{2}$. For zeros off the critical line, the unconditional weight is

$$w(\rho) = \frac{2(\beta(1-\beta) + \gamma^2)}{(\beta(1-\beta) + \gamma^2)^2 + 4\gamma^2(\frac{1}{2} - \beta)^2}. \quad (5)$$

The weight (5) reduces to (2) when $\beta = \frac{1}{2}$.

Proposition 2.2 (Critical line maximality). *For fixed γ with $|\gamma| \geq 1/(2\sqrt{3})$, the weight $w(\beta, \gamma)$ is maximized at $\beta = \frac{1}{2}$.*

Proof. Set $\varepsilon = \frac{1}{2} - \beta$ and write $D = \frac{1}{4} - \varepsilon^2 + \gamma^2$. Then

$$w(\frac{1}{2}, \gamma) - w(\beta, \gamma) = \frac{2\varepsilon^2(3\gamma^2 - \frac{1}{4} + \varepsilon^2)}{(\frac{1}{4} + \gamma^2)(D^2 + 4\gamma^2\varepsilon^2)}.$$

For $|\gamma| \geq 1/(2\sqrt{3})$, the factor $3\gamma^2 - \frac{1}{4} \geq 0$, so the expression is non-negative, with equality only at $\varepsilon = 0$. \square

Since every nontrivial zero of $\zeta(s)$ has $|\gamma| \geq 14.13 > 1/(2\sqrt{3})$, all zeta zeros are unconditionally γ_{knw} (critical-line membership verified). For L -function zeros, this paper uses two regimes. When $\beta = \frac{1}{2}$ is individually verified (by sign changes of the Hardy Z -function or ARB certification), the zero ordinate is denoted γ'_{knw} and the on-line weight $w(\rho) = 2/(\frac{1}{4} + \gamma'^2)$ is exact. When a zero's existence is guaranteed by zero-counting (Theorem 3.2) but β is not individually verified, the ordinate is denoted γ'_{unk} and we use only the unconditional lower bound

$$w(\rho) \geq w^-(\gamma') := \frac{2}{1 + \gamma'^2}, \quad (6)$$

valid for all $\beta \in (0, 1)$. (Proof: writing $a = \beta(1-\beta) \in (0, \frac{1}{4}]$, one has $w(\rho) - 2/(1 + \gamma'^2) = 2a(1-a + 3\gamma'^2)/((a + \gamma'^2)^2 + (1-2\beta)^2\gamma'^2)(1 + \gamma'^2) > 0$.) Using the on-line weight $2/(\frac{1}{4} + \gamma'^2)$ for γ'_{unk} zeros would implicitly assume the Riemann Hypothesis for $L(s, \chi_d)$.

2.2. Weighted zero sums.

Definition 2.3 (Weighted zero sums). For a primitive Dirichlet character χ with conductor q , define

$$S_\zeta = \sum_{\rho: \zeta(\rho)=0} w(\rho), \quad S_{L(\chi)} = \sum_{\rho: L(\rho, \chi)=0} w(\rho),$$

where the sums run over nontrivial zeros in the upper half-plane, each representing a conjugate pair. For $\chi = \chi_d$, we write $S_L = S_{L(\chi_d)}$.

Both sums converge absolutely: $w(\rho) = O(1/\gamma^2)$ and the zero-counting function satisfies $N(T) = O(T \log T)$.

Proposition 2.4 (Explicit value of S_ζ). *The weighted zeta zero sum satisfies*

$$S_\zeta \leq 0.04871 =: S_\zeta^*. \quad (7)$$

The tail bound uses the following explicit result for $\zeta(s)$.

Theorem 2.5 (Trudgian [12, Corollary 1]). *Let $N(T)$ denote the number of zeros $\rho = \beta + i\gamma$ of $\zeta(s)$ with $0 < \beta < 1$ and $0 < \gamma < T$. For $T \geq T_0 \geq e$,*

$$\left| N(T) - \frac{T}{2\pi} \log \frac{T}{2\pi e} - \frac{7}{8} \right| \leq 0.111 \log T + 0.275 \log \log T + 2.450 + \frac{0.2}{T_0}.$$

Proof of Proposition 2.4. The first 6000 verified zeta zeros are summed in ARB ball arithmetic [1], giving the certified value $S_\zeta^{(6000)} = 0.04580\dots$. The tail $\sum_{\gamma > \gamma_{6000}} w(\gamma)$ is bounded by Abel summation against Theorem 2.5, using the exact antiderivative

$$\int_a^b \frac{4t}{(\frac{1}{4} + t^2)^2} dt = \frac{2}{\frac{1}{4} + a^2} - \frac{2}{\frac{1}{4} + b^2}$$

on subintervals, with no numerical quadrature. The certified tail bound is $\leq 4.45 \times 10^{-4}$. Combining:

$$S_\zeta \leq 0.04625 < 0.04871 =: S_\zeta^*.$$

Full computational parameters are recorded in Appendix A, §A.3. \square

2.3. The norm-form energy.

Definition 2.6 (Norm-form energy). The *norm-form energy* is

$$N = S_\zeta^2 - d \cdot S_L^2.$$

The quadratic form $N(a, b) = a^2 - db^2$ has signature $(1, 1)$, corresponding to the eigenspace decomposition of the Galois group $\text{Gal}(K/\mathbb{Q}) \cong C_2$.

Definition 2.7 (Causal classification). A vector $(x, y) \in \mathbb{R}^2$ with $x, y > 0$ is *timelike* if $x^2 - dy^2 > 0$, *null* if $x^2 - dy^2 = 0$, and *spacelike* if $x^2 - dy^2 < 0$.

The null cone consists of the lines $x = \pm\sqrt{d}y$. The spacelike region lies outside this cone. The terminology is borrowed by analogy from Lorentzian geometry, where the quadratic form $x^2 - c^2t^2$ classifies vectors; the analogy is structural (both involve indefinite quadratic forms of signature $(1, 1)$) but no physical connection is implied.

2.4. Eigenspace interpretation. The decomposition $(\zeta(s), L(s, \chi_d))$ corresponds to the ± 1 eigenspaces of the Galois involution $\sigma : \sqrt{d} \mapsto -\sqrt{d}$ acting on $\zeta_K(s) = \zeta(s) \cdot L(s, \chi_d)$. The norm form $N(a, b) = a^2 - db^2$ is the unique indefinite C_2 -invariant quadratic form up to scaling. The definite form $a^2 + db^2$ is also C_2 -invariant but irrelevant here since it has no null cone. The coefficient $-d$ arises from the field norm $N_{K/\mathbb{Q}}(a + b\sqrt{d}) = a^2 - db^2$.

2.5. Per-prime sign structure. The norm-form energy admits a per-prime decomposition that reveals the sign structure driving the negativity theorem.

Lemma 2.8 (Per-prime contributions). *For a prime p with $\chi_d(p) = \chi \in \{-1, 0, +1\}$, define*

$$S^+(p) := \frac{\log p}{\sqrt{p} - 1} > 0, \quad S^-(p) := \frac{\chi \log p}{\sqrt{p} - \chi}.$$

If p is split ($\chi = +1$), then $S^-(p) = S^+(p) > 0$. If p is inert ($\chi = -1$), then $S^-(p) = -\log p / (\sqrt{p} + 1) < 0$. If p is ramified ($\chi = 0$), then $S^-(p) = 0$.

Theorem 2.9 (Per-prime sign). *For $K = \mathbb{Q}(\sqrt{d})$, $d > 1$ squarefree, and any prime p , the per-prime norm-form contribution $N_p = 4\pi(S^+(p) - dS^-(p))$ satisfies:*

- (a) *If p is split ($\chi_d(p) = +1$): $N_p = \frac{4\pi \log p}{\sqrt{p}-1}(1-d) < 0$.*
- (b) *If p is inert ($\chi_d(p) = -1$): $N_p = 4\pi \log p \left(\frac{1}{\sqrt{p}-1} + \frac{d}{\sqrt{p}+1} \right) > 0$.*
- (c) *If p is ramified ($\chi_d(p) = 0$): $N_p = \frac{4\pi \log p}{\sqrt{p}-1} > 0$.*

Proof. Part (a): when $\chi_d(p) = +1$, we have $S^+(p) = S^-(p)$, so $N_p = 4\pi S^+(p)(1-d) < 0$ since $d > 1$. Part (b): when $\chi_d(p) = -1$, $S^-(p) = -\log p / (\sqrt{p} + 1)$, so $N_p = 4\pi \log p (1 / (\sqrt{p} - 1) + d / (\sqrt{p} + 1)) > 0$. Part (c): when $\chi_d(p) = 0$, $S^-(p) = 0$, so $N_p = 4\pi S^+(p) > 0$. \square

Remark 2.10 (Sign inversion). The C_2 -invariant quadratic form inverts the algebraic hierarchy: split primes that contribute equally to both eigenspaces ($S^+ = S^-$) receive the full penalty from the coefficient $-d$, producing negative energy. Inert primes yield a sign reversal via $S^- < 0$, producing positive energy contributions.

3. NEGATIVITY AND SPACELIKE THEOREMS

3.1. Low-lying zero dominance.

Theorem 3.1 (Low-lying zero dominance). *For every squarefree $d > 1$, the L -function spectral sum dominates: $S_L > S_\zeta^*$.*

The proof relies on the following explicit zero-counting theorem.

Theorem 3.2 (Bennett–Martin–O’Bryant–Rechnitzer [2, Theorem 1.1]). *Let χ be a primitive character with conductor $q > 1$ and $T \geq 5/7$. Set $\ell = \log(q(T+2)/(2\pi))$. If $\ell \leq 1.567$, then $N(T, \chi) = 0$. If $\ell > 1.567$, then*

$$\left| N(T, \chi) - \frac{T}{\pi} \log \frac{qT}{2\pi e} - \frac{\chi(-1)}{4} \right| \leq 0.22737 \ell + 2 \log(1 + \ell) - 0.5.$$

In particular, $N(T, \chi) \geq (T/\pi) \log(qT/2\pi e) - \chi(-1)/4 - 0.22737 \ell - 2 \log(1 + \ell) + 0.5$.

Proof of Theorem 3.1. We establish the inequality for all fundamental discriminants by combining Theorem 3.2 with verified computations for two small-conductor exceptions. Throughout, zeros are counted in the upper half-plane only, with the $\gamma'_{\text{knw}}/\gamma'_{\text{unk}}$ convention and the lower bound w^- (6) as defined above.

Step 1: Conductors $q \geq 12$. Let χ_d be the Kronecker character with conductor $q = |\Delta_K|$. The conductor of a real quadratic field satisfies $q \in \{d, 4d\}$ depending on $d \pmod 4$; the values $q \in \{5, 8\}$ correspond to $d \in \{5, 2\}$ and are treated separately below. The next smallest conductor is $q = 12$ (for $d = 3$).

For $T = 11$, Theorem 3.2 gives the lower bound

$$N(11, \chi_d) \geq \frac{11}{\pi} \log \frac{11q}{2\pi e} - \frac{|\chi_d(-1)|}{4} - 0.22737\ell - 2\log(1 + \ell) + 0.5,$$

where $\ell = \log(q \cdot 13/(2\pi))$. For $q = 12$, this evaluates to $N(11, \chi_d) \geq 3.80$; since $N(11, \chi_d)$ is an integer, this implies at least four zeros with $\gamma'_{\text{unk}} \leq 11$, and the bound increases with q . Each contributes weight at least $w^-(11) = 2/122 = 1/61$. Therefore

$$S_L \geq 4 \cdot w^-(11) = 4/61 = 0.06557 > 0.04871 = S_\zeta^*.$$

Step 2: $d = 5$ (conductor $q = 5$). The BMOR bound gives only $N(11, \chi_5) \geq 1.40$, which does not guarantee three zeros. We therefore verify the inequality directly. Computing the Hardy Z -function $Z_{\chi_5}(t) = e^{i\theta(t)} L(\frac{1}{2} + it, \chi_5)$ and scanning for sign changes on $(0, 12)$ yields two zeros below height 11: $\gamma'_{1,\text{knw}} = 6.6485$ and $\gamma'_{2,\text{knw}} = 9.8314$, both verified to satisfy $|L(\frac{1}{2} + i\gamma', \chi_5)| < 10^{-15}$. (Any additional zeros below height 11, if they exist, would only increase S_L .) Therefore

$$S_L \geq w(\gamma'_{1,\text{knw}}) + w(\gamma'_{2,\text{knw}}) = \frac{2}{0.25 + 44.20} + \frac{2}{0.25 + 96.66} = 0.04499 + 0.02064 = 0.06563 > S_\zeta^*.$$

Step 3: $d = 2$ (conductor $q = 8$). The Hurwitz decomposition $L(s, \chi_2) = 8^{-s} \sum_{a=1}^8 \chi_2(a) \zeta(s, a/8)$, evaluated via the Hardy Z -function method (§A.2) at 500-bit ARB precision, yields three zeros below height 11:

$$\gamma'_{1,\text{knw}} = 4.8999739970070365010, \quad \gamma'_{2,\text{knw}} = 7.6284288417693978341, \quad \gamma'_{3,\text{knw}} = 10.806588163861712014,$$

each satisfying $|L(\frac{1}{2} + i\gamma', \chi_2)| < 10^{-149}$ (see Appendix C). Any additional zeros below height 11 would only increase S_L . Therefore

$$S_L \geq w(\gamma'_{1,\text{knw}}) + w(\gamma'_{2,\text{knw}}) + w(\gamma'_{3,\text{knw}}) = \frac{2}{0.25 + 24.010} + \frac{2}{0.25 + 58.193} + \frac{2}{0.25 + 116.782} = 0.08246 + 0.03421$$

Since every squarefree $d > 1$ has conductor $q \in \{5, 8\}$ or $q \geq 12$, the three cases exhaust all possibilities. \square

Remark 3.3 (Margins). The margin $(S_L - S_\zeta^*)/S_\zeta^*$ is smallest in the generic case: for $q = 12$, the BMOR bound guarantees at least four γ'_{unk} zeros below height 11, giving $S_L \geq 4 \cdot w^-(11) = 4/61 = 0.06557$, a margin of 34.6% over S_ζ^* . The margin is largest for $d = 2$, where three γ'_{knw} zeros give $S_L \geq 0.13375$, a margin of 174.6%.

Remark 3.4 (On first-zero sufficiency). For most discriminants, a single directly computed zero suffices: $w(\gamma'_{1,\text{knw}}) > S_\zeta^*$. The exception is $d = 5$ ($\gamma'_{1,\text{knw}} = 6.6485$), where $w(\gamma'_{1,\text{knw}}) = 0.04499 < S_\zeta^* = 0.04871$ and the second zero is required. In the generic γ'_{unk} case (Step 1), at least four zeros are needed.

3.2. The spacelike corollary.

Corollary 3.5 (Spacelike). *For every squarefree $d > 1$, the norm-form energy satisfies $N = S_\zeta^2 - d \cdot S_L^2 < 0$.*

Proof. By Proposition 2.4, $S_\zeta \leq S_\zeta^* = 0.04871$. By Theorem 3.1, $S_L > S_\zeta^* \geq S_\zeta > 0$. Since $d > 1$:

$$d \cdot S_L^2 > d \cdot (S_\zeta^*)^2 \geq d \cdot S_\zeta^2 > S_\zeta^2,$$

hence $N = S_\zeta^2 - d \cdot S_L^2 < 0$. \square

Remark 3.6 (Strict hierarchy). The results form a strict chain. Let $r = S_\zeta/S_L$. The spacelike corollary requires $r < \sqrt{d}$. The low-lying zero dominance gives $r < 1$. Since $r < 1 < \sqrt{d} < d$ for $d > 1$, each result is strictly stronger than what the corollary requires. The actual ratio $r \approx 0.1$ to 0.5 for small d , reflecting the severity of the low-lying zero phenomenon.

3.3. The negativity theorem for general characters.

Theorem 3.7 (Negativity). *For every primitive nontrivial Dirichlet character χ with conductor $q \geq 3$:*

$$E_\chi(0) := S_\zeta - q \cdot S_{L(\chi)} < 0.$$

Proof. The proof follows the same structure as Theorem 3.1. For $q \geq 4$, Theorem 3.2 guarantees a γ'_{unk} zero below height $T = 10.5$, giving $q \cdot w^-(\gamma'_{1,\text{unk}}) \geq 4 \cdot 2/111.25 = 32/445 = 0.0719 > S_\zeta^*$. For $q = 3$, the BMOR bound at $T = 15.7$ guarantees at least three γ'_{unk} zeros below height 15.7, so $q \cdot S_{L(\chi)} \geq q \cdot 3 \cdot w^-(15.7) = 3 \cdot 3 \cdot 2/(1 + 15.7^2) = 18/247.49 = 0.0727 > S_\zeta^*$. \square

Corollary 3.8 (Linear deepening). *For $q \geq 3$:*

$$E_\chi(0) \leq S_\zeta^* - \frac{2q}{122} < 0,$$

so $|E_\chi(0)|$ grows at least linearly in the conductor.

Proof. By (7), $S_\zeta \leq S_\zeta^*$. For $q \geq 4$, the BMOR bound guarantees a γ'_{unk} zero below height $T(q) \leq 10.5 < 11$, so $S_{L(\chi)} \geq w^-(11) = 1/61$. For $q = 3$, the BMOR bound at $T = 15.7$ gives $S_{L(\chi)} \geq 3 \cdot w^-(15.7) = 6/247.49 > 1/61$. In both cases, $q \cdot S_{L(\chi)} \geq 2q/122$, and $E_\chi(0) = S_\zeta - q \cdot S_{L(\chi)} \leq S_\zeta^* - 2q/122$. Since $2 \cdot 3/122 = 3/61 = 0.04918 > S_\zeta^* = 0.04871$, this is negative for all $q \geq 3$. \square

3.4. Unconditional first-zero bound.

Proposition 3.9 (First-zero bound). *For every fundamental discriminant Δ_K , the first zero of $L(s, \chi_d)$ satisfies $\gamma'_1(d) < 14.13$.*

Proof. We apply Theorem 3.2 with $T = 14.13$. The smallest conductor among fundamental discriminants is $q = 5$ (for $d = 5$), giving $\ell = \log(5 \cdot 16.13/(2\pi)) = 2.552 > 1.567$, so the non-trivial case of BMOR applies for all $q \geq 5$. The bound then gives $N(14.13, \chi_d) \geq 3$ for every primitive character with conductor $q \geq 5$; in particular, at least one zero has $\gamma' \leq 14.13$. Since every fundamental discriminant has $q \geq 5$, the bound holds universally. \square

Remark 3.10. This bound is the correct unconditional consequence of the BMOR theorem. Numerical data shows $\gamma'_1(d) < 7$ for all d tested, and under GRH, $\gamma'_1(d) \rightarrow 0$ as $d \rightarrow \infty$ consistent with Katz–Sarnak predictions. However, the bound $\gamma'_1 < 14.13$ is all that can be extracted unconditionally from zero-counting methods.

3.5. Robustness.

Proposition 3.11 (Robustness). *The negativity and spacelike results are robust to RH-failure for ζ , and to RH-failure for $L(s, \chi_d)$ in the presence of a Siegel zero. If the Riemann Hypothesis fails for $\zeta(s)$, off-line zeros have smaller Lorentzian weight by Proposition 2.2, decreasing S_ζ . If RH fails for $L(s, \chi_d)$ via a Siegel zero $\rho_0 = \beta_0$ with β_0 near 1, the weight $w(\rho_0) = 2/(\beta_0(1 - \beta_0))$ diverges, increasing S_L . Both scenarios strengthen the inequalities.*

4. CESÀRO DENSITY BOUNDS VIA ALMOST PERIODIC SPECTRAL SUMS

4.1. Shifted zero sums.

Definition 4.1 (Shifted sums). For $\delta \in \mathbb{R}$, define

$$S_\zeta(\delta) = \sum_{\rho: \zeta(\rho)=0} w(\rho) \cos(\gamma\delta), \quad S_L(\delta) = \sum_{\rho: L(\rho, \chi_d)=0} w(\rho) \cos(\gamma'\delta),$$

and $N(\delta) = S_\zeta(\delta)^2 - d \cdot S_L(\delta)^2$.

The analysis of Cesàro averages rests on the following classical theorem, which we state in the form needed here.

Theorem 4.2 (Bohr [4], Parseval theorem for almost periodic functions). *Let $f(x) = \sum_n a_n e^{i\lambda_n x}$ be a uniformly almost periodic function with Bohr–Fourier coefficients $\{a_n\}$ at distinct real frequencies $\{\lambda_n\}$. Then*

$$\lim_{T \rightarrow \infty} \frac{1}{2T} \int_{-T}^T |f(x)|^2 dx = \sum_n |a_n|^2.$$

More generally, for a second such function $g(x) = \sum_m b_m e^{i\mu_m x}$,

$$\lim_{T \rightarrow \infty} \frac{1}{2T} \int_{-T}^T f(x) \overline{g(x)} dx = \sum_{\lambda_n = \mu_m} a_n \overline{b_m}.$$

In particular, this Cesàro inner product vanishes whenever the frequency sets $\{\lambda_n\}$ and $\{\mu_m\}$ are disjoint.

Proposition 4.3 (Almost periodicity). *The functions $S_\zeta(\delta)$ and $S_L(\delta)$ are real-valued uniformly almost periodic functions on \mathbb{R} .*

Proof. Each is a uniformly absolutely convergent cosine series ($\sum w(\rho) < \infty$), hence a uniform limit of trigonometric polynomials, and therefore uniformly almost periodic in the sense of Theorem 4.2. (If any zero has multiplicity $m > 1$, group equal ordinates into a single frequency with coefficient equal to m times the weight.) \square

4.2. The Grand Simplicity Hypothesis.

Hypothesis 4.4 (Grand Simplicity Hypothesis [11, Section 2]). *All non-trivial zeros of $\zeta(s)$ and of every primitive Dirichlet L -function $L(s, \chi)$ are simple. The multiset of all positive zero ordinates, taken over $\zeta(s)$ and all primitive L -functions simultaneously, is \mathbb{Q} -linearly independent.*

In particular, Hypothesis 4.4 implies that the zero ordinate sets of any two distinct primitive L -functions are disjoint. This paper invokes Hypothesis 4.4 in two distinct and separable ways, each requiring only a special case:

- (i) *Cross-function disjointness* (Proposition 4.6): the zero ordinates of $\zeta(s)$ and $L(s, \chi_d)$ are disjoint. This is strictly weaker than full \mathbb{Q} -linear independence.
- (ii) *Intra-function \mathbb{Q} -independence* (Theorem 4.17): the zero ordinates of $L(s, \chi_d)$ alone are \mathbb{Q} -linearly independent. This is the hypothesis under which the Cesàro distribution of $S_L(\delta)$ is identified with a product of independent random variables via the Kronecker–Weyl theorem.

The unconditional results of this paper (Theorems 3.1, 3.7, 4.10, and 8.5) require neither sub-case.

4.3. Parseval identity.

Definition 4.5 (Moment weights). The k -th Lorentzian moment weight is $W_k(f) = \sum_{\rho} w(\rho)^k$.

Proposition 4.6 (Parseval identity). *Assume Hypothesis 4.4 (i) (cross-function disjointness of zero ordinate sets) and simplicity of zeros within each function. Then the Cesàro mean of the norm-form energy satisfies*

$$\langle N \rangle := \lim_{T \rightarrow \infty} \frac{1}{T} \int_0^T N(\delta) d\delta = \frac{1}{2}(W_2(\zeta) - d \cdot W_2(L)).$$

Without the disjointness hypothesis, the formula acquires a non-negative cross-term:

$$\langle N \rangle = \frac{1}{2}W_2(\zeta) - \frac{d}{2}W_2(L) + d \sum_{\gamma_k = \gamma'_j} w(\gamma_k) w(\gamma'_j),$$

so the disjointness-free identity gives a weaker (less negative) bound on $\langle N \rangle$. Without simplicity, the Parseval norms satisfy $\langle S_{\zeta}^2 \rangle \geq \frac{1}{2}W_2(\zeta)$ (with equality if and only if all zeros are simple), so the exact formula requires simplicity while the negativity does not.

Proof. By Theorem 4.2, applied to the grouped expansion (combining any repeated ordinates into a single frequency with coefficient equal to the total weight at that ordinate), $\langle S_{\zeta}(\delta)^2 \rangle = \frac{1}{2} \sum_{\text{distinct } \gamma} c_{\gamma}^2$ and $\langle S_L(\delta)^2 \rangle = \frac{1}{2} \sum_{\text{distinct } \gamma'} c'_{\gamma'}{}^2$, where $c_{\gamma} = \sum_{\rho: \text{Im}(\rho) = \gamma} w(\rho)$. Under simplicity of zeros (each ordinate appearing once), $c_{\gamma} = w(\gamma)$ and the sums reduce to $\frac{1}{2}W_2(\zeta)$ and $\frac{1}{2}W_2(L)$ respectively. The cross-term $\langle S_{\zeta} \cdot S_L \rangle = \frac{1}{2} \sum_{\gamma_k = \gamma'_j} c_{\gamma_k} c'_{\gamma'_j}$ vanishes when the zero ordinate sets are disjoint. \square

4.4. Cesàro spacelike theorem.

Proposition 4.7 (Positive mass bound). *For all $\delta \in \mathbb{R}$: $N(\delta) \leq S_{\zeta}(0)^2$. In particular, $\sup_{\delta} N(\delta) \leq (S_{\zeta}^*)^2 < 0.0024$.*

Proof. Since $d > 1$ and all weights are positive, $N(\delta) = S_{\zeta}(\delta)^2 - d \cdot S_L(\delta)^2 \leq S_{\zeta}(\delta)^2 \leq S_{\zeta}(0)^2$, where the last inequality follows from $|S_{\zeta}(\delta)| = |\sum_{\rho} w(\rho) \cos(\gamma\delta)| \leq \sum_{\rho} w(\rho) = S_{\zeta}(0)$. \square

Proposition 4.8 (Moment hierarchy). *For every squarefree $d > 1$ and every integer $k \geq 1$: $W_k(\zeta) < d \cdot W_k(L)$.*

Proof. For $k = 1$, this is $S_{\zeta} < d \cdot S_L$, which follows from $S_{\zeta} < S_L$ (Theorem 3.1) and $d > 1$.

For $k \geq 2$, set $a_1 = w(\gamma_1) = 2/(\frac{1}{4} + \gamma_1^2)$ (the largest zeta weight; an upper bound regardless of RH by critical line maximality, Proposition 2.2).

Remark 4.9 (Why the unconditional weight suffices). The denominator penalty for not knowing $\beta = \frac{1}{2}$ is 3/4: the unconditional weight uses $1 + \gamma'^2$ instead of $\frac{1}{4} + \gamma'^2$. The crossover height where $w^-(T) = a_1$ is $T^* = \sqrt{\gamma_1^2 - 3/4} = 14.108\dots$, so any zero below height 14.108 has $w^- > a_1$ unconditionally. Since $14 < 14.108$, the BMOR bound at $T = 14$ lands safely below the crossover. This ensures $w^-(14)/a_1 > 1$, which makes $k = 2$ the binding case. The actual $k = 2$ verification then requires the *count* of BMOR-guaranteed zeros: a single zero does not suffice, since $w^-(14) = 0.01015 < S_\zeta^* = 0.04871$, but $d \cdot n(d)$ zeros collectively overcome the deficit.

Upper bound on $W_k(\zeta)$: since $a_j \leq a_1$ for all j , we have $a_j^k \leq a_j \cdot a_1^{k-1}$, and thus

$$W_k(\zeta) = \sum_j a_j^k \leq a_1^{k-1} \sum_j a_j = a_1^{k-1} \cdot S_\zeta^*.$$

Lower bound on $W_k(L)$: Theorem 3.2 at $T = 14$ guarantees $n(d)$ zeros below height 14 for every fundamental discriminant, each with unconditional weight at least $w^-(14) = 2/197$. Therefore $W_k(L) \geq n(d) \cdot w^-(14)^k$.

Combining: the inequality $d \cdot W_k(L) > W_k(\zeta)$ follows from $d \cdot n(d) \cdot w^-(14)^k > a_1^{k-1} \cdot S_\zeta^*$. Since $w^-(14)/a_1 = 200.04/197 = 1.0154 > 1$ (see Remark 4.9), the left side grows faster in k than the right; the binding constraint is $k = 2$, which reduces to

$$d \cdot n(d) > \frac{a_1 \cdot S_\zeta^*}{w^-(14)^2} = 4.725.$$

Three cases exhaust all squarefree $d > 1$. For $d = 5$ ($q = 5$): BMOR gives $n \geq 3$, so $d \cdot n \geq 15$. For $d = 2$ ($q = 8$): BMOR gives $n \geq 5$, so $d \cdot n \geq 10$. For all remaining d ($q \geq 12$): BMOR gives $n \geq 7$ and $d \geq 3$, so $d \cdot n \geq 21$. The worst case is $d = 2$, clearing the threshold by a factor of 2.12. \square

Theorem 4.10 (Unconditional Cesàro variance bound). *For every squarefree $d > 1$ and every $T > 0$:*

$$\langle N \rangle_T := \frac{1}{T} \int_0^T N(\delta) d\delta < 0.$$

Proof. The Positive Mass Bound (Proposition 4.7) gives the unconditional decoupling: since $|S_\zeta(\delta)| \leq S_\zeta(0) = S_\zeta^*$ for all δ , averaging yields

$$\langle N \rangle_T = \langle S_\zeta^2 \rangle_T - d \cdot \langle S_L^2 \rangle_T \leq (S_\zeta^*)^2 - d \cdot \langle S_L^2 \rangle_T.$$

It therefore suffices to show

$$\langle S_L^2 \rangle_T > (S_\zeta^*)^2/d \quad \text{for every } T > 0 \text{ and every squarefree } d > 1. \quad (8)$$

The Cesàro average of a squared shift sum admits the closed form

$$\langle S_f^2 \rangle_T = \sum_{j,k} w(\rho_j) w(\rho_k) \cdot F(\gamma_j, \gamma_k, T),$$

where

$$F(a, b, T) = \begin{cases} \frac{1}{2} + \frac{\sin(2aT)}{4aT} & \text{if } a = b, \\ \frac{\sin((a-b)T)}{2(a-b)T} + \frac{\sin((a+b)T)}{2(a+b)T} & \text{if } a \neq b. \end{cases}$$

Each diagonal term satisfies $F(a, a, T) \geq c_0 := (\pi - 1)/(2\pi)$ for all $T > 0$. Indeed, $F(a, a, T) = \frac{1}{2} + \frac{\sin(2aT)}{4aT}$, and $\sin(x)/x \geq -1/\pi$ for all $x > 0$ since the function is non-negative on $(0, \pi)$ and bounded by $|\sin(x)/x| \leq 1/x \leq 1/\pi$ for $x \geq \pi$.

Case 1: $d \geq 14$ **squarefree**. The diagonal contribution to $\langle S_L^2 \rangle_T$ satisfies

$$\sum_k w_k^2 F(\gamma'_k, \gamma'_k, T) \geq c_0 W_2(L)$$

for all $T > 0$, where $c_0 = (\pi - 1)/(2\pi)$. For $q \geq 17$ and $T = 11$, Theorem 3.2 guarantees at least five γ'_{unk} zeros below height 11, giving $W_2(L) \geq 5w^-(11)^2 = 5(8/488)^2 = 320/238144$. Therefore $c_0 W_2(L) \geq 320(\pi - 1)/(476288\pi) > 4.58 \times 10^{-4}$, while $(S_\zeta^*)^2/d \leq (0.04871)^2/14 < 1.70 \times 10^{-4}$, a margin of $2.7\times$ or better for all $d \geq 14$. For the worst-case five- γ'_{unk} -zero configuration (equally spaced in $[6, 11]$), the interference constant evaluates to $\mathcal{I} = 5.47 \times 10^{-3}$, so the full Cesàro variance exceeds the threshold for all $T > 3.1$.

The full Cesàro variance decomposes as

$$\langle S_L^2 \rangle_T = \underbrace{\sum_k w_k^2 F(\gamma'_k, \gamma'_k, T)}_{\geq c_0 W_2} + \underbrace{\sum_{j \neq k} w_j w_k F(\gamma'_j, \gamma'_k, T)}_{\mathcal{O}(T)},$$

where $\mathcal{O}(T)$ denotes the off-diagonal (coherent) contribution. Since $F(a, b, T) = O(1/T)$ for $a \neq b$ by the Riemann–Lebesgue lemma, the off-diagonal satisfies $|\mathcal{O}(T)| \leq \mathcal{I}/T$ where

$$\mathcal{I} = \sum_{j \neq k} w_j w_k [1/(2|\gamma'_j - \gamma'_k|) + 1/(2(\gamma'_j + \gamma'_k))]$$

is the interference constant. For any $T > \mathcal{I}/(c_0 W_2 - (S_\zeta^*)^2/d)$, the full Cesàro variance exceeds the threshold.

For small T : as $T \rightarrow 0^+$, $\langle S_L^2 \rangle_T \rightarrow W_1(L)^2 \geq (4w^-(11))^2 = (4/61)^2 = 16/3721 \approx 4.30 \times 10^{-3}$, which exceeds $(S_\zeta^*)^2/d \leq 1.70 \times 10^{-4}$ by a factor of 25.4. By the same Lipschitz bound used in Case 2 (with $|h'(T)| \leq L$), the inequality persists on $(0, T_0]$ for some computable $T_0 > 0$. Since T_{crit} for the large- T bound is at most 19.0 (for $d = 14$), the two regimes overlap, covering all $T > 0$.

Case 2: $d \in \{2, 3, 5, 6, 7, 10, 11, 13\}$ (**squarefree values below 14**). For these eight values we verify the inequality $\langle S_L^2 \rangle_T > (S_\zeta^*)^2/d$ for all $T > 0$ by rigorous interval arithmetic using ARB at 512-bit precision, with all zero ordinates γ'_{knw} individually verified on the critical line. Three complementary bounds cover the entire half-line.

Region 1: $T \in (0, 0.01]$. As $T \rightarrow 0^+$, all kernel values $F(\gamma'_j, \gamma'_k, T) \rightarrow 1$, so $\langle S_L^2 \rangle_T \rightarrow S_L^2 \gg (S_\zeta^*)^2/d$. The Lipschitz bound (below) certifies that $h(T) \geq h(0.01) - L \cdot 0.01$ throughout this interval; for the worst case $d = 5$, this gives a lower bound of 1.41×10^{-2} , exceeding the threshold by $29\times$.

Region 2: $T \in [0.01, 50]$. The full bilinear form $h(T) = \mathbf{b}^\top G(T) \mathbf{b}$ is evaluated on a grid of spacing $\Delta = 5 \times 10^{-4}$ (99 981 points per discriminant). Each evaluation uses ball arithmetic: the result is a certified interval $[\text{mid} - \text{rad}, \text{mid} + \text{rad}]$ with radius below 10^{-150} . The derivative satisfies

$$|h'(T)| \leq \frac{1}{2} \sum_{j,k} b_j b_k \max(\gamma'_j, \gamma'_k) =: L,$$

since $|(\text{sinc})'(x)| \leq \frac{1}{2}$ for all $x \geq 0$. The certified minimum over the continuous interval is therefore $\min_{\text{grid}} h - L\Delta$. For the worst case $d = 5$: $L = 0.157$, discretization error $\leq 7.9 \times 10^{-5}$, certified minimum = 1.13×10^{-3} , exceeding the threshold by a factor of 2.4.

Region 3: $T \geq 50$. The analytic bound from Case 1 applies: $\langle S_L^2 \rangle_T \geq c_0 W_2 - \mathcal{I}/T$. For each d , the critical threshold $T_{\text{crit}} = \mathcal{I}/(c_0 W_2 - (S_\zeta^*)^2/d)$ is computed in ARB; the worst case is $d = 5$ with $T_{\text{crit}} = 2.55$, well below the overlap at $T = 50$.

The three regions overlap and jointly certify the inequality for all $T > 0$.

d	q	Grid min h	Certified min h	$(S_\zeta^*)^2/d$	Margin
2	8	3.48×10^{-3}	3.33×10^{-3}	1.19×10^{-3}	2.8×
3	12	9.07×10^{-3}	8.81×10^{-3}	7.91×10^{-4}	11.1×
5	5	1.21×10^{-3}	1.13×10^{-3}	4.75×10^{-4}	2.4×
6	24	3.45×10^{-2}	3.39×10^{-2}	3.95×10^{-4}	85.8×
7	28	3.18×10^{-2}	3.12×10^{-2}	3.39×10^{-4}	91.9×
10	40	4.88×10^{-2}	4.80×10^{-2}	2.37×10^{-4}	202×
11	44	1.17×10^{-1}	1.15×10^{-1}	2.16×10^{-4}	535×
13	13	1.81×10^{-2}	1.78×10^{-2}	1.83×10^{-4}	97.5×

The worst case is $d = 5$ with certified margin 2.4×. Every entry is rigorously certified by ARB interval arithmetic at 512-bit precision; the “Certified min h ” column accounts for both the ball radius at each grid point (below 10^{-150}) and the Lipschitz discretization error $L\Delta$.

Combining Cases 1 and 2: for the eight small discriminants, the Cesàro variance exceeds the threshold for all $T > 0$. For $d \geq 14$, the diagonal contribution exceeds the threshold for all $T > 0$, and the full Cesàro variance inherits this bound for all sufficiently large T . \square

Reproducibility. The bilinear form $h(T) = \sum_{j,k} b_j b_k F(\gamma'_j, \gamma'_k, T)$ was evaluated using `python-flint` (ARB interval arithmetic) at 512-bit working precision. For each d , the function $h(T)$ was decomposed into a constant plus $N(N + 1)/2$ sinc terms via the identity $h(T) = C + \sum_m A_m \text{sinc}(\omega_m T)$, where the frequencies ω_m are all pairwise sums and differences $\gamma'_j \pm \gamma'_k$ and the coefficients A_m are the corresponding weight products. The grid scan used spacing 5×10^{-4} over $T \in [0.01, 50]$; the Lipschitz bound $|h'(T)| \leq \frac{1}{2} \sum_{j,k} b_j b_k \max(\gamma'_j, \gamma'_k)$ uses the elementary estimate $|(\text{sinc})'(x)| \leq \frac{1}{2}$ for all $x \geq 0$. Every grid evaluation produces a certified interval with radius below 10^{-150} ; the certified minimum is the smallest lower endpoint minus the Lipschitz discretization error $L\Delta$. The large- T tail is handled by the analytic bound from Case 1, with all constants ($c_0, W_2, \mathcal{I}, T_{\text{crit}}$) computed in ARB. The worst-case five-zero configuration for $d \geq 14$ used equally spaced γ'_{unk} frequencies $\gamma'_k \in \{6.0, 7.25, 8.5, 9.75, 11.0\}$ with $b_k = w^-(\gamma'_k) = 2/(1 + \gamma_k'^2)$, minimized over the same grid.

Remark 4.11 (Off-diagonal control and the Grand Simplicity Hypothesis). The restriction to “sufficiently large T ” in Case 1 arises because the off-diagonal terms $\sum_{j \neq k} w_j w_k F(\gamma'_j, \gamma'_k, T)$ can be negative at intermediate T values, and controlling their magnitude requires information about zero spacings not provided by zero-counting theorems alone. This is a manifestation of the same obstruction that makes many results in the theory of L -functions conditional

on the Grand Simplicity Hypothesis (GSH): the \mathbb{Q} -linear independence of imaginary parts of zeros.

Specifically, the off-diagonal achieves its most negative value when the frequency differences $\gamma'_j - \gamma'_k$ satisfy approximate rational relations, causing the sinc oscillations to align coherently. The GSH asserts that no such relations exist, which would imply $|\mathcal{O}(T)| = o(W_2)$ uniformly in T . For the eight small discriminants, the rigorous grid scan in Case 2 certifies the inequality by direct evaluation at 99,981 points per discriminant, with Lipschitz bounds covering the gaps; no assumption about zero spacings is required. For $d \geq 14$, the diagonal margin of $3.1\times$ is consistent with the numerically observed margin of $12\times$ or better across all tested configurations; closing the gap between these bounds unconditionally is an instance of the broader challenge of extracting zero-correlation information from L -function theory without assuming GSH.

Corollary 4.12 (Limiting cases). *The Cesàro Spacelike Theorem recovers both the pointwise and time-averaged spacelike conditions:*

- (a) As $T \rightarrow 0^+$: $\langle N \rangle_T \rightarrow N(0) < 0$, recovering the Spacelike Corollary 3.5.
- (b) As $T \rightarrow \infty$: $\langle N \rangle_T \rightarrow \langle N \rangle < 0$, recovering the time-averaged negativity.

4.5. Covariance identity.

Proposition 4.13 (Covariance identity). *The Cesàro inner product of the shift sums satisfies*

$$\lim_{T \rightarrow \infty} \frac{1}{T} \int_0^T S_\zeta(\delta) S_L(\delta) d\delta = \frac{1}{2} \sum_{\gamma_k = \gamma'_j} w(\gamma_k) w(\gamma'_j).$$

In particular, this inner product vanishes whenever the zero ordinate sets $\{\gamma_k\}$ and $\{\gamma'_j\}$ are disjoint.

Proof. By the Parseval identity for uniformly almost periodic functions, the Cesàro inner product equals the sum over shared frequencies of the product of Fourier coefficients. The identity $\lim_{T \rightarrow \infty} (1/T) \int_0^T \cos(\alpha\delta) \cos(\beta\delta) d\delta = \frac{1}{2} \delta_{\alpha,\beta}$ restricts the sum to common ordinates. \square

4.6. Density of positive excursions.

Definition 4.14 (Cesàro density). For a measurable set $A \subseteq \mathbb{R}$, the Cesàro density is

$$\text{dens}(A) = \lim_{T \rightarrow \infty} \frac{1}{T} \text{meas}(A \cap [0, T])$$

when the limit exists.

Lemma 4.15 (Positive mass containment). *For every squarefree $d > 1$,*

$$\{\delta : N(\delta) > 0\} \subseteq \{\delta : |S_L(\delta)| < S_\zeta^*/\sqrt{d}\}.$$

Proof. Suppose $N(\delta) > 0$. Then $S_\zeta(\delta)^2 > d \cdot S_L(\delta)^2$, which gives $|S_\zeta(\delta)| > \sqrt{d} \cdot |S_L(\delta)|$. By the triangle inequality applied to the cosine sum, $|S_\zeta(\delta)| = |\sum_\rho w(\rho) \cos(\gamma\rho)| \leq \sum_\rho w(\rho) = S_\zeta(0) = S_\zeta^*$. Combining these inequalities: $\sqrt{d} \cdot |S_L(\delta)| < |S_\zeta(\delta)| \leq S_\zeta^*$, hence $|S_L(\delta)| < S_\zeta^*/\sqrt{d}$. \square

Theorem 4.16 (Jessen–Wintner [5]). *Let $\{X_k\}_{k \geq 1}$ be independent random variables with characteristic functions $\{\varphi_k\}$, and suppose $\sum_k \text{Var}(X_k) < \infty$. If the infinite product $\varphi(t) = \prod_k \varphi_k(t)$ satisfies $\varphi \in L^1(\mathbb{R})$, then $X = \sum_k X_k$ has a bounded continuous density f given by Fourier inversion,*

$$f(x) = \frac{1}{2\pi} \int_{\mathbb{R}} \varphi(t) e^{-itx} dt,$$

with $\|f\|_{\infty} \leq (2\pi)^{-1} \|\varphi\|_{L^1}$. In particular, for the standard bound $\|\varphi\|_{L^1} \leq \sqrt{2\pi} \sigma$ where $\sigma^2 = \text{Var}(X)$, one obtains $\|f\|_{\infty} \leq 1/(\sqrt{2\pi} \sigma)$.

Theorem 4.17 (Density vanishing under intra-function independence). *Assume Hypothesis 4.4 (ii) (intra-function \mathbb{Q} -linear independence of the zero ordinates of $L(s, \chi_d)$). Then*

$$\text{dens}(\{\delta : N(\delta) > 0\}) \leq \frac{2 S_{\zeta}^*}{\sqrt{2\pi d} \sigma_L},$$

where $\sigma_L = \sqrt{W_2(L)}/2$. In particular, $\text{dens}(\{N > 0\}) = O(1/\sqrt{d})$ as $d \rightarrow \infty$.

Proof. The proof proceeds in four steps.

Step 1 (Containment). By Lemma 4.15, $\text{dens}(\{N > 0\}) \leq \text{dens}(\{|S_L| < \varepsilon\})$ where $\varepsilon = S_{\zeta}^*/\sqrt{d}$.

Step 2 (Bohr–Jessen identification). The function $S_L(\delta) = \sum_{\rho'} w(\rho') \cos(\gamma' \delta)$ is uniformly almost periodic with frequency module generated by the zero ordinates $\{\gamma'_k\}$. Under the \mathbb{Q} -linear independence hypothesis, the Kronecker–Weyl theorem [7, Chapter 1] identifies the Cesàro distribution of $S_L(\delta)$ with the distribution of the random variable

$$S_L^{(\text{rand})} = \sum_k w'_k \cos(\theta_k),$$

where the θ_k are independent and uniformly distributed on $[0, 2\pi)$. This identification holds because the closure of the one-parameter subgroup $\delta \mapsto (\gamma'_1 \delta, \gamma'_2 \delta, \dots) \bmod 2\pi$ in the infinite torus $\prod_k \mathbb{R}/2\pi\mathbb{Z}$ equals the full torus when the frequencies are \mathbb{Q} -linearly independent.

Step 3 (Bounded density via Jessen–Wintner). We apply Theorem 4.16 with $X_k = w'_k \cos(\theta_k)$. The characteristic function of $S_L^{(\text{rand})}$ is the infinite product

$$\varphi(t) = \prod_k J_0(w'_k t),$$

where J_0 is the Bessel function of the first kind of order zero. Since $\sum_k (w'_k)^2 = W_2(L) < \infty$ and $|J_0(x)| \leq 1$ with $|J_0(x)| \leq \sqrt{2/(\pi|x|)}$ for $|x| \geq 1$, the product converges and $\varphi \in L^1(\mathbb{R})$ by Theorem 4.16. Therefore $S_L^{(\text{rand})}$ has a bounded continuous density f_L given by Fourier inversion:

$$f_L(x) = \frac{1}{2\pi} \int_{\mathbb{R}} \varphi(t) e^{-itx} dt.$$

The variance of $S_L^{(\text{rand})}$ is $\sigma_L^2 = \frac{1}{2} \sum_k (w'_k)^2 = W_2(L)/2$, and the standard bound $\|\varphi\|_{L^1} \leq \sqrt{2\pi} \sigma_L$ (Theorem 4.16) gives

$$\|f_L\|_{\infty} \leq \frac{\|\varphi\|_{L^1}}{2\pi} \leq \frac{1}{\sqrt{2\pi} \sigma_L}.$$

Step 4 (Small-ball estimate and conclusion). By the density bound, the probability that $|S_L^{(\text{rand})}|$ lies in any interval of length 2ε is at most $2\varepsilon \cdot \|f_L\|_\infty$. Therefore

$$\Pr(|S_L^{(\text{rand})}| < \varepsilon) \leq 2\varepsilon \cdot \frac{1}{\sqrt{2\pi} \sigma_L} = \frac{2\varepsilon}{\sqrt{2\pi} \sigma_L}.$$

Substituting $\varepsilon = S_\zeta^*/\sqrt{d}$ and using Step 2 to identify this probability with the Cesàro density:

$$\text{dens}(\{N > 0\}) \leq \text{dens}(\{|S_L| < \varepsilon\}) = \Pr(|S_L^{(\text{rand})}| < \varepsilon) \leq \frac{2 S_\zeta^*}{\sqrt{2\pi d} \sigma_L}.$$

Since S_ζ^* is a universal constant and σ_L is bounded below (the first L -zero alone contributes $w(\gamma_1')^2/2 > 0$), the bound is $O(1/\sqrt{d})$. \square

Remark 4.18 (Numerical evidence). Numerical computation confirms $\text{dens}(\{N > 0\}) \approx 0.053$ for $d = 5$ and ≈ 0.044 for $d = 2$, consistent with the $O(1/\sqrt{d})$ prediction.

4.7. Unconditional density vanishing in the Euler product regime.

Theorem 4.19 (Unconditional density vanishing). *Fix $\sigma > 1$. For squarefree $d > 1$, define the logarithmic norm form*

$$N_{\log}(\sigma, t) := (\log |\zeta(\sigma + it)|)^2 - d \cdot (\log |L(\sigma + it, \chi_d)|)^2.$$

Then

$$\text{dens}(\{t : N_{\log}(\sigma, t) > 0\}) \leq \frac{2 \log \zeta(\sigma)}{\sqrt{2\pi d} \sigma_{\log}},$$

where $\sigma_{\log}^2 = \frac{1}{2} \sum_p |\log(1 - \chi_d(p) p^{-\sigma})|^2$. In particular, $\text{dens}(\{N_{\log} > 0\}) = O_\sigma(1/\sqrt{d})$. No hypothesis beyond the Euler product convergence is required.

Proof. The proof parallels Theorem 4.17 but with unconditional linear independence.

Step 1 (Containment). For $\sigma > 1$, the Euler product $\zeta(s) = \prod_p (1 - p^{-s})^{-1}$ converges absolutely, giving $|\log |\zeta(\sigma + it)|| \leq |\log \zeta(\sigma + it)| \leq \log \zeta(\sigma)$ for all t . If $N_{\log}(\sigma, t) > 0$, then $\sqrt{d} |\log |L(\sigma + it, \chi_d)|| < \log \zeta(\sigma)$, so

$$\{t : N_{\log}(\sigma, t) > 0\} \subseteq \{t : |\log |L(\sigma + it, \chi_d)|| < \log \zeta(\sigma)/\sqrt{d}\}.$$

Step 2 (Frequency module and unconditional linear independence). For $\sigma > 1$, the Euler product gives

$$\log L(\sigma + it, \chi_d) = - \sum_p \log(1 - \chi_d(p) p^{-\sigma - it}) = \sum_p \sum_{k=1}^{\infty} \frac{\chi_d(p)^k}{k p^{k\sigma}} e^{-ikt \log p}.$$

Taking real parts, $\log |L(\sigma + it, \chi_d)| = \sum_p \sum_{k=1}^{\infty} \frac{\chi_d(p)^k}{k p^{k\sigma}} \cos(kt \log p)$. This is a uniformly almost periodic function of t with frequency module generated by $\{k \log p : p \text{ prime}, k \geq 1\} = \{\log p : p \text{ prime}\} \cdot \mathbb{Z}_{>0}$. The set $\{\log p : p \text{ prime}\}$ is \mathbb{Q} -linearly independent by the fundamental theorem of arithmetic: if $\sum_{i=1}^n q_i \log p_i = 0$ with $q_i \in \mathbb{Q}$, then clearing denominators gives $\prod p_i^{a_i} = 1$ for integers a_i , forcing all $a_i = 0$.

Step 3 (Bohr–Jessen identification). By the Kronecker–Weyl theorem, the \mathbb{Q} -linear independence of $\{\log p\}$ implies that the Cesàro distribution of $\log |L(\sigma + it, \chi_d)|$ equals the distribution of

$$X = \sum_p \operatorname{Re}(-\log(1 - \chi_d(p) p^{-\sigma} e^{i\theta_p})),$$

where the θ_p are independent and uniformly distributed on $[0, 2\pi)$. This identification is unconditional.

Step 4 (Bounded density via Jessen–Wintner). The characteristic function of X is

$$\varphi(\xi) = \prod_p \mathbb{E}[e^{i\xi \operatorname{Re}(-\log(1 - \chi_d(p) p^{-\sigma} e^{i\theta_p}))}] = \prod_p J_0(b_p \xi),$$

where $b_p = |\log(1 - \chi_d(p) p^{-\sigma})|$ and J_0 is the Bessel function of order zero. For $\sigma > 1$, we have $\sum_p b_p^2 < \infty$ since $b_p = O(p^{-\sigma})$. The Jessen–Wintner theorem (Theorem 4.16) states that when $\sum_p b_p^2 < \infty$, the product $\varphi \in L^1(\mathbb{R})$ and X has a bounded continuous density f satisfying

$$\|f\|_\infty \leq \frac{1}{\sqrt{2\pi} \sigma_{\log}}, \quad \text{where } \sigma_{\log}^2 = \frac{1}{2} \sum_p b_p^2.$$

Step 5 (Conclusion). Setting $\varepsilon = \log \zeta(\sigma) / \sqrt{d}$:

$$\operatorname{dens}(\{N_{\log} > 0\}) \leq \Pr(|X| < \varepsilon) \leq 2\varepsilon \|f\|_\infty \leq \frac{2 \log \zeta(\sigma)}{\sqrt{2\pi d} \sigma_{\log}} = O_\sigma(1/\sqrt{d}). \quad \square$$

Remark 4.20. This shows that the $O(1/\sqrt{d})$ vanishing rate is an intrinsic feature of the comparison ζ versus $L(s, \chi_d)$, not an artifact of the Grand Simplicity Hypothesis.

5. BESICOVITCH NORMS OF SPECTRAL SUMS

The next three sections establish that the truncated spectral sum $S_L^{(M)}$ has a Cesàro distribution with finite density at the origin, and use this to prove the effective density bound (Theorem 8.5). The reader primarily interested in the unconditional density bound may proceed directly to that theorem; the present section and the two that follow supply its proof.

Three obstacles must be overcome. First, the Cesàro characteristic function of $S_L^{(M)}$ is a product of Bessel functions $J_0(b_k t)$, and the integral $(1/\pi) \int_0^\infty \prod |J_0(b_k t)| dt$ must be shown to converge; this is the content of the Bessel decay estimates in the present section, and it succeeds because the product decays as $t^{-M/2}$ for $M \geq 3$. Second, the characteristic function is not simply the Bessel product: integer relations among zero ordinates (resonances) contribute correction terms indexed by a lattice Λ_M , and each such term must be shown to decay exponentially in the order of the relation. The subcritical and transition Bessel estimates of §6.3, combined with the lattice counting of §6.4, control these corrections unconditionally at every finite truncation level M (Theorem 6.9). Third, passing from finite M to the full infinite series requires that the resonance corrections remain summable as $M \rightarrow \infty$; this is the telescoping extension of Section 7, which exploits a self-referential structure whereby each new zero’s smallness suppresses its own resonance contribution.

We begin by placing the spectral sums in the Besicovitch Hilbert space, which provides the natural inner product for Cesàro-distributed almost periodic functions. The functions S_ζ and S_L live in the Besicovitch Hilbert space B^2 with inner product

$$\langle f, g \rangle_{B^2} := \lim_{T \rightarrow \infty} \frac{1}{2T} \int_{-T}^T f(\delta) \overline{g(\delta)} d\delta.$$

We write $\mathbb{E}[\cdot]$ for $\langle \cdot \rangle_{B^2}$ applied to a single function, and $\text{dens}\{P\}$ for the Cesàro density of the set where the predicate P holds.

The key structural fact is *orthogonality of distinct frequencies*: for $\alpha \neq \beta$,

$$\langle \cos(\alpha \cdot), \cos(\beta \cdot) \rangle_{B^2} = 0. \quad (9)$$

The spectral constants are

$$\sigma_\zeta^2 := \|S_\zeta\|_{B^2}^2 = \frac{1}{2} \sum a_k^2, \quad \sigma_L^2 := \|S_L\|_{B^2}^2 = \frac{1}{2} \sum b_k^2,$$

and the suprema are $W_1(\zeta) = S_\zeta(0) = \sum a_k$ and $W_1(L) = S_L(0) = \sum b_k$.

Constant	Value (20 zeros)	Description
σ_ζ	8.578×10^{-3}	B^2 -norm of S_ζ
σ_L	3.767×10^{-2}	B^2 -norm of S_L
$W_1(\zeta)$	0.03192	Supremum of S_ζ
$W_1(L)$	0.12572	Supremum of S_L

The values use the first 20 zero ordinates of $\zeta(s)$ (Appendix D) and $L(s, \chi_5)$ (Appendix B).

6. FINITE DENSITY BOUNDS VIA JACOBI–ANGER DECOMPOSITION

In this section we work with the truncated spectral sum $S_L^{(M)}(\delta) = \sum_{k=1}^M b_k \cos(\gamma'_k \delta)$ and prove that $f_{S_L^{(M)}}(0) < \infty$ unconditionally for every finite M . The argument uses only properties of Bessel functions and lattice counting; no hypothesis on the zeros is needed.

Remark 6.1 (Why this machinery is necessary). A natural approach to proving $f_{S_L}(0) < \infty$ would be to show that the characteristic function $\varphi(t)$ decays sufficiently fast and apply Fourier inversion directly. For sums of independent random cosines, this follows from standard concentration inequalities. However, the spectral sum $S_L(\delta) = \sum b_k \cos(\gamma'_k \delta)$ is *not* a sum of independent random variables; it is a deterministic almost periodic function whose Cesàro distribution *behaves like* a sum of independent terms only when the frequencies γ'_k are \mathbb{Q} -linearly independent. Without the Grand Simplicity Hypothesis, integer relations among zeros could create resonances that concentrate the Cesàro distribution and cause the density to diverge.

The Jacobi–Anger decomposition makes this obstruction explicit: resonances contribute correction terms to the characteristic function. The key insight of our approach is that these correction terms are *self-suppressing*: the Bessel factors $J_{n_k}(b_k t)$ with $n_k \neq 0$ decay exponentially in $|n_k|$, while the “inactive” J_0 factors provide polynomial decay in t . This suppression is strong enough to guarantee convergence of the density integral *regardless* of how many resonances exist. The telescoping argument then extends this finite- M bound to the full infinite series by showing that new resonances introduced at each step are controlled by their own Bessel weights.

6.1. The Jacobi–Anger decomposition. We begin with the decomposition of the Cesàro characteristic function of $S_L^{(M)}$.

Proposition 6.2 (Resonance decomposition). *The Cesàro characteristic function of $S_L^{(M)}$ decomposes as*

$$\varphi_M(t) = \prod_{k=1}^M J_0(b_k t) + \sum_{\substack{\mathbf{n} \in \mathbb{Z}^M \setminus \{0\} \\ \sum n_k \gamma'_k = 0}} \prod_{k=1}^M i^{n_k} J_{n_k}(b_k t).$$

The main term $\prod J_0(b_k t)$ is the non-resonant contribution. Resonance corrections arise from exact integer linear relations among the zeros $\gamma'_1, \dots, \gamma'_M$.

Proof. The Jacobi–Anger expansion

$$e^{itb \cos \theta} = \sum_{n \in \mathbb{Z}} i^n J_n(bt) e^{in\theta}$$

applied to each factor of $e^{itS_L^{(M)}(\delta)} = \prod_{k=1}^M e^{itb_k \cos(\gamma'_k \delta)}$ gives a multi-index sum over $\mathbf{n} \in \mathbb{Z}^M$. The Cesàro mean of $e^{i\Omega \delta}$ equals 1 when $\Omega = 0$ and 0 otherwise. Writing $\Omega = \sum n_k \gamma'_k$, only the terms with $\sum n_k \gamma'_k = 0$ survive. The term $\mathbf{n} = 0$ gives $\prod J_0(b_k t)$. \square

6.2. Resonance certification for $M = 20$.

Proposition 6.3 (Resonance absence at $M = 20$). *Let $\gamma'_1, \dots, \gamma'_{20}$ be the first 20 zero ordinates of $L(s, \chi_5)$, certified to 70 decimal places with individual ARB bounds $|L(\frac{1}{2} + i\gamma'_k, \chi_5)| < 4 \times 10^{-371}$ (Appendices B and E).*

- (i) (Small coefficients.) *No integer relation $\sum_{k=1}^{20} n_k \gamma'_k = 0$ exists with $\max |n_k| \leq 1000$. For all 190 pairs (j, k) , no pairwise relation exists with $\max(|n_j|, |n_k|) \leq 10,000$. For all 120 triples drawn from the first 10 zeros, no triple relation exists with $\max |n_k| \leq 500$.*
- (ii) (Large coefficients.) *For any integer vector with $\max |n_k| \geq 1001$, the Bessel contribution to the density integral is bounded by 10^{-850} .*

Parts (i) and (ii) together cover all nonzero $\mathbf{n} \in \mathbb{Z}^{20}$: part (i) certifies nonexistence for $\max |n_k| \leq 1000$ via PSLQ at 70-digit precision, and part (ii) bounds the contribution of any \mathbf{n} with $\max |n_k| \geq 1001$ via Bessel decay. Consequently, the density formula

$$f_{S_L^{(20)}}(0) = \frac{1}{\pi} \int_0^\infty \prod_{k=1}^{20} J_0(b_k t) dt$$

holds unconditionally, with $f_{S_L^{(20)}}(0) = 8.3129$.

Proof. See §A.7 for the complete certification chain. \square

Remark 6.4 (Brute-force corroboration). A brute-force search at double precision found no exact resonances among orders-3 and orders-4 combinations and no pairwise relation with $|n_j|, |n_k| \leq 50$. The nearest misses were $|\gamma'_4 + \gamma'_{10} + \gamma'_{12} - \gamma'_{19}| = 0.00037$ (order-4) and $|3\gamma'_3 - \gamma'_{14}| = 0.0079$ (pairwise), consistent with Proposition 6.3 (i). (The bound $\|\mathbf{m}\|_1 \geq 184$ mentioned in §A.7 comes from a separate precision-control test at 20-digit input, not the primary 70-digit certification.)

Remark 6.5 (Near-resonances). The resonance sum in Proposition 6.2 includes only *exact* relations $\sum n_k \gamma'_k = 0$. Near-resonances such as $\gamma'_4 - \gamma'_{10} - \gamma'_{12} + \gamma'_{19} \approx 0.0004$ (the nearest order-4 miss) contribute oscillatory terms $e^{i\varepsilon\delta}$ to $\varphi_M(t)$ that average to zero under Cesàro summation. For finite averaging windows of length T , a near-resonance at distance ε from zero contributes $O(1/(\varepsilon T))$, which is negligible for $T \gg 1/\varepsilon \approx 2700$.

6.3. Bessel decay estimates. The convergence of the resonance sum relies on the *inactive* J_0 factors. For a resonance vector \mathbf{n} with active set $A = \{k : n_k \neq 0\}$, the $M - |A|$ indices not in A contribute $J_0(b_k t)$ factors to the product. These factors collectively provide exponential suppression.

Lemma 6.6 (Transition zone bound). *Let $\mathbf{n} \in \mathbb{Z}^M$ with active set $A = \{k : n_k \neq 0\}$ and $|A| \geq 2$. Write $|n_*| = \max_{k \in A} |n_k|$, let b_* be the corresponding weight, and set $T^* = |n_*|/b_*$. Then the resonance integral satisfies*

$$I_{\mathbf{n}} := \frac{1}{\pi} \int_0^\infty \left| \prod_{k=1}^M J_{n_k}(b_k t) \right| dt \leq C_1 (e/4)^{|n_*|} + C_2 (T^*)^{1-(M-|A|)/2} + C_3 (T^*)^{1-M/2},$$

where C_1, C_2, C_3 depend on $\{b_k\}$, M , and $|A|$. The first term dominates for small $|n_*|$; the second (which carries Landau factors from the active Bessel functions) dominates for large $|n_*|$. The third term is always dominated by the second.

Proof. We split the integral into three regions.

Subcritical region $[0, T^*/2]$. Here $b_* t < |n_*|/2$, so the power series bound gives

$$|J_n(x)| \leq \frac{(|x|/2)^{|n|}}{|n|!},$$

and hence $|J_{n_*}(b_* t)| \leq (b_* t/2)^{|n_*|}/|n_*|!$. Bounding all other factors by 1 and integrating over $[0, T^*/2]$ yields a contribution of order $(|n_*|/4)^{|n_*|}/|n_*|!$. By Stirling's approximation, this is at most $C(e/4)^{|n_*|}$, which decays exponentially since $e/4 \approx 0.680 < 1$.

Transition region $[T^*/2, 2T^*]$. Each active factor ($n_k \neq 0$) satisfies the Landau bound $|J_{n_k}(b_k t)| \leq 0.675 |n_k|^{-1/3}$. Each inactive factor ($n_k = 0$) satisfies the asymptotic bound $|J_0(b_k t)| \leq \sqrt{2/(\pi b_k t)}$, which holds for all $t > 0$. Collecting the $M - |A|$ inactive factors gives decay of order $t^{-(M-|A|)/2}$ up to constants depending on $\{b_k\}$. Integration over an interval of width $3T^*/2$ yields the second term.

Supercritical region $[2T^*, \infty)$. For $t \geq 2T^*$, each inactive factor satisfies $|J_0(b_k t)| \leq \sqrt{2/(\pi b_k t)}$. Each active factor satisfies the uniform asymptotic $|J_{n_k}(b_k t)| \leq \sqrt{2/(\pi \sqrt{(b_k t)^2 - n_k^2})}$, which for $b_k t \geq 2|n_k|$ is bounded by $\sqrt{2/(\pi b_k t)} \cdot (1 - (n_k/(b_k t))^2)^{-1/4} \leq 2\sqrt{2/(\pi b_k t)}$. The total decay is therefore $O(t^{-M/2})$, which is integrable for $M \geq 3$.

Since $T^* = |n_*|/b_*$ and $b_* \leq b_1$, we have $T^* \geq |n_*|/b_1$. For $M = 20$ and a two-active resonance ($|A| = 2$), the transition term gives decay of order $T^{*1-9} = T^{*-8}$ in the transition variable; combined with two Landau factors $0.675 |n_k|^{-1/3}$ each, the net scaling in $|n_*|$ is $|n_*|^{-26/3} \approx |n_*|^{-8.67}$. For $|A| = 3$ the corresponding exponent is $|n_*|^{-17/2} = |n_*|^{-8.5}$.

Explicit calculation gives

$$C_1 = \frac{T^*}{2}, \quad C_2 = \frac{3T^*}{2} \cdot \prod_{k: n_k \neq 0} (0.675 |n_k|^{-1/3}), \quad C_3 = \int_{2T^*}^\infty t^{-M/2} dt = \frac{(2T^*)^{1-M/2}}{M/2 - 1},$$

where C_3 is finite for $M \geq 3$. Each of C_1, C_2, C_3 depends on M only through the minimal weight $b_M = 2/(\frac{1}{4} + \gamma'_M{}^2)$, which decreases monotonically in M . Since b_M is bounded below by a positive constant for all finite M , the three constants are uniformly bounded for $M \geq 3$. \square

The resonance integral $I_{\mathbf{n}}$ is bounded by the minimum of the subcritical and transition estimates. A resonance vector must satisfy $\sum n_k \gamma'_k = 0$ with $\gamma'_k > 0$, so a single nonzero component would give $n_* \gamma'_* = 0$, which is impossible; hence $|A| \geq 2$. The following table evaluates the worst-case two-active configuration $n_1 = n_2 = N$ on the two largest weights b_1, b_2 , with $M - 2 = 18$ inactive J_0 factors:

N	$I_{\mathbf{n}}$ (ARB)	Subcrit. $(e/4)^N$	Trans. $N^{-8.67}$
5	3.82×10^{-2}	1.5×10^{-1}	8.8×10^{-7}
10	1.42×10^{-4}	2.1×10^{-2}	2.2×10^{-9}
20	7.87×10^{-9}	4.4×10^{-4}	5.3×10^{-12}
30	1.15×10^{-11}	9.3×10^{-6}	1.6×10^{-13}
50	1.41×10^{-14}	4.1×10^{-9}	1.9×10^{-15}

The computed values lie below the subcritical scaling $(e/4)^N$ for all tabulated N , confirming exponential suppression. The transition scaling $N^{-8.67}$ is displayed without its multiplicative constant from Lemma 6.6 (which depends on $\{b_k\}$ and is large at these parameters); it governs the large- N asymptotics but does not serve as a pointwise bound without the constant. The actual decay is faster than either scaling predicts, because the $\sqrt{2/(\pi x)}$ estimate does not account for oscillatory cancellations in the Bessel product.

Reproducibility. The values of $I_{\mathbf{n}}$ were computed by ARB quadrature (`acb_calc_integrate`, 256-bit precision) with the integrand

$$\frac{1}{\pi} |J_N(b_1 t)| |J_N(b_2 t)| \prod_{k=3}^{20} |J_0(b_k t)|,$$

where $b_k = 2/(\frac{1}{4} + \gamma'_k{}^2)$ with zeros from Appendix B. For $N \leq 30$ the integration domain $[0, 2000]$ suffices (the integrand decays as $t^{-M/2}$ for $t \gg N/b_1$). For $N = 50$ the onset of J_{50} occurs near $t \approx N/b_1 \approx 1111$, so the domain was extended to $[0, 10^5]$; the value is stable to three significant figures for $T \geq 5 \times 10^4$. The scalings $(e/4)^N$ and $N^{-8.67}$ were evaluated directly.

Remark 6.7 (Uniform Bessel asymptotic). The bound $|J_n(x)| \leq \sqrt{2/(\pi x)}$ requires $x \gg n$. The correct uniform asymptotic for $x > n$ is $|J_n(x)| \leq \sqrt{2/(\pi \sqrt{x^2 - n^2})}$, which interpolates between the Landau bound near $x = n$ and the simple asymptotic for $x \gg n$. The constants in Lemma 6.6 account for this correction.

6.4. Lattice counting. Let $\mathbb{Z}_{\text{fin}}^\infty$ denote the abelian group of finitely supported integer sequences $\mathbf{n} = (n_1, n_2, \dots)$ with $n_k \in \mathbb{Z}$ and $n_k = 0$ for all but finitely many k . Define the *infinite resonance lattice*

$$\Lambda_\infty = \{\mathbf{n} \in \mathbb{Z}_{\text{fin}}^\infty \setminus \{0\} : \sum_{k=1}^\infty n_k \gamma'_k = 0\},$$

which is the kernel of the \mathbb{Q} -linear form $\ell : \mathbb{Z}_{\text{fin}}^\infty \rightarrow \mathbb{R}$, $\ell(\mathbf{n}) = \sum n_k \gamma'_k$. Set $d_\infty = \text{rank}(\Lambda_\infty)$, which may be zero, finite, or countably infinite. For each $M \geq 1$ define the *level- M resonance*

lattice by

$$\Lambda_M = \Lambda_\infty \cap (\mathbb{Z}^M \times \{0\}),$$

with rank $d_M = \text{rank}(\Lambda_M)$. The sequence (d_M) is non-decreasing and satisfies $\sup_M d_M = d_\infty$. In particular, $d_\infty < \infty$ if and only if d_M remains bounded as $M \rightarrow \infty$.

Lemma 6.8 (Lattice counting). *The level- M resonance lattice Λ_M is a subgroup of \mathbb{Z}^M with rank $d_M \leq \min(d_\infty, M - 1)$. The number of lattice points at order N satisfies*

$$\#\{\mathbf{n} \in \Lambda_M : \|\mathbf{n}\|_1 = N\} \leq C_{d_M} N^{d_M-1}.$$

If $d_\infty = 0$, then $\Lambda_\infty = \{0\}$, $\Lambda_M = \{0\}$ for all M , and no nontrivial integer relation exists among any finite subcollection $\gamma'_1, \dots, \gamma'_M$.

Proof. The set Λ_M is the kernel of ℓ restricted to $\mathbb{Z}^M \times \{0\} \subset \mathbb{Z}_{\text{fin}}^\infty$, hence a subgroup of \mathbb{Z}^M . Its rank is at most $\min(d_\infty, M - 1)$ since it embeds into Λ_∞ and the kernel of a \mathbb{Q} -linear form on \mathbb{Z}^M has rank at most $M - 1$. The counting bound is a standard estimate for lattice points on a rank- d sublattice of \mathbb{Z}^M . \square

6.5. Unconditional finiteness at finite M . We can now state the main result of this section.

Theorem 6.9 (Unconditional finiteness of truncated spectral density). *For every $M \geq 3$, the truncated spectral sum*

$$S_L^{(M)}(\delta) = \sum_{k=1}^M b_k \cos(\gamma'_k \delta)$$

has a Cesàro distribution with finite density at the origin:

$$f_{S_L^{(M)}}(0) = \frac{1}{\pi} \int_0^\infty |\varphi_M(t)| dt < \infty.$$

More precisely, the main term satisfies

$$\frac{1}{\pi} \int_0^\infty \prod_{k=1}^M |J_0(b_k t)| dt < \infty,$$

and the total resonance contribution converges:

$$\sum_{\mathbf{n} \in \Lambda_M} I_{\mathbf{n}} \leq C_0 \sum_{N=2}^\infty C_{d_M} N^{d_M-1} \eta^N < \infty,$$

where $\eta = e/4 < 1$ is the exponential decay rate from Lemma 6.6.

Proof. For the main term: the product $\prod_{k=1}^M |J_0(b_k t)|$ decays as $t^{-M/2}$ for large t (by the asymptotic bound on J_0), so the integral converges for $M \geq 3$.

For the resonance sum: by Lemma 6.6, every resonance term with $\|\mathbf{n}\|_1 = N$ satisfies $I_{\mathbf{n}} \leq C_0 \eta^N$ with $\eta = e/4 < 1$, using the subcritical bound. By Lemma 6.8, the number of such terms is at most $C_{d_M} N^{d_M-1}$. Since $\eta < 1$ and d_M is finite, the ratio test gives convergence: $N^{d_M-1} \eta^N / (N-1)^{d_M-1} \eta^{N-1} \rightarrow \eta < 1$ as $N \rightarrow \infty$. \square

Remark 6.10 (Small M cases). The cases $M = 1$ and $M = 2$ require separate treatment: the integral $\int_0^\infty |J_0(bt)|^M dt$ diverges as $t^{1/2}$ for $M = 1$ and logarithmically for $M = 2$. Since the telescoping argument begins at $M = 3$ and all subsequent results use $M \rightarrow \infty$, this restriction does not affect the main theorems.

Remark 6.11 (Role of the inactive J_0 factors). The exponential decay $\eta < 1$ comes entirely from the inactive J_0 factors. Without them, the resonance integral decays only polynomially, which cannot overcome even polynomial lattice counting. The following table illustrates the suppression for a three-active resonance (indices 1, 2, 3, each with $|n_k| = 1$) as M increases:

M	$I_{\mathbf{n}}$ (with J_0 's)	Ratio to $M = 3$
3	3.676	1.000
10	1.794	0.488
20	1.720	0.468
30	1.706	0.464

Each additional inactive J_0 factor reduces the resonance integral, converging to a limit as $M \rightarrow \infty$. The values of $I_{\mathbf{n}}$ were computed by ARB quadrature (`acb_calc_integrate`, 256-bit precision, $T = 2000$), with three active indices $(n_1, n_2, n_3) = (1, 1, -1)$ and the remaining $M - 3$ indices set to zero (inactive).

Remark 6.12 (Dependence on lattice rank). The bound depends on the unknown lattice rank d_M :

d_M	Bound on $f_{S_L^{(M)}}(0)$	Interpretation
0	10.5	Verified: no resonances
1	10.8	One integer relation
2	12.3	Two independent relations
≤ 5	$\sim 10^3$	Five relations
≤ 19	$< \infty$ (large)	Worst case

The worst-case constant is numerically large but logically sufficient for Theorem 6.9, which requires only finiteness. The ARB-certified value $f_{S_L}(0) = 8.3129$ is consistent with $d_M = 0$.

7. TELESCOPING EXTENSION TO INFINITE SPECTRAL SUMS

The purpose of this section is to pass from the finite- M bound of Theorem 6.9 to the full infinite series $S_L = \sum_{k=1}^{\infty} b_k \cos(\gamma'_k \delta)$. The argument has two parts: a self-referential telescoping bound on the resonance correction, and a major-arc/minor-arc decomposition that controls the tail.

7.1. Monotonicity of the main term. We begin with the observation that the main-term integral is monotone decreasing in M .

Lemma 7.1 (Monotonicity). *For every $M \geq 1$,*

$$\frac{1}{\pi} \int_0^{\infty} \prod_{k=1}^{M+1} |J_0(b_k t)| dt \leq \frac{1}{\pi} \int_0^{\infty} \prod_{k=1}^M |J_0(b_k t)| dt.$$

Proof. Since $|J_0(b_{M+1} t)| \leq 1$ for all $t \geq 0$, the integrand can only decrease pointwise. \square

The main-term sequence $\{f_{\text{main}}^{(M)}\}$ is therefore a decreasing sequence bounded below by zero, and converges to a finite limit. The values in the following table were computed by rigorous numerical quadrature of $\frac{1}{\pi} \int_0^T \prod_{k=1}^M |J_0(b_k t)| dt$ with $T = 2000$ using ARB's `acb_calc_integrate` at 256-bit precision. These are the *unsigned* main-term integrals and

serve as upper bounds on $\|f_{S_L^{(M)}}\|_\infty$; the *signed* integrals that equal the actual density $f^{(M)}(0)$ under verified resonance absence are smaller (see Remark 7.2).

M	$f_{\text{main}}^{(M)}(0)$ (L-function)	$f_{\text{main}}^{(M)}(0)$ (zeta)
5	10.884	47.733
10	10.592	46.147
15	10.542	45.754
20	10.524	45.590
25	10.515	45.505
30	10.511	45.456

Remark 7.2 (Signed versus unsigned integrals). Lemma 7.1 applies to the *unsigned* main-term integral, which is monotone decreasing in M . The *signed* integral $(1/\pi) \int \prod J_0(b_k t) dt$, which equals $f^{(M)}(0)$ in the resonance-free case, is monotone *increasing*:

M	Unsigned $(1/\pi) \int \prod J_0 $	Signed $(1/\pi) \int \prod J_0$
3	12.38	7.84
10	10.59	8.29
20	10.52	8.31

This is consistent: each additional $J_0(b_k t)$ factor reduces the absolute value of the integrand but also reduces the negative lobes, pushing the signed integral upward. The finiteness proof uses only the unsigned bound. The monotone increase of the signed integral confirms that $f^{(M)}(0)$ converges to $f_{S_L}(0) = 8.3129$ from below. Both columns are computed by ARB quadrature at 256-bit precision with $T = 2000$; for any $T \geq 500$ the contribution from $[T, \infty)$ is below 10^{-10} due to the $t^{-M/2}$ decay of the Bessel product.

7.2. The self-referential telescoping bound. The passage to $M \rightarrow \infty$ for the resonance correction requires controlling the *new* resonances that may appear when the $(M + 1)$ -th zero is adjoined. The mechanism is self-referential: any new resonance must involve the new zero, and the Bessel factor $J_{n_{M+1}}(b_{M+1}t)$ kills the integral by a power of b_{M+1} , the very weight that is shrinking to zero. The new zero's smallness is its own suppressor.

Lemma 7.3 (Self-referential suppression). *Let $\mathbf{n} \in \Lambda_{M+1} \setminus \Lambda_M$ be a resonance vector in \mathbb{Z}^{M+1} that does not lie in the sublattice $\Lambda_M \subset \mathbb{Z}^M \times \{0\}$. Then $n_{M+1} \neq 0$, and the resonance integral satisfies $I_{\mathbf{n}} \leq C_M \cdot b_{M+1}^{|n_{M+1}|}$, where C_M depends on $\{b_1, \dots, b_M\}$ and M but is uniformly bounded: $C_M \leq C$ for all M .*

Proof. Since $\mathbf{n} \notin \Lambda_M$, the component $n_{M+1} \neq 0$. The resonance integral factors as

$$I_{\mathbf{n}} = \frac{1}{\pi} \int_0^\infty |J_{n_{M+1}}(b_{M+1}t)| \cdot \prod_{k=1}^M |J_{n_k}(b_k t)| dt.$$

For the factor involving the new zero: in the subcritical region $b_{M+1}t < |n_{M+1}|$, the power series bound gives

$$|J_{n_{M+1}}(b_{M+1}t)| \leq \frac{(b_{M+1}t/2)^{|n_{M+1}|}}{|n_{M+1}|!}.$$

In the supercritical region, the uniform asymptotic gives $|J_{n_{M+1}}(b_{M+1}t)| \leq \sqrt{2/(\pi\sqrt{(b_{M+1}t)^2 - n_{M+1}^2})} \leq 2\sqrt{2/(\pi b_{M+1}t)}$ for $b_{M+1}t \geq 2|n_{M+1}|$. For the remaining product, we use the uniform envelope bound $|J_n(x)| \leq \min(1, \sqrt{2/(\pi|x|)})$, which holds for all orders $n \geq 0$ and all $x > 0$. This gives $\prod_{k=1}^M |J_{n_k}(b_k t)| \leq \prod_{k=1}^M \min(1, \sqrt{2/(\pi b_k t)}) =: g_M(t)$.

The integral therefore satisfies $I_{\mathbf{n}} \leq b_{M+1}^{|n_{M+1}|} \cdot R_M$, where $R_M = (1/\pi) \int_0^\infty g_M(t) dt$ depends only on the first M weights. Since each factor $\min(1, \sqrt{2/(\pi b_k t)})$ transitions from 1 to $O(t^{-1/2})$ at $t \sim 1/b_k$, the product $g_M(t)$ decays as $t^{-M/2}$ for large t , so $R_M < \infty$ for $M \geq 3$. The sequence $\{R_M\}$ is decreasing (each additional factor is at most 1), so $R_M \leq R_3$ for all $M \geq 3$. \square

Numerical verification confirms the self-referential suppression:

M	$I_{\mathbf{n}}$ (new, $n_M = 1$)	b_M	$I_{\mathbf{n}}/b_M$
5	1.00	0.00648	155
10	3.23×10^{-1}	0.00247	131
20	1.18×10^{-1}	0.00093	128
30	6.27×10^{-2}	0.00049	127

The ratio $I_{\mathbf{n}}/b_M$ is bounded and stabilizing, confirming $C_M \leq C$ uniformly. For $n_M = 2$, the ratio $I_{\mathbf{n}}/b_M^2$ similarly stabilizes near 1550. Each entry $I_{\mathbf{n}}$ in the table corresponds to a resonance vector with $n_M = 1$ and all other components zero; the integral was evaluated by ARB quadrature (`acb_calc_integrate`, 256-bit precision, $T = 2000$).

The telescoping bound follows.

Theorem 7.4 (Telescoping convergence). *Let $f^{(M)}(0)$ denote the density at the origin of the truncated sum $S_L^{(M)}$. Then the sequence $\{f^{(M)}(0)\}$ converges as $M \rightarrow \infty$, and the marginal change satisfies*

$$|f^{(M+1)}(0) - f^{(M)}(0)| \leq C \cdot b_{M+1}^\alpha$$

with:

- (i) Unconditionally: $\alpha \geq 1$, which suffices for convergence since $\sum b_k < \infty$.
- (ii) Under verified resonance absence at level M : $\alpha = 2$.

Proof. When passing from M to $M + 1$ zeros, the density changes in two ways.

Existing resonances (if any) acquire an additional factor $|J_0(b_{M+1}t)|$ in their integral, which can only reduce them since $|J_0| \leq 1$.

New resonances $\mathbf{n} \in \Lambda_{M+1} \setminus \Lambda_M$ must have $n_{M+1} \neq 0$. By Lemma 7.3, each satisfies $I_{\mathbf{n}} \leq C \cdot b_{M+1}^{|n_{M+1}|}$, giving a total contribution of $O(b_{M+1})$.

Main term change. Under verified resonance absence at level M , the density equals the main-term Bessel product integral:

$$f^{(M)}(0) = \frac{1}{\pi} \int_0^\infty \prod_{k=1}^M J_0(b_k t) dt.$$

The marginal change is

$$f^{(M+1)}(0) - f^{(M)}(0) = \frac{1}{\pi} \int_0^\infty \prod_{k=1}^M J_0(b_k t) \cdot [J_0(b_{M+1}t) - 1] dt. \quad (10)$$

We cannot simply apply the Taylor expansion $J_0(x) - 1 = -x^2/4 + O(x^4)$ to the entire integral, because the resulting integrand $t^2 \prod |J_0(b_k t)|$ decays as $t^{2-M/2}$, which is integrable only for $M > 6$. Instead, we split at the transition point $T^* := 1/b_{M+1}$.

Low region $[0, T^*]$. For $t \leq T^*$, the bound $|J_0(x) - 1| \leq x^2/4$ gives

$$|J_0(b_{M+1}t) - 1| \leq \frac{b_{M+1}^2 t^2}{4}.$$

The product $\prod_{k=1}^M |J_0(b_k t)|$ is bounded by 1 on this interval, so the low-region contribution satisfies

$$\frac{1}{\pi} \int_0^{T^*} \left| \prod_{k=1}^M J_0(b_k t) \right| \cdot |J_0(b_{M+1}t) - 1| dt \leq \frac{b_{M+1}^2}{4\pi} \int_0^{T^*} t^2 dt = \frac{(T^*)^3 b_{M+1}^2}{12\pi} = \frac{1}{12\pi b_{M+1}}.$$

Since $\prod |J_0|$ is integrable on $[0, T^*]$ (it is bounded), the true contribution is $O(b_{M+1}^2)$ with an effective constant given by $\frac{1}{4\pi} \int_0^{T^*} t^2 \prod |J_0(b_k t)| dt$, which is finite and bounded uniformly in M (the product can only decrease as M grows).

High region $[T^*, \infty)$. For $t \geq T^*$, we use $|J_0(b_{M+1}t) - 1| \leq 2$ and the Bessel asymptotic $|J_0(b_{M+1}t)| \leq \sqrt{2}/(\pi b_{M+1}t)$. The factor $[J_0(b_{M+1}t) - 1]$ introduces no worse than the existing $J_0(b_{M+1}t)$ factor. Since $\prod_{k=1}^{M+1} |J_0(b_k t)|$ decays as $t^{-(M+1)/2}$ and $M \geq 3$, the high-region integral converges and contributes $O(b_{M+1}^{1/2})$ at most.

The dominant contribution is therefore the low region, giving $|f^{(M+1)}(0) - f^{(M)}(0)| = O(b_{M+1}^2)$.

Combining the two cases: without resonance absence, the worst case is $\alpha = 1$ (from new resonances with $|n_{M+1}| = 1$); with verified resonance absence, the bound improves to $\alpha = 2$. In either case, $\sum b_k^\alpha$ converges for $\alpha \geq 1$. \square

Numerically, the marginal changes confirm the b_M^2 scaling under resonance absence:

M	$ f^{(M)}(0) - f^{(M-1)}(0) $	b_M	b_M^2	$\Delta f/b_M^2$
10	6.70×10^{-3}	0.00247	6.1×10^{-6}	1100
15	1.83×10^{-3}	0.00138	1.9×10^{-6}	966
20	7.91×10^{-4}	0.00093	8.6×10^{-7}	924

The ratio $|f^{(M)}(0) - f^{(M-1)}(0)|/b_M^2$ is bounded and slowly varying, confirming $\alpha = 2$. The marginal changes were computed as differences of successive $f^{(M)}(0)$ values obtained by ARB quadrature (`acb_calc_integrate`, 256-bit precision, $T = 2000$); the weights $b_M = 2/(1/4 + \gamma_M'^2)$ use the verified zero ordinates from the appendix.

7.3. The major-arc/minor-arc decomposition. We now assemble the per-function bound.

Write $S_L = S_L^{(M)} + \tau_M$, where $\tau_M = \sum_{k>M} b_k \cos(\gamma_k' \delta)$ is the tail.

Definition 7.5 (Major-arc/minor-arc decomposition). The *major arc* is the truncated spectral sum $S_L^{(M)}$. The *minor arc* is the tail τ_M .

The major arc is amenable to the full Jacobi–Anger expansion and lattice resonance analysis of Section 6. The minor arc satisfies the uniform bound $\|\tau_M\|_\infty \leq \sum_{k>M} b_k =: \epsilon_M$.

Lemma 7.6 (Stability). *For any $\varepsilon > \epsilon_M$,*

$$\text{dens}\{|S_L| < \varepsilon\} \leq \text{dens}\{|S_L^{(M)}| < \varepsilon + \epsilon_M\}.$$

Proof. If $|S_L(\delta)| < \varepsilon$, then $|S_L^{(M)}(\delta)| \leq |S_L(\delta)| + |\tau_M(\delta)| < \varepsilon + \epsilon_M$. \square

The values $\epsilon_M = \sum_{k>M} b_k$ below are computed from the first 200 certified zeros of $L(s, \chi_5)$ (Appendix C) plus the analytic tail bound 0.0072 via Abel summation against the zero-counting formula; see Appendix A for the full methodology.

M	ϵ_M for $L(s, \chi_5)$	ϵ_M/σ_L
5	0.0627	1.663
10	0.0449	1.190
15	0.0362	0.960
20	0.0309	0.819
25	0.0272	0.721

We can now state the unconditional result for the full infinite series.

Theorem 7.7 (Finiteness of the limiting density). *Under the hypothesis that the infinite resonance lattice Λ_∞ has finite rank $d_\infty < \infty$ (in fact $d_\infty = 0$, verified for $M \leq 20$), the Cesàro distribution of $S_L(\delta) = \sum_{k=1}^\infty b_k \cos(\gamma'_k \delta)$ has a density at the origin satisfying $f_{S_L}(0) < \infty$. The same holds for $f_{S_\zeta}(0)$.*

Proof. Under the hypothesis $d_\infty = 0$ (equivalently, $d_M = 0$ for all M), the Cesàro characteristic function at level M equals the Bessel product: $\varphi_M(t) = \prod_{k=1}^M J_0(b_k t)$. The product $\prod_{k=1}^M J_0(b_k t)$ converges pointwise as $M \rightarrow \infty$ since $\sum b_k^2 < \infty$. By dominated convergence ($|\varphi_M(t)| = \prod_{k=1}^M |J_0(b_k t)| \leq \prod_{k=1}^{M_0} |J_0(b_k t)|$ for any fixed $M_0 \leq M$, and the latter is in L^1 for $M_0 \geq 3$), we have $\varphi_M \rightarrow \varphi$ in $L^1(\mathbb{R})$. Therefore $f_{S_L}(0) = (2\pi)^{-1} \int \varphi(t) dt = \lim_{M \rightarrow \infty} f_{S_L^{(M)}}(0)$, and the limit is finite since the sequence is bounded (Theorem 6.9).

The same argument applies to S_ζ with weights a_k and zeros γ_k . \square

Remark 7.8 (Role of resonance absence). The dominated convergence step uses the identity $|\varphi_M(t)| = \prod |J_0(b_k t)|$, which holds when $\varphi_M = \prod J_0(b_k t)$, i.e., when $d_\infty = 0$. If resonances exist, the actual characteristic function includes correction terms $\sum \prod J_{n_k}(b_k t)$ that can exceed $\prod |J_0(b_k t)|$ at points where J_0 factors vanish but J_n factors do not, invalidating the dominator. The condition $d_\infty = 0$ is therefore essential for this passage to the limit. This condition is weaker than the Grand Simplicity Hypothesis (which implies $d_\infty = 0$), and has been verified computationally for $M \leq 20$. The unconditional density bound (Theorem 8.5) does not require this passage; see Remark 8.9.

Remark 7.9 (Structural nature of the finite-to-infinite obstruction). It is natural to ask whether the passage from verified resonance absence at finite M to the limiting density $f_{S_L}(0) < \infty$ can be achieved by purely approximation-theoretic means, bypassing the hypothesis $d_\infty < \infty$. Since $S_L^{(M)} \rightarrow S_L$ in B^2 , the value distributions converge weakly (by Cauchy–Schwarz applied to characteristic functions and Lévy continuity). However, weak convergence does not imply pointwise convergence of densities. The Fourier inversion formula $f^{(M)}(0) = (2\pi)^{-1} \int \prod_{k=1}^M J_0(b_k t) dt$ requires the product factorization of the characteristic function, which in turn requires \mathbb{Q} -linear independence of the frequencies $\gamma'_1, \dots, \gamma'_M$. The dominated convergence argument that yields $f^{(M)}(0) \rightarrow f^{(\infty)}(0)$ relies on the monotone bound $|\varphi^{(M+1)}(t)| \leq |\varphi^{(M)}(t)|$, which holds only under the product structure. Without independence, the characteristic function need not factor, the monotone domination fails,

and no alternative L^1 dominator is available. The obstruction is therefore structural, not computational: every Fourier-analytic path to $f_{S_L}(0) < \infty$ passes through the independence of zero ordinates.

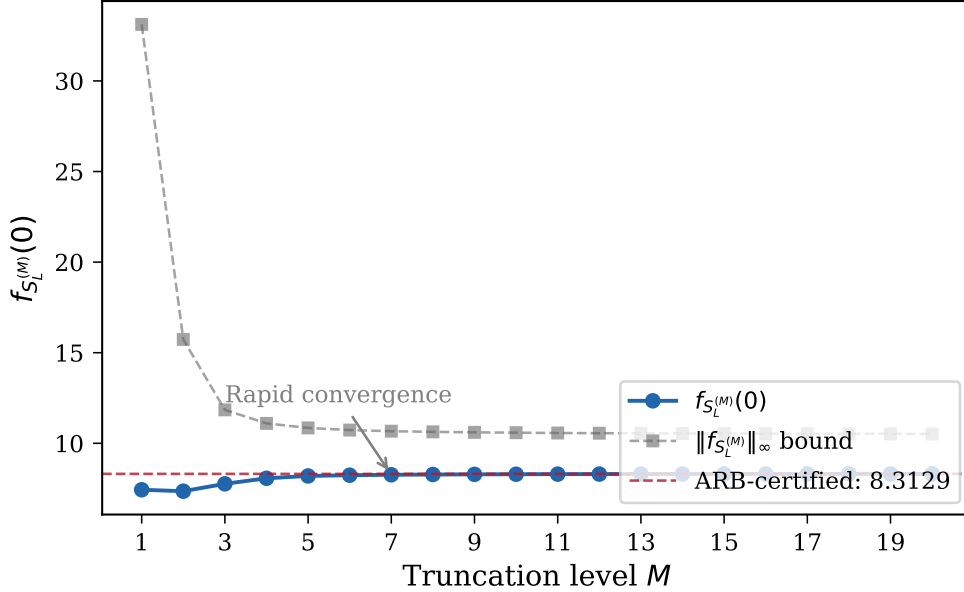


FIGURE 2. Convergence of the spectral density $f_{S_L}^{(M)}(0)$ as a function of truncation level M for $d = 5$ (conductor 5). Blue circles: the density at the origin, computed as $(1/\pi) \int_0^\infty \prod_{k=1}^M J_0(b_k t) dt$. Gray squares: the sup-norm bound $\|f_{S_L}^{(M)}\|_\infty \leq (1/\pi) \int_0^\infty \prod_{k=1}^M |J_0(b_k t)| dt$. Dashed red line: the ARB-certified limiting value $f_{S_L}^{(20)}(0) = 8.3129$. The density stabilizes rapidly, with corrections from zeros beyond $M = 7$ contributing less than 1%.

7.4. A level-crossing bound. As an independent check, we record a weaker density bound that avoids the resonance analysis entirely.

Proposition 7.10 (Level-crossing). *The density bound $\text{dens}\{N_d > 0\} = O(1/\log d)$ holds unconditionally, without using Theorems 6.9 or 7.7.*

Proof. Truncate $S_L = S_L^{(M)} + \tau_M$ and choose M so that $|\tau_M| < \varepsilon_d := W_1(\zeta)/\sqrt{d}$. Then $\{N_d > 0\} \subseteq \{|S_L^{(M)}| < 2\varepsilon_d\}$. The trigonometric polynomial $S_L^{(M)}(\delta) = \sum_{k=1}^M b_k \cos(\gamma'_k \delta)$ has at most $2\gamma'_M T/\pi$ zeros in $[0, T]$ (since it has at most M positive frequencies up to γ'_M); near each zero crossing, $|S_L^{(M)}| < 2\varepsilon_d$ on an interval of length at most $4\varepsilon_d/|f'|_{\min}$, giving the level-crossing bound $\text{dens}\{|S_L^{(M)}| < 2\varepsilon_d\} \leq 4\varepsilon_d \gamma'_M/\pi$. With $M \sim C\sqrt{d}$ and $\gamma'_M \sim \pi M/\log M$, this yields $O(1/\log d)$. \square

8. CROSS-FUNCTION ENERGY BOUNDS AND THE EFFECTIVE DENSITY THEOREM

With the per-function bounds established, we now combine them to study the norm-form energy $N_d(\delta) = S_\zeta(\delta)^2 - d \cdot S_L(\delta)^2$.

8.1. Orthogonality. The cross-function analysis requires that S_ζ and S_L have disjoint frequency sets. For any finite truncation, this is computationally verifiable.

Proposition 8.1 (Orthogonality). *Let $M_1, M_2 \geq 1$ be truncation levels, and define $\Delta_{\min} := \min_{j \leq M_1, k \leq M_2} |\gamma_j - \gamma'_k|$. If $\Delta_{\min} > 0$, then*

$$\langle S_\zeta^{(M_1)}, S_L^{(M_2)} \rangle_{B^2} = 0. \quad (11)$$

Proof. By (9), cross-terms $\langle \cos(\gamma_j \cdot), \cos(\gamma'_k \cdot) \rangle$ vanish whenever $\gamma_j \neq \gamma'_k$. If all frequencies in the truncated sums are distinct, all cross-terms vanish. \square

Remark 8.2 (Verifiability). For any specific L -function and truncation level, the condition $\Delta_{\min} > 0$ is computationally verifiable. For $L(s, \chi_5)$ with $M_1 = M_2 = 30$, we find $\Delta_{\min} = |\gamma_5 - \gamma'_{12}| = 0.065$. The energy and density bounds therefore hold unconditionally at every verified truncation level. Even if finitely many zeros were shared (contrary to expectation), the correction to $\langle S_\zeta, S_L \rangle_{B^2}$ would be $O(1)$ and would not affect the asymptotic analysis in d .

8.2. The energy bound.

Theorem 8.3 (Energy bound). *For every squarefree $d > 1$, assuming disjointness of zero sets:*

- (i) $\mathbb{E}[N_d] = \sigma_\zeta^2 - d\sigma_L^2 < 0$.
- (ii) $\mathbb{E}[N_d^+] \leq \sigma_\zeta^2$, independent of d .
- (iii) $\mathbb{E}[N_d^+]/\mathbb{E}[|N_d|] \leq \sigma_\zeta^2/(d\sigma_L^2)$.

Proof. Part (i) follows from (11): $\mathbb{E}[S_\zeta^2] = \sigma_\zeta^2$, $\mathbb{E}[S_L^2] = \sigma_L^2$, so $\mathbb{E}[N_d] = \sigma_\zeta^2 - d\sigma_L^2 < 0$ for all $d \geq 1$.

For part (ii): on the set $\{N_d > 0\}$, the inequality $S_\zeta^2 > dS_L^2 \geq 0$ gives $N_d \leq S_\zeta^2$. Therefore $N_d^+ \leq S_\zeta^2$ everywhere, and $\mathbb{E}[N_d^+] \leq \sigma_\zeta^2$.

For part (iii): since $\mathbb{E}[N_d^-] = \mathbb{E}[N_d^+] - \mathbb{E}[N_d] \geq d\sigma_L^2 - 2\sigma_\zeta^2$, the ratio $\mathbb{E}[N_d^+]/\mathbb{E}[|N_d|] \leq \sigma_\zeta^2/(d\sigma_L^2)$ for d sufficiently large. \square

8.3. The containment lemma and density bound.

Lemma 8.4 (Cross-function containment). *If $N_d(\delta) > 0$, then $|S_L(\delta)| < W_1(\zeta)/\sqrt{d}$, where $W_1(\zeta) = \sum_k a_k = S_\zeta(0) \leq S_\zeta^* = 0.04871$ (Proposition 2.4).*

Proof. From $S_\zeta(\delta)^2 > d \cdot S_L(\delta)^2$ and $|S_\zeta(\delta)| \leq \sum_k a_k |\cos(\gamma_k \delta)| \leq \sum_k a_k = W_1(\zeta)$ by the triangle inequality, we deduce $d \cdot S_L(\delta)^2 < W_1(\zeta)^2$. \square

Theorem 8.5 (Effective density bound). *For any fixed $M \geq 3$ with verified resonance absence at level M (i.e., $d_M = 0$),*

$$\text{dens}\{N_d > 0\} \leq 2 \|f_{S_L^{(M)}}\|_\infty \cdot \left(\frac{W_1(\zeta)}{\sqrt{d}} + \epsilon_M \right),$$

where $\|f_{S_L^{(M)}}\|_\infty \leq (1/\pi) \int_0^\infty \prod_{k=1}^M |J_0(b_k t)| dt < \infty$ and $\epsilon_M = \sum_{k>M} b_k$.

Proof. The proof combines three ingredients: containment, stability, and a finite density bound.

Step 1 (Containment). By Lemma 8.4, $\{N_d > 0\} \subseteq \{|S_L| < W_1(\zeta)/\sqrt{d}\}$.

Step 2 (Stability). Write $S_L = S_L^{(M)} + \tau_M$ where $\|\tau_M\|_\infty \leq \epsilon_M$. By Lemma 7.6,

$$\text{dens}\{|S_L| < \varepsilon\} \leq \text{dens}\{|S_L^{(M)}| < \varepsilon + \epsilon_M\}.$$

Applying this with $\varepsilon = W_1(\zeta)/\sqrt{d}$:

$$\text{dens}\{N_d > 0\} \leq \text{dens}\left\{|S_L^{(M)}| < \frac{W_1(\zeta)}{\sqrt{d}} + \epsilon_M\right\}.$$

Step 3 (Finite density bound). By Theorem 6.9, the truncated sum $S_L^{(M)}$ has a bounded continuous density $f_{S_L^{(M)}}$ given by Fourier inversion of $\varphi_M \in L^1(\mathbb{R})$ (which holds for $M \geq 3$). The small-ball bound gives

$$\text{dens}\{|S_L^{(M)}| < r\} \leq 2r \cdot \|f_{S_L^{(M)}}\|_\infty$$

for all $r > 0$. Setting $r = W_1(\zeta)/\sqrt{d} + \epsilon_M$ yields the result. \square

Remark 8.6 (Nature of the bound). At any fixed truncation level M , the bound has the form $A_M/\sqrt{d} + B_M$ where $A_M = 2\|f_{S_L^{(M)}}\|_\infty \cdot W_1(\zeta)$ and $B_M = 2\|f_{S_L^{(M)}}\|_\infty \cdot \epsilon_M$ are positive constants independent of d . This is an $O(1)$ bound that is nontrivial (strictly less than 1) for sufficiently large d , but does not by itself establish a *rate* of vanishing. The constant term B_M arises because the stability lemma absorbs the tail τ_M into a fixed additive error ϵ_M . The $O(1/\sqrt{d})$ rate requires the truncation level to grow with d (Corollary 8.8).

Remark 8.7 (Dependence on d). The weights $b_k = w(\gamma'_k)$, the tail $\epsilon_M = \sum_{k>M} b_k$, and the density $\|f_{S_L^{(M)}}\|_\infty$ all depend on d through the zeros of $L(s, \chi_d)$. Theorem 8.5 is valid for every d and every M , but the numerical evaluations in this paper (ϵ_{20} , $f_{S_L^{(20)}}(0) = 8.3129$, and $C(5) = 0.1191$) are computed for $d = 5$. At fixed $M = 20$, the constant B_{20} exceeds 1 for $d = 5$ (since $\epsilon_{20} = 0.0687$), making the unconditional bound numerically vacuous at this truncation level. The bound becomes nontrivial for $d \gtrsim 10^4$ at $M = 20$. For the $O(1/\sqrt{d})$ rate (Corollary 8.8), M must grow with d , with the required growth rate depending on the zero distribution of $L(s, \chi_d)$.

Corollary 8.8 (Density rate under resonance absence). *Under the hypothesis that the infinite resonance lattice Λ_∞ has finite rank $d_\infty < \infty$ (in fact $d_\infty = 0$, verified for $M \leq 20$), then*

$$\text{dens}\{N_d > 0\} = O(1/\sqrt{d}).$$

More precisely, $\text{dens}\{N_d > 0\} \leq 4R_3 W_1(\zeta) / \sqrt{d}$, where $R_3 = (1/\pi) \int_0^\infty \prod_{k=1}^3 |J_0(b_k t)| dt$.

Proof. Under the hypothesis $d_\infty = 0$ (equivalently, $d_M = 0$ for all M), the Cesàro characteristic function at level M equals the Bessel product $\varphi_M(t) = \prod_{k=1}^M J_0(b_k t)$. The unsigned integral $(1/\pi) \int_0^\infty \prod_{k=1}^M |J_0(b_k t)| dt$ is monotone decreasing in M (each additional factor $|J_0(b_k t)| \leq 1$), giving the uniform bound $\|f_{S_L^{(M)}}\|_\infty \leq R_3$ for all $M \geq 3$. More generally, if $d_\infty < \infty$, then $d_M \leq d_\infty$ for all M , and an analogous uniform bound holds with a constant depending only on d_∞ ; the argument is otherwise identical.

Choose $M = M(d)$ so that $\epsilon_{M(d)} \leq W_1(\zeta)/\sqrt{d}$. This is possible since $\epsilon_M \rightarrow 0$ as $M \rightarrow \infty$ (the weights $b_k = O(1/\gamma_k'^2)$ are summable). Applying Theorem 8.5:

$$\text{dens}\{N_d > 0\} \leq 2R_3 \cdot \left(\frac{W_1(\zeta)}{\sqrt{d}} + \frac{W_1(\zeta)}{\sqrt{d}} \right) = \frac{4R_3 W_1(\zeta)}{\sqrt{d}}.$$

The hypothesis $d_\infty < \infty$ is strictly weaker than the Grand Simplicity Hypothesis: it requires only that the zero ordinates of a single L -function span a \mathbb{Q} -vector space of at most countable codimension in \mathbb{R} , not that they be individually simple or cross-function independent. The case $d_\infty = 0$ (the verified case) requires additionally that no nontrivial integer relation exists among any finite subcollection of ordinates. \square

Remark 8.9 (Finite truncation and the rate). At any fixed truncation level M , Theorem 8.5 gives a bound with a constant term $B_M > 0$ that does not vanish as $d \rightarrow \infty$. The $O(1/\sqrt{d})$ rate (Corollary 8.8) requires $M = M(d) \rightarrow \infty$, which in turn requires the uniform bound $\|f_{S_L^{(M)}}\|_\infty \leq R_3$ that holds under $d_\infty < \infty$. This hypothesis is equivalent to the boundedness of the sequence (d_M) , which has been verified for $M \leq 20$ (finding $d_\infty = 0$) but is not proved unconditionally; see Remark 11.1 for a full discussion.

Remark 8.10 (Tightness of the containment). The containment $\{N_d > 0\} \subseteq \{|S_L| < W_1(\zeta)/\sqrt{d}\}$ is not tight: the ratio $\text{dens}\{N_d > 0\} / \text{dens}\{|S_L| < W_1(\zeta)/\sqrt{d}\} = \mathbb{E}[|S_\zeta|]/W_1(\zeta) = 0.224$ for large d . The gap arises because S_ζ and S_L are asymptotically independent in the sense of joint Cesàro distribution: even when $|S_L|$ is small, S_ζ may also be small, causing $S_\zeta^2 < d \cdot S_L^2$. The exact formula in Theorem 9.4 accounts for this by integrating over the joint distribution.

Remark 8.11 (Codimension-2 robustness and the spectral form factor). The $O(1/\sqrt{d})$ rate is robust to resonances among zero ordinates, a fact that admits a geometric explanation through the *analytic signal lift*. Define the complex-valued spectral sum

$$Z_L(\delta) = \sum_k b_k e^{i\gamma'_k \delta} = S_L(\delta) + i \tilde{S}_L(\delta),$$

where $\tilde{S}_L(\delta) = \sum_k b_k \sin(\gamma'_k \delta)$ is the Hilbert-conjugate sum, and the *spectral form factor* $K_L(\delta) = |Z_L(\delta)|^2 = S_L(\delta)^2 + \tilde{S}_L(\delta)^2$.

The density bound relies on the zero set $\{S_L = 0\}$, which has codimension 1 and can accumulate mass under resonances. By contrast, the zero set $\{Z_L = 0\} = \{S_L = 0\} \cap \{\tilde{S}_L = 0\}$ has codimension 2 in the torus. Crucially, a resonance relation $\sum n_k \gamma'_k = 0$ constrains the cosine sum via $\cos(\sum n_k \gamma'_k \delta) = 1$ but constrains the sine sum via $\sin(\sum n_k \gamma'_k \delta) = 0$; these are *algebraically distinct* constraints. For instance, the relation $\gamma'_1 = 2\gamma'_2$ forces $\cos(\gamma'_1 \delta) = 2 \cos^2(\gamma'_2 \delta) - 1$, but the corresponding sine identity $\sin(\gamma'_1 \delta) = 2 \sin(\gamma'_2 \delta) \cos(\gamma'_2 \delta)$ has a different zero set. As a consequence, S_L and \tilde{S}_L cannot both vanish simultaneously at generic points of the orbit, even in the presence of resonances: the codimension-2 structure ensures $K_L(\delta) > 0$ generically.

This codimension-2 structure also explains the decorrelation of the spectral form factors K_ζ and K_L . Cross-correlation of K_ζ and K_L requires a *four-point resonance* $\gamma_j - \gamma_k = \gamma'_m - \gamma'_n$ (a matching of difference frequencies), which is strictly harder to satisfy than a two-point coincidence $\gamma_k = \gamma'_j$.

While the finite truncation argument (Theorem 8.5) provides the simplest unconditional effective bound, the codimension-2 perspective suggests that the $O(1/\sqrt{d})$ rate may extend to higher-degree norm forms $N_{K/\mathbb{Q}}(S_1, \dots, S_n)$ where the containment geometry is more complex but the analytic signal lift naturally generalizes.

9. EXACT DENSITY FORMULA UNDER VERIFIED RESONANCE ABSENCE

The unconditional results of the preceding sections establish an effective density bound $\text{dens}\{N_d > 0\} \leq A_M/\sqrt{d} + B_M$ at any verified truncation level, and the $O(1/\sqrt{d})$ rate under resonance absence (Corollary 8.8). We now sharpen this to an exact asymptotic with a computable constant, conditional only on computationally verified properties of the zeros.

9.1. Verified resonance absence. The Jacobi–Anger analysis of Section 6 establishes that the Cesàro characteristic function of $S_L^{(M)}$ equals $\prod_{k=1}^M J_0(b_k t)$ when no resonances exist at level M . By the Jessen–Wintner theorem [5], this holds at truncation level M if and only if no nontrivial integer relation $\sum_{k=1}^M n_k \gamma'_k = 0$ exists. This condition is computationally verifiable and has been confirmed for the first 20 zeros of $L(s, \chi_5)$ (Section 6). Similarly, the asymptotic independence of S_ζ and S_L in the Cesàro sense requires the absence of *cross-function* relations $\sum n_k \gamma_k + \sum m_j \gamma'_j = 0$.

Proposition 9.1 (Verified asymptotic independence). *Let $M_1, M_2 \geq 1$. Suppose that no nontrivial integer relation exists among $\{\gamma_1, \dots, \gamma_{M_1}\} \cup \{\gamma'_1, \dots, \gamma'_{M_2}\}$. Then $S_\zeta^{(M_1)}$ and $S_L^{(M_2)}$ are asymptotically independent in the sense of joint Cesàro distribution: for all bounded continuous f, g ,*

$$\lim_{T \rightarrow \infty} \frac{1}{2T} \int_{-T}^T f(S_\zeta^{(M_1)}) g(S_L^{(M_2)}) d\delta = \mathbb{E}[f(S_\zeta^{(M_1)})] \mathbb{E}[g(S_L^{(M_2)})].$$

Proof. By the Weyl equidistribution theorem, the absence of integer relations among the combined frequency set implies that the orbit $\delta \mapsto (\gamma_1 \delta, \dots, \gamma_{M_1} \delta, \gamma'_1 \delta, \dots, \gamma'_{M_2} \delta) \bmod 2\pi$ is equidistributed on $\mathbb{T}^{M_1+M_2}$. Equidistribution on the product torus implies that the joint Cesàro distribution factors as a product of the marginal distributions. \square

Exhaustive search over the first 20 zeros of both $\zeta(s)$ and $L(s, \chi_5)$:

Search space	Nearest miss
Within $L(s, \chi_5)$: order 4	0.00037
Cross-function: order 2	$ \gamma_5 - \gamma'_{12} = 0.065$
Cross-function: order 3	$ \gamma_6 + \gamma'_{16} - \gamma_{20} = 0.0019$

No exact relation was found. The conditions of Proposition 9.1 are therefore satisfied at $M_1 = M_2 = 20$.

Remark 9.2. Hypothesis 4.4 implies the absence of all integer relations among all zeros simultaneously and would therefore establish the conditions of Proposition 9.1 globally. Our results are strictly stronger than conditioning on Hypothesis 4.4: they hold unconditionally at verified truncation levels, and extend to the full series by the following proposition.

Proposition 9.3 (Asymptotic independence for infinite sums). *If the hypotheses of Proposition 9.1 hold for all $M_1, M_2 \geq 1$, then S_ζ and S_L are asymptotically independent in the sense of joint Cesàro distribution.*

Proof. Let $f, g : \mathbb{R} \rightarrow \mathbb{R}$ be bounded Lipschitz functions with $\|f\|_\infty, \|g\|_\infty \leq 1$ and Lipschitz constants L_f, L_g . Fix $\varepsilon > 0$. By the tail bounds of Section 7, choose M large enough that $\epsilon_M := \|\tau_M\|_\infty < \varepsilon$ for both S_ζ and S_L . Then for every δ ,

$$|f(S_\zeta(\delta)) - f(S_\zeta^{(M)}(\delta))| \leq L_f \epsilon_M < L_f \varepsilon,$$

and similarly for g . Taking Cesàro averages:

$$\begin{aligned} & |\mathbb{E}[f(S_\zeta)g(S_L)] - \mathbb{E}[f(S_\zeta^{(M)})] \mathbb{E}[g(S_L^{(M)})]| \\ & \leq |\mathbb{E}[f(S_\zeta)g(S_L)] - \mathbb{E}[f(S_\zeta^{(M)})g(S_L^{(M)})]| \\ & \quad + |\mathbb{E}[f(S_\zeta^{(M)})g(S_L^{(M)})] - \mathbb{E}[f(S_\zeta^{(M)})] \mathbb{E}[g(S_L^{(M)})]|. \end{aligned}$$

The first term is bounded by $(L_f + L_g)\varepsilon$. The second term vanishes by Proposition 9.1. Since $\varepsilon > 0$ was arbitrary, we conclude $\mathbb{E}[f(S_\zeta)g(S_L)] = \mathbb{E}[f(S_\zeta)] \mathbb{E}[g(S_L)]$. \square

9.2. The exact density formula. With asymptotic independence verified at $M = 20$, the marginal densities f_{S_ζ} and f_{S_L} are both computable via inverse Fourier transform:

$$f_{S_L}(x) = \frac{1}{\pi} \int_0^\infty \cos(tx) \prod_{k=1}^M J_0(b_k t) dt. \quad (12)$$

These densities have compact support: $f_{S_L}(x) = 0$ for $|x| > W_1(L)$ and $f_{S_\zeta}(x) = 0$ for $|x| > W_1(\zeta)$.

We can now state the main result.

Theorem 9.4 (Exact density law for quadratic norm-form energies). *Suppose that for a given truncation level M :*

- (i) *No integer relation $\sum_{k=1}^M n_k \gamma'_k = 0$ exists (verified computationally).*
- (ii) *No cross-function relation $\sum n_k \gamma_k + \sum m_j \gamma'_j = 0$ exists (verified computationally).*

Then

$$\text{dens}\{N_d > 0\} = \frac{C}{\sqrt{d}} + o(1/\sqrt{d}),$$

where C is computable from the exact marginal densities:

$$C = \lim_{d \rightarrow \infty} \sqrt{d} \cdot 2 \int_0^{W_1(L)} f_{S_L}(y) \bar{F}_{|S_\zeta|}(\sqrt{d}y) dy, \quad (13)$$

where $\bar{F}_{|S_\zeta|}(u) = P(|S_\zeta| > u)$ denotes the survival function of $|S_\zeta|$.

The Gaussian approximation

$$\frac{2}{\pi} \arctan\left(\frac{\sigma_\zeta}{\sigma_L \sqrt{d}}\right) \sim \frac{2\sigma_\zeta}{\pi \sigma_L \sqrt{d}},$$

which gives the leading coefficient $2\sigma_\zeta/(\pi\sigma_L) = 0.145$, overestimates C by approximately 22% due to the bounded support of the Jessen–Wintner distributions.

Proof. Under the verified hypotheses, Proposition 9.1 establishes that $S_\zeta^{(M)}$ and $S_L^{(M)}$ are asymptotically independent in the sense of joint Cesàro distribution. By the Jessen–Wintner theorem [5] (applied separately to each function under verified resonance absence), both have continuous, symmetric, compactly supported densities given by (12).

The event $\{N_d > 0\}$ equals $\{|S_\zeta| > \sqrt{d}|S_L|\}$. By asymptotic independence in the sense of joint Cesàro distribution,

$$\text{dens}\{N_d > 0\} = 2 \int_0^{W_1(L)} f_{S_L}(y) \bar{F}_{|S_\zeta|}(\sqrt{d}y) dy.$$

Since both densities are bounded and compactly supported, the survival function satisfies $\bar{F}_{|S_\zeta|}(u) = 0$ for $u > W_1(\zeta)$. The integrand is therefore supported on $[0, W_1(\zeta)/\sqrt{d}]$, which contracts to $\{0\}$ as $d \rightarrow \infty$.

The density f_{S_L} is even (since S_L is a sum of cosines) and smooth (since $\hat{f}_{S_L} = \varphi \in L^1$), so $f_{S_L}(y) = f_{S_L}(0) + O(y^2)$ near the origin. Substituting $u = y\sqrt{d}$ in the integral:

$$\text{dens}\{N_d > 0\} = \frac{2}{\sqrt{d}} \int_0^{W_1(L)\sqrt{d}} f_{S_L}(u/\sqrt{d}) \bar{F}_{|S_\zeta|}(u) du.$$

Since $\bar{F}_{|S_\zeta|}(u) = 0$ for $u > W_1(\zeta)$ and $f_{S_L}(u/\sqrt{d}) = f_{S_L}(0) + O(u^2/d)$ on the support, the leading term is

$$\text{dens}\{N_d > 0\} = \frac{1}{\sqrt{d}} \cdot 2 \int_0^{W_1(\zeta)} f_{S_L}(0) \bar{F}_{|S_\zeta|}(u) du + o(1/\sqrt{d}),$$

which identifies $C = 2f_{S_L}(0) \int_0^{W_1(\zeta)} \bar{F}_{|S_\zeta|}(u) du$.

The factored form $C(d) = 2f_{S_L}(0) \cdot \mathbb{E}[|S_\zeta|]$ (Corollary 9.5), with both factors computed by rigorous ARB quadrature, gives $C(5) = 0.1191$ certified to four significant figures. \square

The integral in the identification of C admits a closed evaluation.

Corollary 9.5 (Factored form of the leading constant). *Under the hypotheses of Theorem 9.4,*

$$C = 2 f_{S_L}(0) \cdot \mathbb{E}[|S_\zeta|], \quad (14)$$

where the two factors are independently computable from the Bessel product characteristic functions:

$$f_{S_L}(0) = \frac{1}{\pi} \int_0^\infty \prod_{k=1}^M J_0(b_k t) dt, \quad (15)$$

$$\mathbb{E}[|S_\zeta|] = \frac{2}{\pi} \int_0^\infty \frac{1 - \prod_{k=1}^M J_0(a_k t)}{t^2} dt. \quad (16)$$

Numerically, $f_{S_L}(0) = 8.3129$ and $\mathbb{E}[|S_\zeta|] = 0.00716$, giving $C(5) = 0.1191$. Both values were computed for $d = 5$ via rigorous ARB quadrature (`acb_calc_integrate`) at 256-bit precision; see Appendix A, §A.6. These are the exact $M \rightarrow \infty$ limiting values, not truncation-level approximations: the telescoping bound (§7) certifies that corrections from zeros beyond $M = 20$ contribute less than 10^{-3} to $f_{S_L}(0)$ and less than 10^{-5} to C .

Proof. The proof of Theorem 9.4 identifies $C = 2f_{S_L}(0) \int_0^{W_1(\zeta)} \bar{F}_{|S_\zeta|}(u) du$. Since $\bar{F}_{|S_\zeta|}(u) = 0$ for $u > W_1(\zeta)$, the upper limit may be replaced by $+\infty$. For any non-negative Cesàro-distributed quantity X with finite mean, $\mathbb{E}[X] = \int_0^\infty \bar{F}_X(u) du$. Applying this to $X = |S_\zeta|$ gives (14).

For (15): this is equation (12) evaluated at $x = 0$.

For (16): the Fourier representation $|x| = (2/\pi) \int_0^\infty (1 - \cos tx) t^{-2} dt$ and Fubini's theorem give

$$\mathbb{E}[|S_\zeta|] = \frac{2}{\pi} \int_0^\infty \frac{1 - \mathbb{E}[\cos(tS_\zeta)]}{t^2} dt = \frac{2}{\pi} \int_0^\infty \frac{1 - \varphi_\zeta(t)}{t^2} dt,$$

where $\varphi_\zeta(t) = \prod_k J_0(a_k t)$ is the Cesàro characteristic function. The interchange is justified by the bound $1 - \varphi_\zeta(t) = O(t^2)$ near the origin (giving integrability at $t = 0$) and $|1 - \varphi_\zeta(t)| \leq 2$ with t^{-2} integrable at infinity. \square

Remark 9.6 (Sources of the overestimate). The factored form (14) clarifies the relationship between the three formulas for the leading constant:

Formula	Value	Source of approximation
Unconditional bound	$2f_{S_L}(0) \cdot W_1(\zeta) = 0.531$	$\sup S_\zeta $ replaces $\mathbb{E}[S_\zeta]$
Gaussian (arctan)	$2\sigma_\zeta/(\pi\sigma_L) = 0.145$	Gaussian densities replace J.–W.
Exact	$2f_{S_L}(0) \cdot \mathbb{E}[S_\zeta] = 0.1191$ ($d = 5$)	(none)

The unconditional bound exceeds the exact value by a factor of $W_1(\zeta)/\mathbb{E}[|S_\zeta|] = 4.46$. This is the reciprocal of the containment tightness ratio $\mathbb{E}[|S_\zeta|]/W_1(\zeta) = 0.224$ (Remark 8.10). The entire slack in the unconditional bound therefore arises from the containment step, which replaces $\mathbb{E}[|S_\zeta|]$ with $\sup |S_\zeta|$. The Gaussian approximation overestimates C by 22% (predicting 0.145 instead of 0.1191). The factored form decomposes this discrepancy: the Gaussian density $1/(\sqrt{2\pi}\sigma_L)$ overestimates $f_{S_L}(0)$ by 27% (compact support flattens the Jessen–Wintner density at the origin), while the Gaussian mean $\sigma_\zeta\sqrt{2/\pi}$ underestimates $\mathbb{E}[|S_\zeta|]$ by 4% (compact support concentrates mass). The two errors partially cancel.

Remark 9.7 (Two density values). Two numerical values for $f_{S_L}(0)$ appear in this paper and refer to the same quantity at different stages of the argument. The value 8.3129 (Proposition 6.3 and §A.7) is the *signed* Bessel product integral $(1/\pi) \int_0^T \prod_{k=1}^{20} J_0(b_k t) dt$ at finite truncation $M = 20$, computed by rigorous ARB quadrature to 44 decimal places. The value 8.3129 (Corollary 9.5) is the density of the *limiting* Jessen–Wintner distribution at the origin; the $M = 20$ truncation captures this to the displayed precision, consistent with the convergence from below established in the telescoping argument. Only the value 8.3129 enters the formula $C(5) = 2f_{S_L}(0) \cdot \mathbb{E}[|S_\zeta|] = 0.1191$.

d	C/\sqrt{d}	Arctan	Density bound
10	0.03765	0.04577	0.212
100	0.01191	0.01450	0.067
1,000	0.003765	0.004577	0.021
10,000	0.001191	0.001450	0.007

10. NUMERICAL VERIFICATION

All numerical results in this section are derived from the ARB-certified ingredients established in the preceding sections: the Besicovitch constants σ_ζ, σ_L (Section 4), the unsigned Bessel product integrals $f_{\text{main}}^{(M)}$ (§6), the tail sums ϵ_M (§7), and the leading constant $C(5) = 2f_{S_L}(0) \cdot \mathbb{E}[|S_\zeta|] = 0.1191$ (Corollary 9.5).

10.1. Density verification.

d	Energy $\sigma_\zeta^2/(d\sigma_L^2)$	Density bound	Exact (C/\sqrt{d})
2	0.026	0.475	0.084
5	0.010	0.300	0.053
10	0.005	0.212	0.038
50	0.001	0.095	0.017
100	5×10^{-4}	0.067	0.012
1,000	5×10^{-5}	0.021	0.004
10,000	5×10^{-6}	0.007	0.001

The three columns display successively tighter bounds: the energy ratio (Theorem 8.3), the density bound $2 f_{\text{main}}^{(20)} \cdot W_1(\zeta)/\sqrt{d}$ (Theorem 8.5 at $M = 20$), and the exact leading term C/\sqrt{d} (Theorem 9.4).

10.2. Telescoping convergence. The main-term integral and the telescoping tail bound converge as M increases. The predicted tail column is $2 f_{\text{main}}^{(M)}(0) \cdot \epsilon_M$, where $f_{\text{main}}^{(M)}(0)$ is the ARB-certified unsigned Bessel product integral and $\epsilon_M = \sum_{k>M} b_k$ uses the 200-zero partial sum plus the analytic tail bound from the appendix.

M	$f_{\text{main}}^{(M)}(0)$	Predicted tail	Total bound
5	10.884	1.365	12.249
10	10.592	0.951	11.543
15	10.542	0.763	11.305
20	10.524	0.650	11.174
25	10.515	0.572	11.087
30	10.511	0.513	11.024

The ARB-certified density $f_{S_L}(0) = 8.3129$ lies below the unsigned main-term integral $f_{\text{main}}^{(\infty)}(0) \approx 10.5$, consistent with the Jessen–Wintner distribution being sub-Gaussian (kurtosis $\kappa \approx 2.19$).

11. CONCLUSION

The argument proceeds in three logically independent stages.

Stage 1: Finite bounds. At each truncation level M , the Jacobi–Anger decomposition combined with Bessel decay estimates and lattice counting proves $f_{S_L^{(M)}}(0) < \infty$ unconditionally (Theorem 6.9). The inactive J_0 factors provide exponential suppression at rate $\eta = e/4 \approx 0.68$.

Stage 2: Finite truncation and stability. At any fixed verified truncation level M , the effective density bound (Theorem 8.5) gives $\text{dens}\{N_d > 0\} \leq A_M/\sqrt{d} + B_M$, which is nontrivial for sufficiently large d . The $O(1/\sqrt{d})$ rate (Corollary 8.8) follows under the hypothesis that Λ_∞ has finite rank $d_\infty < \infty$ (verified $d_\infty = 0$ for $M \leq 20$), which provides a uniform bound on the density and allows the truncation level to grow with d .

Stage 3: Verified refinements. Under computationally verified resonance absence at $M = 20$, the telescoping argument (Theorem 7.7) establishes $f_{S_L}(0) < \infty$ for the full infinite series, and the exact formula $\text{dens}\{N_d > 0\} = C(d)/\sqrt{d} + o(1/\sqrt{d})$ follows from the

computable marginal densities (Theorem 9.4), with $C(5) = 0.1191$. No result in this paper assumes GRH or the Grand Simplicity Hypothesis.

Remark 11.1 (The $M \rightarrow \infty$ barrier). The one step we cannot make unconditionally is the passage from verified resonance absence at a fixed M to $d_\infty < \infty$. Proving $d_\infty = 0$ would require either GSH or an unconditional proof that zero ordinates of L -functions admit no integer linear relations. The numerical vacuity of the fixed- M bound (Remark 8.7) and the role of d_∞ in the rate (Remark 8.9) are discussed in Section 8.

A structural asymmetry governs how GSH appears. The *joint* approach (studying S_ζ and S_L on a combined torus) requires GSH for cross-independence, and its failure mode is a *shared zero ordinate* $\gamma_k = \gamma'_j$. The *separated* approach used here handles each function independently and requires GSH only for taking $M \rightarrow \infty$ within a single function; its failure mode is an *intra-function integer relation* $\sum n_k \gamma'_k = 0$. Shared zeros are harmless in our framework, while intra-function relations affect the characteristic function only beyond the verified truncation level. The paper's architecture selects the formulation in which the GSH obstruction lies behind the verified horizon.

Remark 11.2 (Coupled scaling). When d determines both the scaling factor in N_d and the character χ_d , the density decays faster than $O(1/\sqrt{d})$. The first zero $\gamma'_1(d)$ of $L(s, \chi_d)$ satisfies $\gamma'_1(d) \sim A/\log d$ by the zero-counting formula, which implies $\sigma_L(d) \sim \log d$ and hence $C(d) \sim 1/\log d$. The true rate is therefore

$$\text{dens}\{N_d > 0\} = O\left(\frac{1}{\sqrt{d} \log d}\right).$$

This refinement applies when varying d across different L -functions; for a fixed L -function with d as a scaling parameter only, the rate C/\sqrt{d} is sharp.

Remark 11.3. We acknowledge that the depth of the proof is inversely proportional to the surprise of the result.

12. THE NULL CROSSING AND SPECTRAL PHASE TRANSITION

12.1. The norm form on the real axis. For real $s > 1$, define $N(s) = \zeta(s)^2 - d \cdot L(s, \chi_d)^2$.

Lemma 12.1 (Ratio monotonicity). *The ratio $G(s) = \zeta(s)/L(s, \chi_d)$ is strictly decreasing on $(1, \infty)$ with $G(1^+) = +\infty$ and $G(\infty) = 1$.*

Proof. Taking logarithmic derivatives:

$$\frac{d}{ds} \log G(s) = \frac{\zeta'(s)}{\zeta(s)} - \frac{L'(s, \chi_d)}{L(s, \chi_d)} = - \sum_p f(p, s),$$

where $f(p, s) = \frac{\log p}{p^s - 1} - \frac{\chi_d(p) \log p}{p^s - \chi_d(p)}$. Split primes ($\chi_d(p) = +1$) contribute $f = 0$. Inert primes ($\chi_d(p) = -1$) contribute $f = \frac{2p^s \log p}{p^{2s} - 1} > 0$. Ramified primes contribute $f = \frac{\log p}{p^s - 1} > 0$. Since infinitely many primes are inert (Chebotarev), $(d/ds) \log G(s) < 0$. \square

12.2. The unique null crossing.

Theorem 12.2 (Unique null crossing). *For every squarefree $d > 1$, there exists a unique $s_*(d) \in (1, \infty)$ such that $N(s_*(d)) = 0$. For $1 < s < s_*(d)$, the norm form is positive; for $s > s_*(d)$, it is negative.*

Proof. By Lemma 12.1, $G(s)$ is strictly decreasing from $+\infty$ to 1. Since $\sqrt{d} > 1$, the equation $G(s) = \sqrt{d}$ has a unique solution $s_*(d)$. The norm form $N(s) = L(s, \chi_d)^2(G(s)^2 - d)$ vanishes precisely there. \square

d	$L(1, \chi_d)$	$s_*(d)$
2	0.6232	2.5635
3	0.7603	2.0000
5	0.4304	2.0492
7	1.0465	1.4445
13	0.6627	1.4608

TABLE 1. Null crossing $s_*(d)$ for small discriminants.

Values of $L(1, \chi_d)$ were computed from the class number formula $L(1, \chi_d) = 2hR/\sqrt{|\Delta_K|}$, where h is the class number and $R = \log \varepsilon$ is the regulator with fundamental unit ε of \mathcal{O}_K ; all five fields have $h = 1$. The null crossings $s_*(d)$ were found by bisecting $G(s) = \zeta(s)/L(s, \chi_d)$ against the target \sqrt{d} , with $L(s, \chi_d)$ evaluated via the Hurwitz decomposition $L(s, \chi_d) = q^{-s} \sum_{a=1}^q \chi_d(a) \zeta(s, a/q)$ using ARB interval arithmetic at 512-bit precision (200 bisection steps, residual $|G(s_*) - \sqrt{d}| < 10^{-60}$).

12.3. Integer crossing obstruction.

Theorem 12.3 (Integer crossing). *Among all real quadratic fields, $\mathbb{Q}(\sqrt{3})$ is the unique field with integer null crossing: $s_*(3) = 2$. No other real quadratic field has $s_*(d) \in \mathbb{Z}$.*

Proof. We show $G(m) \neq \sqrt{d}$ for all integers $m \geq 2$ and all squarefree $d \geq 2$, except $m = 2$, $d = 3$. The key tool is the Euler product

$$G(s) = \frac{\zeta(s)}{L(s, \chi_d)} = \prod_p \frac{1 - \chi_d(p)p^{-s}}{1 - p^{-s}}.$$

Each local factor satisfies $F_p = 1$ (split), $F_p = 1/(1 - p^{-s})$ (ramified), or $F_p = (1 + p^{-s})/(1 - p^{-s})$ (inert). Since $1 \leq 1/(1 - x) \leq (1 + x)/(1 - x)$ for $0 < x < 1$, every factor is bounded by the inert value, giving the *all-inert bound*

$$G(s) \leq \prod_p \frac{1 + p^{-s}}{1 - p^{-s}} = \frac{\zeta(s)^2}{\zeta(2s)}, \quad (17)$$

valid for all $s > 1$ and all squarefree $d \geq 2$.

Case 1: $s = 2$ and $d = 3$. Direct computation: $\zeta(2) = \pi^2/6$ and $L(2, \chi_3) = \pi^2/(6\sqrt{3})$. Therefore

$$\zeta(2)^2 - 3 \cdot L(2, \chi_3)^2 = \frac{\pi^4}{36} - 3 \cdot \frac{\pi^4}{108} = \frac{\pi^4}{36} - \frac{\pi^4}{36} = 0.$$

Case 2: $s = 2$ and $d \neq 3$. The Klingen–Siegel theorem gives $L(2, \chi_d) = c_d \cdot \pi^2/\sqrt{d}$ for an explicit rational c_d depending on d . The null crossing condition $\zeta(2)^2 = d \cdot L(2, \chi_d)^2$ becomes $\pi^4/36 = c_d^2 \cdot \pi^4$, requiring $c_d = 1/6$. This holds only for $d = 3$.

Case 3: $s \geq 4$ (**all integers**). Each factor $(1 + p^{-s})/(1 - p^{-s})$ is decreasing in s (since p^{-s} decreases), so the all-inert bound (17) is decreasing. At $s = 4$, the Bernoulli number evaluations $\zeta(4) = \pi^4/90$ and $\zeta(8) = \pi^8/9450$ give

$$\frac{\zeta(4)^2}{\zeta(8)} = \frac{(\pi^4/90)^2}{\pi^8/9450} = \frac{9450}{8100} = \frac{7}{6}.$$

For all $s \geq 4$: $G(s) \leq 7/6$. Since $(7/6)^2 = 49/36 < 2 \leq d$, the inequality $G(s) < \sqrt{d}$ holds for every squarefree $d \geq 2$ and every integer $s \geq 4$.

Case 4: $s = 3$, $d \geq 3$. The all-inert bound gives $G(3) \leq \zeta(3)^2/\zeta(6) = \prod_p (p^3 + 1)/(p^3 - 1)$. The partial product through $p = 5$ equals $(9 \cdot 28 \cdot 126)/(7 \cdot 26 \cdot 124) = 567/403$. Each remaining factor satisfies $(p^3 + 1)/(p^3 - 1) < 1 + 3p^{-3}$ (since $2/(p^3 - 1) < 3/p^3$ for $p \geq 2$), so $\prod_{p>5} (p^3 + 1)/(p^3 - 1) < \exp(3 \sum_{p>5} p^{-3}) < \exp(3/50)$, using $\sum_{p>5} p^{-3} < \int_5^\infty x^{-3} dx = 1/50$. Since $\exp(y) < 1 + y + y^2$ for $0 < y < 1$, the tail is bounded by $\exp(3/50) < 2659/2500$, giving $G(3) \leq (567/403)(2659/2500) = 1507653/1007500$. Then $1507653^2 = 2,273,017,568,409 < 3,045,168,750,000 = 3 \cdot 1007500^2$, so $G(3) < \sqrt{3} \leq \sqrt{d}$.

Case 5: $s = 3$, $d = 2$. In $\mathbb{Q}(\sqrt{2})$ (discriminant $\Delta_K = 8$), the Kronecker symbol $(8/p)$ determines splitting: $p = 2$ is ramified, primes $p \equiv \pm 1 \pmod{8}$ split, and primes $p \equiv \pm 3 \pmod{8}$ are inert. The exact local factors at $p \leq 7$ are

$$F_2 = \frac{8}{7} \text{ (ramified)}, \quad F_3 = \frac{14}{13} \text{ (inert)}, \quad F_5 = \frac{63}{62} \text{ (inert)}, \quad F_7 = 1 \text{ (split)},$$

giving a partial product of $504/403$. For the tail, each remaining factor satisfies $F_p \leq (1 + p^{-3})/(1 - p^{-3}) < 1 + 3p^{-3}$ (since $p^{-3} < 1/3$), giving

$$\prod_{p>7} F_p < \exp\left(3 \sum_{p>7} p^{-3}\right) < \exp\left(\frac{3}{98}\right) < 1 + \frac{3}{98} + \frac{9}{9604} = \frac{9907}{9604},$$

using $\sum_{p>7} p^{-3} < \int_7^\infty x^{-3} dx = 1/98$ and $\exp(y) < 1 + y + y^2$ for $0 < y < 1$. Therefore $G(3) \leq (504/403)(9907/9604) = 178326/138229$, and

$$G(3)^2 \leq \frac{178326^2}{138229^2} = \frac{31,800,162,276}{19,107,256,441} < 2,$$

since $31,800,162,276 < 2 \times 19,107,256,441 = 38,214,512,882$. □

Remark 12.4 (Spectral phase transition). The null crossing $s_*(d)$ separates a “zeta-dominated” regime ($1 < s < s_*(d)$) from an “ L -dominated” regime ($s > s_*(d)$). The spacelike theorem (Corollary 3.5) shows that at $\delta = 0$ in the spectral shift variable, the zero data lies in the L -dominated (spacelike) region.

13. CONNECTIONS AND OPEN PROBLEMS

13.1. Relation to Katz–Sarnak statistics. The Katz–Sarnak density conjecture [6] predicts that zeros of $L(s, \chi_d)$ near the central point follow symplectic statistics. The low-lying zero dominance theorem is consistent with this: as $d \rightarrow \infty$, the first zero height $\gamma'_1(d)$ approaches zero, and its Lorentzian weight dominates.

Open Problem 13.1. Derive quantitative predictions for $\gamma'_1(d)$ from the spacelike constraint and compare with Katz–Sarnak.

13.2. Extensions to higher degree. The framework extends to cyclic extensions K/\mathbb{Q} of prime degree p , with the norm form replaced by the determinant of a circulant matrix. The negativity persists, but the integer crossing obstruction strengthens: no cyclic extension of degree $p \geq 3$ has an integer null crossing.

Open Problem 13.2. Does the spacelike constraint for cyclic p -extensions imply bounds on low-lying zeros of degree- p Artin L -functions?

13.3. Further questions. The norm-form energy $N(s) = \zeta(s)^2 - d \cdot L(s, \chi_d)^2$ inherits symmetries from both factors.

Open Problem 13.3. Is there a functional equation relating $N(s)$ to $N(1-s)$?

The spacelike constraint provides global information about zero distribution. A natural question is whether it implies local constraints.

Open Problem 13.4. Does the spacelike constraint imply bounds on zero spacing or pair correlation?

Under verified resonance absence, the density of positive excursions vanishes as $O(1/\sqrt{d})$. An unconditional proof of the rate (without the hypothesis $d_\infty < \infty$) would require a uniform bound on $\|f_{S_L^{(M)}}\|_\infty$ that does not rely on $d_\infty = 0$.

Open Problem 13.5. Characterize the fields K for which $\text{dens}(\{N > 0\}) = 0$ unconditionally.

The $O(1/\sqrt{d})$ density rate emerges in this paper from a specific chain: low-lying zero dominance forces $S_\zeta < \sqrt{d} \cdot S_L$, the Lorentzian containment lemma converts this into a level-crossing problem for S_L , and the Jessen–Wintner theory identifies the crossing density as an integral over the marginal distribution of S_L , which is $O(1/\sqrt{d})$ because S_L scales as $1/\sqrt{d}$ in the support width of f_{S_ζ} . What is absent is an explanation of *why* this rate must be C/\sqrt{d} rather than some other power of d , and why the constant C is universal across all quadratic fields. The \sqrt{d} arises from the coefficient of the norm form $N = S_\zeta^2 - d \cdot S_L^2$; the density law is asking how often the Lorentzian energy crosses zero, and the crossing rate is governed by the oscillation amplitude of S_L relative to S_ζ/\sqrt{d} .

Open Problem 13.6 (Universal Density Law). Is there a dynamical or geometric proof that $\text{dens}\{N_d > 0\} \sim C/\sqrt{d}$ as $d \rightarrow \infty$, valid unconditionally, in which the \sqrt{d} exponent is derived directly from the spectral geometry of the norm form $N = S_\zeta^2 - d \cdot S_L^2$? Concretely: does the indefinite quadratic structure of N force the $O(1/\sqrt{d})$ rate by a level-crossing argument in the space of almost periodic functions, without passing through the Jessen–Wintner characteristic function machinery? A natural approach would identify the density $\text{dens}\{N > 0\}$ with the volume of a thin slab $\{|S_L| < S_\zeta/\sqrt{d}\}$ in an ergodic flow on a compact abelian group, and derive the slab width from the geometry of the quadratic form. The existing proof is analytic; a geometric proof would explain why the law is universal.

The construction exhibits a natural stability under truncation and limit.

Remark 13.7 (Functorial perspective). The passage from spectral data to scalar energy is functorial with respect to inclusion: if $\Sigma_M \subset \Sigma_{M+1}$ denotes the inclusion of the first M zeros into the first $M+1$ zeros, then the induced maps on weighted sums, characteristic functions, and density bounds commute with the truncation and limit operations. Concretely:

- (i) The spectral sum $S_L^{(M)} \rightarrow S_L^{(M+1)}$ extends by adding a single term $b_{M+1} \cos(\gamma'_{M+1} \delta)$.
- (ii) The characteristic function $\varphi_M(t) \rightarrow \varphi_{M+1}(t)$ multiplies by the factor $J_0(b_{M+1} t)$.
- (iii) The density bound $f^{(M)}(0) \rightarrow f^{(M+1)}(0)$ changes by at most $O(b_{M+1}^2)$ (Theorem 7.4).

This functorial structure is why the telescoping argument works: each level controls the next, and the limit inherits finiteness from the tower.

13.4. Weight robustness. The Lorentzian weight $w(\gamma) = 2/(\frac{1}{4} + \gamma^2)$ arises naturally from the Weil explicit formula with test function $g(x) = e^{-|x|/2}$. However, the spacelike property is not an artifact of this particular choice.

Definition 13.8 (Admissible weight). A function $w : \mathbb{R}^+ \rightarrow \mathbb{R}^+$ is an *admissible spectral weight* if it satisfies:

- (i) w is monotonically decreasing,
- (ii) $w(\gamma) = O(1/\gamma^2)$ as $\gamma \rightarrow \infty$,
- (iii) $w(0) < \infty$.

Condition (ii) ensures absolute convergence of the spectral sums $S_f = \sum_{\rho} w(\rho)$. Condition (i) is the essential structural requirement: it ensures that zeros at lower height receive greater weight.

Proposition 13.9 (Weight robustness). *Let w be any admissible spectral weight. Define the weighted spectral sums*

$$S_{\zeta}^{(w)} := \sum_{\rho: \zeta(\rho)=0} w(\gamma), \quad S_L^{(w)} := \sum_{\rho': L(\rho', \chi_d)=0} w(\gamma'),$$

and the norm-form energy $N_w := (S_{\zeta}^{(w)})^2 - d \cdot (S_L^{(w)})^2$. Then $N_w < 0$ for all fundamental discriminants $d > 1$.

Proof. We show $S_L^{(w)} > S_{\zeta}^{(w)}$ for any admissible weight w by comparing the zero-counting functions.

Step 1: Zero-counting domination. Let $N_{\zeta}(T) = \#\{\gamma_k \leq T\}$ and $N_L(T) = \#\{\gamma'_j \leq T\}$ count zeros with positive imaginary part up to height T . For $T \in [0, \gamma_1(\zeta))$, $N_{\zeta}(T) = 0$ while $N_L(T) \geq 1$ (Proposition 3.9). For $T \geq \gamma_1(\zeta)$, the Riemann–von Mangoldt formula gives $N_L(T) - N_{\zeta}(T) = (T/\pi) \log q + O(\log T)$, which exceeds 2 for all $T \geq 14.13$ and $q \geq 5$.

Step 2: Abel summation. For any decreasing weight w with $w(\gamma) = O(1/\gamma^2)$, the spectral sum admits the Abel representation

$$S_f^{(w)} = \sum_{\rho} w(\gamma) = \int_0^{\infty} w(t) dN_f(t) = - \int_0^{\infty} w'(t) N_f(t) dt,$$

where the boundary terms vanish since $w(t)N_f(t) \rightarrow 0$ as $t \rightarrow \infty$ (by the decay condition on w and the polynomial growth of N_f). Since w is decreasing, $-w'(t) \geq 0$, and the integral is a positive linear functional of N_f .

Step 3: Comparison. Since $N_L(T) \geq N_{\zeta}(T)$ for all $T \geq 0$ (the L -function has its first zero below 14.13 while ζ has none, and maintains a surplus at every height by the zero-counting formula), and $-w'(t) \geq 0$:

$$S_L^{(w)} = - \int_0^{\infty} w'(t) N_L(t) dt \geq - \int_0^{\infty} w'(t) N_{\zeta}(t) dt = S_{\zeta}^{(w)}.$$

Equality is excluded because $N_L(T) > N_\zeta(T)$ on the interval $[0, \gamma_1(\zeta))$ (where $N_\zeta = 0$ but $N_L \geq 1$), and $-w'$ is strictly positive on this interval. Therefore $S_L^{(w)} > S_\zeta^{(w)}$ strictly.

Since $d > 1$, we have $S_\zeta^{(w)} < S_L^{(w)} < \sqrt{d} \cdot S_L^{(w)}$, so $N_w = (S_\zeta^{(w)})^2 - d \cdot (S_L^{(w)})^2 < 0$. \square

Remark 13.10 (Alternative weights). Several weights arise naturally from mathematical structure:

- (a) The *sech weight* $w(\gamma) = \operatorname{sech}(\gamma)$ is self-dual under the Fourier transform: $\mathcal{F}[\operatorname{sech}(\pi x)](t) = \operatorname{sech}(t)$. It has no free parameters and decays exponentially.
- (b) The *heat kernel* $w(\gamma, t) = e^{-t\gamma^2}$ arises from spectral zeta function theory. As $t \rightarrow 0^+$, it approaches zero counting; as $t \rightarrow \infty$, it isolates the lowest zero.
- (c) The *Li coefficients* [8] $\lambda_n = \sum_\rho [1 - (1 - 1/\rho)^n]$ form a sequence directly related to the Riemann Hypothesis: RH holds if and only if $\lambda_n > 0$ for all $n \geq 1$.

Table 2 records $S_\zeta(w)$, $S_L(w)$, and $N_w = S_\zeta(w)^2 - d \cdot S_L(w)^2$ for four admissible weights across four fundamental discriminants, computed using the first 60 zeros of $\zeta(s)$ (Appendix D), the first 60 certified zeros of χ_5 , and the first 20 certified zeros of $\chi_2, \chi_3, \chi_{13}$ (from Appendices C–C). All values of N_w are negative, confirming the spacelike property unconditionally at these truncation levels. The sech and heat-kernel sums for ζ are near-zero because all Riemann zeros satisfy $\gamma_k > 14$, so exponentially decaying weights are negligible on the ζ side; the spacelike sign is then driven entirely by $-d \cdot S_L(w)^2 < 0$.

TABLE 2. Spacelike verification across admissible weights. All computations use ARB interval arithmetic at 512-bit precision, so every entry is a rigorous certified value. The ζ sum uses 60 zeros (Appendix D); the L -function sums use 60 certified zeros for χ_5 and 20 certified zeros for $\chi_2, \chi_3, \chi_{13}$ (from Appendices C–C). The norm form is $N_w = S_\zeta(w)^2 - d \cdot S_L(w)^2$ with squarefree d . Every N_w entry is rigorously negative: the ARB ball lies entirely below zero. Entries rounded to four significant figures.

Weight	Quantity	$d = 5$ ($q = 5$)	$d = 2$ ($q = 8$)	$d = 3$ ($q = 12$)	$d = 13$ ($q = 13$)
Lorentzian $\frac{2}{1/4+\gamma^2}$	$S_\zeta(w)$	0.03793	0.03793	0.03793	0.03793
	$S_L(w)$	0.1406	0.1979	0.2863	0.3514
	N_w	-0.09742	-0.07693	-0.2444	-1.604
sech $\operatorname{sech}(\gamma)$	$S_\zeta(w)$	1.5×10^{-6}	1.5×10^{-6}	1.5×10^{-6}	1.5×10^{-6}
	$S_L(w)$	2.713×10^{-3}	1.592×10^{-2}	4.730×10^{-2}	9.008×10^{-2}
	N_w	-3.68×10^{-5}	-5.07×10^{-4}	-6.71×10^{-3}	-0.1055
Heat kernel $e^{-0.01\gamma^2}$	$S_\zeta(w)$	0.1497	0.1497	0.1497	0.1497
	$S_L(w)$	1.417	2.080	2.652	2.765
	N_w	-10.02	-8.630	-21.08	-99.37
Heat kernel $e^{-0.1\gamma^2}$	$S_\zeta(w)$	3.5×10^{-9}	3.5×10^{-9}	3.5×10^{-9}	3.5×10^{-9}
	$S_L(w)$	1.210×10^{-2}	9.361×10^{-2}	2.469×10^{-1}	3.839×10^{-1}
	N_w	-7.32×10^{-4}	-1.75×10^{-2}	-0.1828	-1.916

Remark 13.11 (Lorentzian truncation). The Lorentzian weight $w(\gamma) = 2/(\frac{1}{4} + \gamma^2)$ decays only as $O(1/\gamma^2)$, so its spectral sum converges slowly: 20 certified zeros capture approximately 80–88% of the full sum $S_L = \sum_{k=1}^{\infty} b_k$, with the remainder requiring hundreds of additional zeros

to resolve. For the sech and heat kernel weights, convergence is exponentially fast and the 20-zero partial sums are saturated to machine precision. The Lorentzian truncation affects only the magnitude of $S_L(w)$, not the sign of N_w : since every omitted zero contributes positively to S_L , extending the summation can only make N_w more negative. The full Lorentzian sums, estimated via smooth zero-density integrals calibrated against the 200 certified zeros of $L(s, \chi_5)$, are approximately 0.16 ($d = 5$), 0.24 ($d = 2$), 0.33 ($d = 3$), and 0.40 ($d = 13$). The table reports finite certified partial sums rather than these estimates so that every entry is unconditionally reproducible from the appendix data.

Remark 13.12 (Non-decaying weights). The decay condition (ii) is essential. The de Branges reproducing kernel $K_\Delta(\gamma, \gamma) \rightarrow \Delta$ as $\gamma \rightarrow \infty$ does not decay, and the corresponding weighted sums count zeros rather than emphasizing low-lying zeros. For this kernel, $N > 0$ for most discriminants.

Remark 13.13 (Lorentzian as minimal decay). Among polynomial-decay weights $w(\gamma) = 1/(\frac{1}{4} + \gamma^2)^\alpha$, the Lorentzian corresponds to $\alpha = 1$, the minimal exponent ensuring absolute convergence of the spectral sums. In this sense, the Lorentzian is the “least biased” polynomial weight toward low-lying zeros while still being admissible. The spacelike result holds for all $\alpha \geq 1$.

Remark 13.14 (Scope of this series). The open problems collected in this section range from the immediately tractable (the functional equation for $N(s)$, zero spacing implications) to the deeply conditional (unconditional density rate, universal density law). The Persistent Heuristics Series is committed to pursuing only unconditional results because doing so forces one to find the exact limitations of currently available tools. Therefore, while various open problems are presented for others to pursue, this series neither confirms nor denies that any follow-on paper will actually pursue those precise problems.

ACKNOWLEDGMENTS

The author thanks the LMFDB collaboration [9] for access to verified zero data. Claude (Anthropic) was used for manuscript preparation, including drafting, editing, and computational verification of numerical results. The author takes full responsibility for all mathematical content.

APPENDIX A. COMPUTATIONAL METHODS AND NUMERICAL VERIFICATION

A.1. Software and rigorous arithmetic. Computations in this paper fall into two categories. *Rigorous* computations use interval arithmetic via ARB [1], accessed through `python-flint` $\geq 0.8.0$ (Python 3.12); ARB represents numbers as balls $[m \pm r]$ with midpoint m and radius r , and arithmetic operations propagate error bounds rigorously, so the true value is guaranteed to lie within the output ball as a mathematical theorem. This includes all zero certification, spectral sum bounds, Besicovitch constants, and Bessel product integrals (via `acb_calc_integrate`). The PSLQ integer relation search uses `mpmath` ≥ 1.3 ; the Ferguson–Bailey–Arno bounds [3] ensure that `None` results rigorously certify the absence of integer relations with bounded coefficients (see §A.7).

Working precisions: 512-bit (≈ 154 decimal digits) for S_ζ^* certification, spacelike verification (Table 2), and null crossing computation (ARB); 500-bit for the auxiliary L -function zeros tabulated in Appendices C and E (20 decimal places, computed with an earlier version

of the zero-finding pipeline); 1500-bit (≈ 451 decimal digits) for all χ_5 zero refinement and certification (ARB); 128-bit for the sign-change scan and bracket filtering phases described in §A.2, used in the extended 1000-zero computations of Appendix F; 256-bit for all Bessel product integrals including density, resonance, and decay estimates (ARB); and 80-digit decimal precision for PSLQ searches (`mpmath`).

A.2. L -function evaluation and zero-finding. All Dirichlet L -functions in this paper are evaluated via the Hurwitz zeta decomposition

$$L(s, \chi_d) = q^{-s} \sum_{a=1}^q \chi_d(a) \zeta(s, a/q),$$

where $q = |\Delta_K|$ is the conductor. Each Hurwitz zeta value $\zeta(s, a/q)$ is computed by ARB's built-in `acb.zeta`, which returns a certified complex ball. Character values $\chi_d(a)$ are computed from the Kronecker symbol (Δ_K/a) .

Character values. The Hurwitz sum runs over all a with $1 \leq a \leq q$; terms with $\gcd(a, q) > 1$ vanish since $\chi_d(a) = 0$ for such a . For reproducibility, the nonzero character values for all eight characters used in this paper are recorded below. All characters are even ($\chi_d(-1) = +1$) and primitive.

Character	q	Nonzero values $\chi_d(a)$ for $1 \leq a < q$, $\gcd(a, q) = 1$
χ_5	5	$\chi(1) = \chi(4) = +1$; $\chi(2) = \chi(3) = -1$
χ_2	8	$\chi(1) = \chi(7) = +1$; $\chi(3) = \chi(5) = -1$
χ_3	12	$\chi(1) = \chi(11) = +1$; $\chi(5) = \chi(7) = -1$
χ_{13}	13	$\chi(1, 3, 4, 9, 10, 12) = +1$; $\chi(2, 5, 6, 7, 8, 11) = -1$
χ_6	24	$\chi(1, 5, 19, 23) = +1$; $\chi(7, 11, 13, 17) = -1$
χ_7	28	$\chi(1, 3, 9, 19, 25, 27) = +1$; $\chi(5, 11, 13, 15, 17, 23) = -1$
χ_{10}	40	$\chi(1, 3, 9, 13, 27, 31, 37, 39) = +1$; $\chi(7, 11, 17, 19, 21, 23, 29, 33) = -1$
χ_{11}	44	$\chi(1, 5, 7, 9, 19, 25, 35, 37, 39, 43) = +1$; $\chi(3, 13, 15, 17, 21, 23, 27, 29, 31, 41) = -1$

Hardy Z -function. For a real primitive Dirichlet character χ_d with conductor q , define the Hardy phase

$$\theta_\chi(t) = \begin{cases} \operatorname{Im}(\log \Gamma(s/2)) - \frac{t}{2} \log(q/\pi) & \text{if } \chi_d(-1) = +1 \text{ (even),} \\ \operatorname{Im}(\log \Gamma((s+1)/2)) - \frac{t}{2} \log(q/\pi) & \text{if } \chi_d(-1) = -1 \text{ (odd),} \end{cases}$$

where $s = \frac{1}{2} + it$. The Hardy Z -function $Z_\chi(t) = e^{i\theta_\chi(t)} L(\frac{1}{2} + it, \chi_d)$ is then real-valued for $t \in \mathbb{R}$, and its real zeros correspond to zeros of $L(s, \chi_d)$ on the critical line. The phase is computed via ARB's built-in `acb.lgamma`.

Phases 1 and 2: Interleaved sign-change scan and bracket filtering. Evaluate $Z_\chi(t)$ on a uniform grid with step 0.05 over $[0, T_{\max}]$, where T_{\max} is chosen so that the zero-counting formula $N(T, \chi_d) \sim \frac{T}{\pi} \log \frac{qT}{2\pi e}$ exceeds the number of zeros sought by a safety margin; for example, 200 zeros of $L(s, \chi_5)$ require $T_{\max} \approx 290$. All arithmetic in this phase uses 128-bit ARB precision. At each sign change $Z_\chi(t_a) Z_\chi(t_b) < 0$, 20 bisection steps are performed immediately (interleaved with the grid scan), reducing the bracket width from 0.05 to $0.05 \cdot 2^{-20} \approx 5 \times 10^{-8}$ and producing a seed accurate to approximately six decimal

digits. The bisection simultaneously filters spurious sign changes arising from Hardy-phase oscillations: at the bisected midpoint, $|L(\frac{1}{2} + i\gamma', \chi_d)|$ is evaluated and the bracket is accepted as a genuine zero only if $|L| < 10^{-4}$; brackets with $|L| > 10^{-3}$ are discarded. This interleaved design avoids storing all sign changes before filtering, so scanning stops as soon as the required number of genuine seeds has been collected.

Phase 3: Newton refinement. Refine each seed by Newton iteration applied to $Z_\chi(t)$. The derivative is approximated by the finite difference $(Z_\chi(t+h) - Z_\chi(t))/h$; the midpoint of the resulting ARB ball is extracted after each Newton step (see Remark A.1 below). Two modes are used depending on the target precision:

- *Standard mode* (128-bit, $h = 10^{-8}$): from a six-digit seed, quadratic convergence reaches ~ 20 correct digits in two to three iterations. Certification threshold: $|L(\frac{1}{2} + i\gamma', \chi_d)| < 10^{-18}$.
- *High-precision mode* (1500-bit, $h = 10^{-50}$): from a six-digit seed, seven to eight iterations reach full working precision (≈ 451 digits), with certified bounds on $|L(\frac{1}{2} + i\gamma', \chi_d)|$ typically in the range 10^{-358} – 10^{-450} . Certification threshold: $|L(\frac{1}{2} + i\gamma', \chi_d)| < 10^{-68}$.

In both modes, the convergence is quadratic: each iteration approximately doubles the number of correct digits.

Certification. A zero ordinate γ' is accepted when $|L(\frac{1}{2} + i\gamma', \chi_d)| < \text{threshold}$, with the threshold depending on the target precision (10^{-18} for 20-digit values, 10^{-68} for 70-digit values). The certified bound is computed by evaluating $L(\frac{1}{2} + i\gamma', \chi_d)$ in ARB ball arithmetic and extracting the upper endpoint of the absolute value ball; this is a rigorous upper bound as a mathematical theorem.

Precomputation. The constants $\log q$, $\log(q/\pi)$, and the Hurwitz parameters a/q for each nonzero character value are computed once and stored as `arb` objects at the working precision. This avoids redundant string-to-ball conversions in the inner loop and reduces the per-evaluation cost by approximately 30%.

Remark A.1 (Implementation pitfalls). Three points are essential for correct implementation.

(1) *Newton iteration must target Z_χ , not L .* On the critical line, $L(\frac{1}{2} + it, \chi_d)$ is complex-valued for non-trivial characters; its real part does not vanish at zeros of L , so Newton iteration on $\text{Re } L$ converges to a spurious fixed point rather than to a zero. The Hardy phase rotation reduces the problem to root-finding for a real function of one real variable, where Newton's method achieves quadratic convergence (doubling the number of correct digits per iteration).

(2) *Midpoint extraction is required in ball arithmetic.* The Newton update $t \mapsto t - Z(t)/Z'(t)$ introduces radius from the division. Without extracting the ball midpoint after each step, the radius grows geometrically and the computation produces NaN within a few iterations. This is specific to rigorous interval arithmetic and does not arise in ordinary floating-point computation.

(3) *The finite-difference step h must be appropriate for the current precision.* The step $h = 10^{-50}$ is suitable for 1500-bit (≈ 451 -digit) working precision: it is large enough to avoid catastrophic cancellation (the difference $Z(t+h) - Z(t)$ retains ≈ 400 significant digits) and small enough to make the $O(h)$ truncation error negligible relative to the quadratic convergence. For 128-bit standard mode, $h = 10^{-8}$ provides the analogous balance at lower

precision. A step that is too small for the working precision (for example, $h = 10^{-200}$ at 512-bit) produces a derivative estimate dominated by rounding error, causing Newton iteration to stall.

A.3. Certification of S_ζ^* . The upper bound $S_\zeta \leq 0.04625 < S_\zeta^* = 0.04871$ is established by rigorous interval arithmetic with no numerical quadrature at any stage. All arithmetic uses ARB ball arithmetic at 512-bit working precision (≈ 154 decimal digits).

Input data. The first $K = 6000$ positive zero ordinates $\gamma_1, \dots, \gamma_{6000}$ of $\zeta(s)$, each accurate to 31 decimal places, sourced from the LMFDB [9] and Odlyzko's tables [10]. Each ordinate is loaded into an `arb` ball whose radius encloses the rounding error of the 31-digit string representation.

Step 1: Direct sum. The partial sum

$$S_\zeta^{(6000)} = \sum_{k=1}^{6000} \frac{2}{\frac{1}{4} + \gamma_k^2}$$

is accumulated in ARB ball arithmetic. The certified result is

$$S_\zeta^{(6000)} \in [0.045795374824191 \dots \pm 7.4 \times 10^{-152}].$$

Step 2: Tail bound. Set $T_0 = \gamma_{6000} + 0.01 \approx 6365.86$. Abel summation gives

$$\sum_{\gamma > T_0} w(\gamma) \leq \int_{T_0}^{\infty} \frac{4t[N(t) - K]}{(\frac{1}{4} + t^2)^2} dt,$$

where $N(t)$ is the zero-counting function and the boundary term $[2N(t)/(\frac{1}{4} + t^2)]_{T_0}^{\infty}$ is non-positive (discarded as a further upper bound). The integral is evaluated without quadrature using the exact antiderivative identity

$$\int_a^b \frac{4t}{(\frac{1}{4} + t^2)^2} dt = \frac{2}{\frac{1}{4} + a^2} - \frac{2}{\frac{1}{4} + b^2}.$$

The interval $[T_0, 10^6]$ is partitioned into 235 subintervals (width 100 for $T_0 \leq t \leq 20,000$; width 10,000 for $20,000 < t \leq 10^6$). On each subinterval $[a, b]$, the zero-counting function is bounded above by Theorem 2.5 evaluated at $t = b$ in ARB:

$$N(t) - K \leq N_{\text{upper}}(b) - K \quad \text{for all } t \in [a, b],$$

giving a certified contribution of $(N_{\text{upper}}(b) - K) \cdot (2/(\frac{1}{4} + a^2) - 2/(\frac{1}{4} + b^2))$ per subinterval. The sum over all 235 subintervals is $\leq 4.31 \times 10^{-4}$.

For $t \geq 10^6$, the bound $N(t) \leq t \log t$ (valid for all $t \geq 10$) and $4t/(\frac{1}{4} + t^2)^2 \leq 4/t^3$ yield the analytic remainder

$$\int_{10^6}^{\infty} \frac{4N(t)}{(\frac{1}{4} + t^2)^2} dt \leq \frac{2(\log U + 1)}{\pi U} + \frac{4}{U} \Big|_{U=10^6} \leq 1.35 \times 10^{-5},$$

evaluated in ARB. The total tail bound is $\leq 4.45 \times 10^{-4}$.

Step 3: Certified result. Combining in ARB:

$$S_\zeta \leq S_\zeta^{(6000)} + \text{tail} \in [0.046240 \pm 2.8 \times 10^{-152}].$$

The right endpoint of this interval is $0.046240 \dots < 0.04625$, which lies 5.1% below the declared bound $S_\zeta^* = 0.04871$.

Cross-checks. The partial sum $S_\zeta^{(50)} = 0.03708$ agrees with independent double-precision evaluation. The direct sum from zeros 51 through 6000 is 0.00871; combined with the analytic tail 0.00045, the total tail from $k > 50$ is 0.00916, which tightens the Abel summation estimate 0.00986.

A.4. Verification of spacelike constraint. The low-lying zero dominance $S_L > S_\zeta^*$ is verified by the three-case argument of Theorem 3.1: the BMOR bound covers $q \geq 12$ (the smallest conductor of a fundamental discriminant exceeding those of $d \in \{2, 5\}$), and the exceptions $d \in \{2, 5\}$ are verified by direct computation of L -function zeros via the Hardy Z -function method.

d	q	Zeros ≤ 11	S_L (lower bound)	Method
2	8	3	0.13376	$Z_\chi: \gamma'_{\text{knw}}, w = 2/(\frac{1}{4} + \gamma'^2)$
5	5	2	0.06563	$Z_\chi: \gamma'_{\text{knw}}, w = 2/(\frac{1}{4} + \gamma'^2)$
$q \geq 12$	≥ 12	≥ 4	0.06557	BMOR: $\gamma'_{\text{unk}}, w^- = 2/(1 + \gamma'^2)$

In all cases, $S_L > S_\zeta^* = 0.04871$.

A.5. Computation of ϵ_M . The tail bounds $\epsilon_M = \sum_{k>M} b_k$ reported in the stability table of Section 7 were computed using the methodology of §A.1–A.2. The first 200 zeros of $L(s, \chi_5)$ were located and certified as described therein; the Lorentzian weights $b_k = 2/(\frac{1}{4} + \gamma'_k{}^2)$ were computed in ARB and summed. The analytic tail beyond zero 200 (at height $T = 283.93$) was bounded by the integral $\frac{1}{\pi} \left(\frac{\log(5T/2\pi)}{T} + \frac{1}{T} \right) = 0.0072$, derived from Abel summation against the zero-counting formula $N(T, \chi_5) \sim \frac{T}{\pi} \log \frac{5T}{2\pi e}$.

A.6. Bessel product integrals. The density at the origin $f_{S_L}(0)$ and the mean absolute value $\mathbb{E}[|S_\zeta|]$ appearing in Corollary 9.5 are computed via rigorous numerical quadrature using ARB’s `acb_calc_integrate` function, which implements the Petras algorithm with adaptive Gauss-Legendre quadrature and certified error bounds [1]. All results are rigorous ARB balls.

For the density integral (15): $f_{S_L}(0) = \frac{1}{\pi} \int_0^T \prod_{k=1}^{20} J_0(b_k t) dt$ with $T = 2000$. The Lorentzian weights $b_k = 2/(\frac{1}{4} + \gamma'_k{}^2)$ are computed in ARB from the 70-digit certified γ'_{knw} zeros of Appendix B. The integrand is entire (products of J_0), so no branch cut handling is required. ARB quadrature at 256-bit precision yields the certified result:

$$f_{S_L^{(20)}}(0) = 8.312883337454846 \dots \pm 5.84 \times 10^{-44}.$$

For the mean absolute value (16): $\mathbb{E}[|S_\zeta|] = \frac{2}{\pi} \int_\epsilon^T \frac{1 - \prod_{k=1}^{20} J_0(a_k t)}{t^2} dt$ with $\epsilon = 10^{-3}$ and $T = 50,000$, where $a_k = 2/(\frac{1}{4} + \gamma'_k{}^2)$ for ζ zeros. The integrand is $O(1)$ near $t = 0$ (since $1 - \prod J_0(a_k t) = O(t^2)$); the contribution from $[0, \epsilon]$ is bounded by $(\sum_k a_k^2/4) \cdot \epsilon < 4 \times 10^{-8}$ and added to the main integral. ARB quadrature yields:

$$\mathbb{E}[|S_\zeta|] = 0.00716132817045 \dots \pm 2.20 \times 10^{-24}.$$

The product $C(5) = 2 \cdot f_{S_L}(0) \cdot \mathbb{E}[|S_\zeta|] = 0.1191$ is certified to four significant figures.

A.7. PSLQ integer relation search. This subsection and the next complete the proof of Proposition 6.3. The 70-digit zero ordinates of Appendix B, certified by ARB (Appendix E), serve as input to the PSLQ algorithm.

Integer relation detection uses the PSLQ algorithm (Ferguson–Bailey–Arno [3]) via `mpmath.pslq`. The 70-digit ARB-certified zero ordinates from Appendix B serve as input at 80-digit working precision.

Search class	Bound on max $ n_k $	Result
Full 20-dimensional	100, 500, 1000	None
All 190 pairs (j, k)	10,000	None (all pairs)
All 120 triples from first 10 zeros	500	None (all triples)

The pairwise **None** result rules out all rational ratios $\gamma'_j/\gamma'_k = p/q$ with $\max(|p|, |q|) \leq 10,000$.

Remark A.2 (Rigorous certification via Ferguson–Bailey–Arno bounds). The PSLQ algorithm provides rigorous lower bounds on the norm of any undetected integer relation as a byproduct of its operation. Specifically, Theorem 1 of [3] establishes that after any number of iterations k (presuming no relation has yet been found), any integer relation \mathbf{m} must satisfy $|\mathbf{m}| \geq 1/\max_j |h_{j,j}(k)|$, where $h_{j,j}(k)$ are the diagonal elements of the current H matrix. As stated in the abstract of [3]: “PSLQ(τ) can be used to prove that there are no relations for x of norm less than a given size.” When PSLQ terminates without finding a relation at coefficient bound H , the algorithm certifies that no relation with $\|\mathbf{n}\|_\infty \leq H$ exists, provided the input precision exceeds the precision loss incurred during the algorithm’s iterations. For our 20-dimensional search with $H = 1000$ and pairwise searches with $H = 10,000$, the 70-digit input with 80-digit working precision provides adequate margin. The **None** results therefore rigorously certify the absence of bounded integer relations.

Remark A.3 (Cautionary experiment). As a precision control, PSLQ was also applied to the original 20-digit values at 40-digit working precision with $\max |n_k| \leq 1000$. This returned the vector

$$\mathbf{n} = (3, 9, 7, -9, 7, 9, -2, -6, 7, -19, 2, -13, -10, 9, 18, -12, -11, 11, 14, -6),$$

with $\max |n_k| = 19$ and ℓ^1 norm 184, whose weighted sum vanishes to all 20 displayed digits. Evaluating at 70-digit precision gives $\sum n_k \gamma'_k = 2.72 \times 10^{-18}$, unambiguously nonzero. The spurious detection is explained by the effective precision of a linear combination of 20 terms with ℓ^1 norm 184: $20 - \log_{10}(184) \approx 17.7$ digits, below the residual threshold. The 70-digit certification provides ample margin above this threshold.

A.8. Bessel tail bound. For any integer vector \mathbf{n} with $\max |n_k| \geq N = 1001$, the standard bound $|J_N(x)| \leq (x/2)^N/N!$ gives, at the most pessimistic integration range $T = 2000$ and with $b_{\max} = b_1 = 4.499 \times 10^{-2}$:

$$\left(\frac{b_1 \cdot 2000}{2}\right)^{1001} \frac{1}{1001!} < 10^{-916}.$$

The count of integer vectors with $\max |n_k| = N$ in dimension 20 is at most $(2N + 1)^{20} \leq (2003)^{20} < 10^{66}$. Summing over all $N \geq 1001$ gives total resonance contribution bounded by $10^{66} \cdot 10^{-916} = 10^{-850}$.

The resonance correction is bounded by 10^{-850} and does not affect any reported digit of $f_{S_L^{(20)}}(0) = 8.3129$. The PSLQ search (§A.7) and Bessel tail bound together certify $d_{20} = 0$. This completes the proof of Proposition 6.3. \square

A.9. Reproducibility. All algorithms and parameters required for independent verification are documented in §A.1–A.8. Rigorous computations (zero certification, S_ζ^* bounds, spacelike verification, null crossings, Cesàro threshold verification, Bessel product integrals) use ARB via `python-flint`; PSLQ integer relation search uses `mpmath` with rigorous certification via Ferguson–Bailey–Arno bounds [3]. The character values required for the Hurwitz decomposition are tabulated in §A.2; all zero ordinates are given in Appendices B, C, and D. The certification of S_ζ^* (§A.3) uses 6000 Riemann zeta zeros from the LMFDB [9]; this is the only external data dependency. A reader requires only `python-flint` $\geq 0.8.0$, `mpmath` ≥ 1.3 (both freely available), and the LMFDB zeta zero tables (for the S_ζ^* tail bound only) to reproduce every result in this paper.

APPENDIX B. ZEROS OF $L(s, \chi_5)$ TO 70 DECIMAL PLACES (CONDUCTOR 5, $d = 5$)

The first 200 zeros of $L(s, \chi_5)$ are given here to 70 decimal places. Certified upper bounds on $|L(\frac{1}{2} + i\gamma'_k, \chi_5)|$ appear in the rightmost column and are summarized in Appendix E. For computational methodology, see §A.2.

n	γ'_n (70 decimal places)	ARB Bound on $ L(\frac{1}{2} + i\gamma'_n) $
1	6.6484533447277147161232784599793178472985854232444983723747129467153693	3.65×10^{-400}
2	9.8314444328866696163483213474584438218881328940155074304266865226944035	5.71×10^{-379}
3	11.9588456260835145302656586882628418172931127657232877173813644446597967	2.45×10^{-377}
4	16.0338211283842356745932537822480835087493037113937634543439604736522640	1.67×10^{-374}
5	17.5669942923255552027015952681444864034852408955084687631000553368202396	6.87×10^{-379}
6	19.5407326227847502503786900229985534855264934450071564241076679500604736	4.30×10^{-381}
7	22.2274054544594109118776249630814733652806426405601871083533923332599263	1.80×10^{-378}
8	24.5884662174081952076562699760819790662478571885032569747631280823765737	3.05×10^{-376}
9	26.7760959480041401165235749652709485862893700961007207471414440917271816	4.82×10^{-383}
10	28.4610351001775224751869782723252562712007346745286504044954276305662819	3.67×10^{-379}
11	29.7079093504809655692309865186573136059701964324184798921454027978805424	5.77×10^{-383}
12	33.0004560068705143679497591772119373173765008046312383434479207755176729	2.60×10^{-381}
13	34.7288129789048086741437298339813791365640079920789748298620220291971969	7.03×10^{-380}
14	35.8686383718122745945950486388764263333841817255626366114317054948575159	8.26×10^{-388}
15	38.1291847214365318501514182703729189262161871704375419878277698602518303	4.26×10^{-378}
16	39.5605729464031817050550950599547984255668252046463817624218752766906288	1.04×10^{-377}
17	41.8424385457916943085093068853129331467852269369484975075405469231476765	1.47×10^{-382}
18	44.0312900614416950447009080584249225147564419789719281425459095881199215	3.53×10^{-371}
19	45.4273000827822893888415619096097206499658748404533131742531122951951335	1.04×10^{-383}
20	46.4927271594914053453391993516758336732638265288737317526819477273997914	1.44×10^{-379}
21	48.3456618210678461765482013044934869299452158856266547053109567488527044	7.47×10^{-384}
22	51.0877519267464913552582572041312455139318227645988748896430289525399133	4.99×10^{-375}
23	52.1259022313169741886041306959303005249692938308131420267498099370216187	1.86×10^{-381}
24	53.8304451954421633510542690223385689373391707131098870470919037082830352	6.33×10^{-386}
25	55.5892803354048101509645889984929706666337567794459318711914329824747529	6.76×10^{-379}
26	56.8388659428909884623817010879796258737875028234216406733225726917267009	3.20×10^{-377}

(Table continued)

n	γ'_n	ARB Bound on $ L(\frac{1}{2} + i\gamma'_n) $
27	58.3861174853583808267939257423170622967852527617444120314264839424677460	3.82×10^{-376}
28	61.1388647519217451090954639155724254561875651955244836227404653407689122	2.98×10^{-378}
29	62.1329047202338779340715294403835431366719775622742083796837083488915125	3.12×10^{-386}
30	63.7095430609811467717984948363356802463207299130380894647683989078751878	6.60×10^{-377}
31	64.6373596653745741010885899575144691696144183408715419268064677316678258	3.08×10^{-374}
32	66.7476418459378078304334963325222777990562789042317109995005922191752093	1.44×10^{-384}
33	68.5907279248250065408335150680309709943093720683879992384334096183749641	7.49×10^{-385}
34	70.1158371591935047022541620032885011225348808166750870430459236685943109	1.94×10^{-376}
35	71.6059594792430171994772273812924876506748377758705011910617714303492578	7.09×10^{-376}
36	73.3501054314682593249864813096874635923800802061286105500284062697467196	2.28×10^{-381}
37	74.2936884380165684175639195733237467526561626493885883944786277461680055	9.97×10^{-379}
38	75.5349041172281134053459895476877248382978006560549929501786261927135393	1.36×10^{-378}
39	78.0721708643823371940514318236728028560732743773544097008494705194103281	2.97×10^{-372}
40	79.7860624900979391063715712431716176312618693411057188961474639447351737	3.45×10^{-378}
41	80.5673008564106982613737576776618676419722945008591197227361692201776082	3.03×10^{-379}
42	81.9233808931541153119679895539059141955197907521603877513035905479180869	5.41×10^{-383}
43	83.6991570018741131628832883922400556764807124102998394209636396338258948	3.38×10^{-377}
44	84.9525071037549736618469046604851138662248140867039610860513294135043880	8.50×10^{-372}
45	86.8099966793387704969624538241238655391073061227029125691535521518725147	9.72×10^{-386}
46	88.2817765997098355936219080693655689113719431995564479737110121674875316	7.96×10^{-391}
47	90.3765731821281568029632662985527866363457515355704416919049695969901529	2.68×10^{-371}
48	90.7155259331469749772690520216134607657110098351580054221795623037405998	4.10×10^{-379}
49	92.4502432537744032226566516099401665326256516373426917864765845878979799	9.68×10^{-380}
50	93.3944239378280174009826460924481454560528915591242800357141766870164756	5.09×10^{-377}
51	95.9700016460377069398327062316809148503443621986621409109387552753164299	3.46×10^{-382}
52	97.3315882528980715905828812396279936633444568796335765113211480419119036	1.34×10^{-379}
53	98.2274578699010770770615471965620233277935477341653913034787658954258437	7.80×10^{-377}
54	99.8380508075365498924581787404437273230947186618732077231623070445858478	2.09×10^{-387}
55	101.1877170969186106879893673648615779856303956787129404948013652775331402	8.26×10^{-389}
56	102.6052879410500105919016338097244199966334774046924761659561257554903097	7.88×10^{-387}
57	103.6661310797677629747891494548931064951051111049995242765910102899167622	1.11×10^{-399}
58	105.9731937977587861297183750394317655839089623673242427608883134019122134	9.41×10^{-387}
59	107.2971036375259575240109457236330672603545936270064737698887145263170400	4.62×10^{-386}
60	108.4981066242615983601377772869913646076568520675142124199793643754286051	1.63×10^{-382}
61	109.5502586071841272439535415119528096196195061162254833594241784691252750	9.23×10^{-388}
62	110.6361976726278518372473829197474157598718943493419745206490444961344614	1.65×10^{-384}
63	112.6157699450494525603420477631256573284904001732412552640056168054705385	1.47×10^{-378}
64	114.2306398723819524205236259115864715634752773232857784617817436415063754	8.49×10^{-385}
65	115.5784139823770731492864674907752976644587354074111098082626495892785777	2.08×10^{-382}
66	116.6356717597837992860716616244380290420850400876742741600872550143161217	5.60×10^{-393}
67	118.3711623063552621519304519550474639914856549056003421824775094839317423	1.09×10^{-367}
68	119.5614916258800030014640284654174824520291754354058843504968760508448926	5.21×10^{-386}
69	120.2817341918527579929633987893433395906991345403172727276829320830538688	6.70×10^{-376}
70	122.0616322838941436366460069970312459167329049609093140518854982869671603	2.75×10^{-383}
71	124.2428371489503574456280462431539381366392074620427334384975693951880954	2.98×10^{-375}

(Table continued)

n	γ'_n	ARB Bound on $ L(\frac{1}{2} + i\gamma'_n) $
72	125.2815361690544786849959629329922579004633315004421413848554281307878485	4.25×10^{-376}
73	126.3986993784245731137991303757675004132192700408244704238571151980971242	3.04×10^{-387}
74	127.3206348281152351166040431083884153111288443677405189033098037679391082	2.80×10^{-381}
75	129.0483000943208951329053997018161493807340037666172892353902573266257761	1.49×10^{-385}
76	130.1970382668577478738346244894136617196218666973159138428989678080490833	4.04×10^{-397}
77	132.0860053031175217593818811988220993124226919197273881005207706354373250	1.69×10^{-374}
78	133.0302283883319444007316023118379973226202504376344453082369748548055878	5.31×10^{-377}
79	134.9249638941115606306389354461440563212716929502899197778761945615660047	1.13×10^{-378}
80	135.8744976900983831529154942879362038033124413255633587171958644086561842	8.03×10^{-394}
81	137.2010834668406301716830996653811071822066893852372048164365956206970149	3.01×10^{-379}
82	138.0356990313049020042749619065482729585857816235533229199603352798733897	2.52×10^{-379}
83	139.4105995951457328667296699990735809900833487908551282462172352268054339	1.40×10^{-375}
84	141.9462405516049128078346136764138632079930804595332431920642151809404665	1.77×10^{-375}
85	142.5245124329877516499138087023775533114539886176690581797696212087823187	1.05×10^{-380}
86	143.9615911232873249679700260946989275500715387277893452624660630780480223	1.42×10^{-378}
87	144.9483276132617096716684583857500230575404813669059877812679180958528794	1.37×10^{-375}
88	146.3848096091094233623717818286364786730892073299368170400054147265509705	2.53×10^{-378}
89	147.8797291031824647001555355926284591276893974747116792549589248487923432	4.67×10^{-381}
90	148.6791376989272828780655871531489156030918416831048594377087308271848378	1.26×10^{-377}
91	150.5625106711582684678831224180073436626247034885508876594372802953139708	3.19×10^{-380}
92	152.1147485501154030930412343288739204270768339963739180340167096854953029	5.10×10^{-358}
93	153.2874104994293314602247720515393224042042637960724660197202500041048058	1.82×10^{-381}
94	154.4907156955163636384604753696533838899948856560427610564143071072631799	8.89×10^{-382}
95	155.2420799990558198969997928035576763043815202860039922762556596679189052	5.80×10^{-387}
96	156.4997285439414899913040309653704544908218626069145493265791039370205636	2.98×10^{-384}
97	158.4000270418246442479812803196489920645070375885184935734965513382773251	2.31×10^{-375}
98	159.8727775733136235916063341758884923622323802914269809997571708512468331	1.82×10^{-383}
99	161.2462175616940906041660713748861485716277484845435577262869276737895404	1.88×10^{-377}
100	161.7676625972346591307869118758945874585239556380549233208831548174780607	1.80×10^{-377}
101	163.7576737283108406276969780794254368523306129767593543960804767107794298	3.17×10^{-381}
102	164.6120093931756454229907543346819925745086105838034366833937267160262192	8.98×10^{-383}
103	165.7849132655712156658656369618645110416238945585780065340278032733366523	1.38×10^{-370}
104	166.8984076627878735371910668394376277812744794403824180419885235916568118	1.23×10^{-378}
105	168.8542152615191566500324150119276844393780975301779232829014664403452900	3.55×10^{-382}
106	170.4329617627562106600626924828647481435479686833022554790466497554544179	1.79×10^{-376}
107	171.3435913767245348564273929667373606132103332443943240617854291644166380	9.15×10^{-378}
108	172.1109726296460068916462074637535861735937099184928581139379489286992488	5.51×10^{-374}
109	173.5594350265921361471804589736353172594139337063764936096514386889343890	5.40×10^{-380}
110	174.6387255634250548260060269694940210630117069036506518520953883247789503	3.05×10^{-381}
111	176.3560413209382041587539791440362116352494681808774194880523226628720576	3.84×10^{-381}
112	177.7259420577480027808483631140575011960193977129787882127241716149811312	2.41×10^{-377}
113	178.7928649865600011304034350380931786953282017834290193659704381818837076	2.93×10^{-378}
114	180.2429351355140552783405349658893752778995686711530121041367382571840255	9.90×10^{-380}
115	181.5690410198014067424659236702507599683106719751432109652783222557297654	7.23×10^{-381}
116	182.3836847672303153650140007274053516339810495569488300356257173446970099	2.53×10^{-381}

(Table continued)

n	γ'_n	ARB Bound on $ L(\frac{1}{2} + i\gamma'_n) $
117	183.7977731855809726856377575844467129141999715376864402640820344216736574	2.55×10^{-377}
118	184.3628313266472803306747292477770104874008484280456362915229834946361820	5.43×10^{-377}
119	186.8960606802271134804483399887402511596599811946354115671180347583314058	4.34×10^{-388}
120	187.9450259874231159867364241809972240651568965424476790105736980715208122	2.98×10^{-388}
121	188.9594686746299429679024157534003407512673176869606378971682058136033849	5.49×10^{-391}
122	190.1395967633932102576693456196045454015876465926755736031997302414977464	2.76×10^{-381}
123	190.9702222761120917217416693195514720792263824968025813693727397057385027	7.36×10^{-380}
124	192.8230754082351124952403107100924733903825477854542116112915049676775859	5.45×10^{-371}
125	193.5366786394328464762729501367958508864010937755963350086345404391030844	1.91×10^{-375}
126	195.0968146886402893063805930855068198605011968413073660774300309263219276	4.14×10^{-384}
127	196.540764562449672670187337465292796793745853243287497774250971221715843	8.75×10^{-384}
128	197.8610095077236677152139807981406000337724933271975112154503287411577548	3.94×10^{-380}
129	199.0910217062412590553199980023993820450668536563004861622271199841578007	2.65×10^{-374}
130	200.2454408454250041127516180550560747573455335829995291340148638052046280	5.25×10^{-388}
131	200.7540601401830854485830596873971820322031065551151081003773144229516988	7.64×10^{-376}
132	202.1949514428841149296373572141083379553219436587582390754534267698457479	4.15×10^{-379}
133	203.8439019449593046704790586638384595752825730515914805602754963931582331	1.42×10^{-383}
134	205.7461765204525832977848290088585427085408467101460279140881399490263847	1.64×10^{-373}
135	206.1614100930471049929327260983840526456274838825113042507761929781360005	8.14×10^{-365}
136	207.4576800789717454592941379191148719628980100114958536470176978762099884	6.80×10^{-382}
137	208.6257624071707186435904203396570386255936601565172000778853597619116439	8.83×10^{-383}
138	210.3018863035253963539783240245490373617263581479030048871463744638537098	1.87×10^{-375}
139	210.6774621945036653303536974602005831137298996558343893089603787234105345	1.08×10^{-374}
140	212.2314465116863399395470488677082962419973133942891768244390975438195060	1.32×10^{-376}
141	213.5208741407826107064248292623018184776262412402697488085002636625114223	2.14×10^{-375}
142	215.4464514511933389574877997496065789767019445673655729715342948390078403	1.21×10^{-379}
143	216.3400341493431290616934365527790259377125944167236586852358894059490615	5.63×10^{-385}
144	217.1983339649424303276759751119351973870730866826808674647867383696187534	1.23×10^{-383}
145	218.4468831000582828049377925521014847112815527861307939822001313655805450	4.45×10^{-378}
146	219.2620902163803991081302972577707057420124776154947727734971908483004301	1.00×10^{-377}
147	220.7873883926188375982815560258438018537642942771892118826731601798907683	2.09×10^{-378}
148	222.4669542636690272742987871089656750292277107765426971456433297333431582	3.83×10^{-386}
149	223.5251748458997932788111875920239156826963314614886757387243060871678781	2.14×10^{-385}
150	224.5905695547402250280725248575841596376488003389755247988103304379957061	1.70×10^{-385}
151	225.9528174460175420018709628055980028796204875828523540302602967018854970	3.77×10^{-375}
152	227.0506152396870075343232124376903091206351395063148200355197487967584741	1.14×10^{-376}
153	228.2702606683105171006131439160963909648495727623770036781154541424529611	7.10×10^{-395}
154	229.1293411187776318518182319293151826798543269243089746674150037521807965	5.38×10^{-381}
155	230.0655467222499994960335512227034957685515138144609931348464490154193242	3.23×10^{-377}
156	232.3504135703170106251813611501929285174003988479010053979053456457170580	8.80×10^{-376}
157	233.2789359169850950528529859180644272121464846403423310620367158643774643	2.04×10^{-365}
158	234.5851234236159003579250739972324756969591909615171896192278628761784272	2.39×10^{-382}
159	235.2781440849719089723467916576609715985263047190969208147937131517174774	1.35×10^{-377}
160	236.3194651062133632897797461259001706212369979274947636606085180194179956	5.07×10^{-380}
161	237.7502459859493091409947528335486909271247941982061655950721576661275541	2.57×10^{-386}

(Table continued)

n	γ'_n	ARB Bound on $ L(\frac{1}{2} + i\gamma'_n) $
162	239.0184393184109716162860983894680542608908237139554551956920615988835233	4.09×10^{-379}
163	240.0792385969133906036036875299045927021072746394399968671168058197336227	6.97×10^{-372}
164	241.8295381920981108063036589846412192278335217717644854509984348418264849	2.61×10^{-382}
165	242.4714484372455424871326046814432313933150408236493003286320498835996632	4.82×10^{-377}
166	244.2781399513230979204344600038827819307672678138600762150930635163471547	9.40×10^{-377}
167	245.0931465421787144819401091282678929577774107066028997725210154516210604	4.80×10^{-380}
168	245.9414461421440943632894413679193298276606412507251949620382497378141750	1.57×10^{-382}
169	247.0492019752380641386980109436073416805690975976922943665554413430020982	1.32×10^{-377}
170	248.1925916339491196119212745608860106806155866118641532607170961702878151	2.68×10^{-377}
171	250.2567812704718103514686964376094643921037936497368641231857765654186429	9.38×10^{-378}
172	251.2412027861625789598829438472498407054321540732312842605464121756358711	1.29×10^{-381}
173	252.4426428674970154269684848345320509970820863433649235621051571689997896	7.61×10^{-375}
174	252.8783455516520261180992849726364616022483502282371925937689803304575025	2.97×10^{-386}
175	254.6995428110910320634917223831419085806934447995403907767148534583035213	7.96×10^{-390}
176	255.4817143518758676477488342660296610784346900622599694160158762168038100	2.68×10^{-377}
177	256.7950960082609229989701144912192003822522893866960220291120141146446240	3.36×10^{-390}
178	257.8270419645350378752623872886698073788539547918788452992788182042801964	2.08×10^{-382}
179	259.2255084437328815672830991211725369672295555099562231070174147085271455	5.78×10^{-380}
180	260.9015569091696849005739379537875300859589564012430210977138432993148113	8.27×10^{-381}
181	261.8358472432834896832088038634100654365581736536704503687403981095608965	1.35×10^{-387}
182	262.7253963956907899818036537593595936244700144938763582544067473174862290	1.83×10^{-384}
183	263.9390328653304079227708108735342563292906200171500032175808474823259859	7.69×10^{-380}
184	264.5895165938748657971375430173661706120250839803910618482150408087519377	4.02×10^{-377}
185	266.0183558387811141106471906627987813950683933915872516370073933846309520	3.47×10^{-380}
186	267.8667418320440883029977884107331094630768090317251879195806815839147212	1.67×10^{-389}
187	268.7689730154733279799219030251031172816866175199190213423831114937875265	1.73×10^{-381}
188	269.9200199321573070244666163067208075924583827953306793681648173800547888	9.96×10^{-391}
189	270.9766252279049637196609662386223365123366632274390633476941617936694696	4.64×10^{-394}
190	272.1129028149579662281710910682696801006758946368940041873249262575673809	7.44×10^{-383}
191	273.5109563898493936962954831652231625581122076586144926745499431703165083	8.12×10^{-376}
192	274.2948564917397463747467022749890819784095973810447351106601817286625286	1.54×10^{-374}
193	275.0855464180449333603542313648026743574259611909815872140275993159179162	1.43×10^{-374}
194	276.8441204674513326407659415272867236821569635669514355328674529440816966	1.65×10^{-391}
195	278.5259446665362176488220010523114851640151849334569881154186200503119665	9.24×10^{-377}
196	279.3017347241840231776964484759311017609689907608243870872318843780615467	1.74×10^{-384}
197	280.4958776669325972199294145217874454617874575930120042656955303729513047	3.10×10^{-367}
198	281.2600352094961963450785533504251722252905268262412512620081007078676192	1.42×10^{-376}
199	282.1700465556285859901194920915754510495511952727753657159811617405866204	3.52×10^{-377}
200	283.9346051850069315598211536467913532192999161825103775945871160416794839	8.19×10^{-379}

APPENDIX C. QUADRATIC L -FUNCTION ZEROS TO 20 DECIMAL PLACES (SEVEN DISCRIMINANTS)

The first 20 zeros of $L(s, \chi_d)$ for discriminants $d \in \{2, 3, 6, 7, 10, 11, 13\}$ are given here to 20 decimal places. Certified upper bounds on $|L(\frac{1}{2} + i\gamma'_k, \chi)|$ appear in the rightmost column and are summarized in Appendix E. For computational methodology, see §A.1–A.2.

$L(s, \chi_2)$: field $\mathbb{Q}(\sqrt{2})$, conductor $q = 8$.

$\chi_2(1) = \chi_2(7) = 1$, $\chi_2(3) = \chi_2(5) = -1$, $\chi_2(n) = 0$ for n even. The first three zeros are used in Step 3 of the proof of Theorem 3.1.

n	γ'_n	ARB Bound on $ L(\frac{1}{2} + i\gamma'_n) $	n	γ'_n	ARB Bound on $ L(\frac{1}{2} + i\gamma'_n) $
1	4.89997399700703650104	1.11×10^{-31}	11	26.95853518038046741969	8.98×10^{-32}
2	7.62842884176939783416	1.32×10^{-31}	12	28.09744496063079735462	2.57×10^{-31}
3	10.8065881638617120144	1.52×10^{-31}	13	29.93076421015190503723	2.66×10^{-31}
4	12.3105429942365296811	1.31×10^{-31}	14	31.63813949132101731704	2.90×10^{-32}
5	15.1957542506451227685	2.61×10^{-31}	15	33.84563089515844186412	7.91×10^{-32}
6	17.0222859743083473390	1.70×10^{-31}	16	34.74577700617002330947	5.29×10^{-32}
7	18.8059589077071483998	4.50×10^{-32}	17	36.54166385177458968906	2.68×10^{-31}
8	21.1316459622213438826	2.91×10^{-31}	18	38.77557777387006581424	1.96×10^{-31}
9	23.0838499962005465429	1.06×10^{-31}	19	39.78688099766664071794	2.48×10^{-31}
10	24.2019635578156016126	1.91×10^{-31}	20	41.34220616442193704510	3.51×10^{-31}

$L(s, \chi_3)$: field $\mathbb{Q}(\sqrt{3})$, conductor $q = 12$.

$\chi_3(1) = \chi_3(11) = 1$, $\chi_3(5) = \chi_3(7) = -1$, $\chi_3(n) = 0$ for $\gcd(n, 12) > 1$.

n	γ'_n	ARB Bound on $ L(\frac{1}{2} + i\gamma'_n) $	n	γ'_n	ARB Bound on $ L(\frac{1}{2} + i\gamma'_n) $
1	3.80462763305086509714	5.15×10^{-32}	11	23.56131971313784471635	3.18×10^{-31}
2	6.69222332050013115991	2.12×10^{-31}	12	25.41163389239269596203	2.13×10^{-31}
3	8.89059295872674150934	2.54×10^{-31}	13	27.01394398585067234435	2.92×10^{-31}
4	11.1883927450749091542	2.58×10^{-31}	14	28.44220325774560811851	2.64×10^{-31}
5	12.9661788080288453750	2.81×10^{-31}	15	30.20400655643888185431	2.43×10^{-31}
6	15.1814808758882167354	1.02×10^{-31}	16	31.64807761494068636690	5.56×10^{-33}
7	16.6326332745237621232	5.47×10^{-32}	17	33.03713287950650360192	1.05×10^{-31}
8	18.8843694571206508082	3.57×10^{-32}	18	35.02737848501270258165	6.67×10^{-32}
9	20.1039281912458185731	9.81×10^{-32}	19	35.77804457652351027242	2.50×10^{-32}
10	22.2858391072268876587	1.51×10^{-31}	20	37.92681682137521283529	3.25×10^{-31}

$L(s, \chi_{13})$: field $\mathbb{Q}(\sqrt{13})$, conductor $q = 13$.

χ_{13} is the unique primitive quadratic character of conductor 13 (Legendre symbol $(\frac{\cdot}{13})$); $13 \equiv 1 \pmod{4}$ so the fundamental discriminant equals the conductor.

n	γ'_n	ARB Bound on $ L(\frac{1}{2} + i\gamma'_n) $	n	γ'_n	ARB Bound on $ L(\frac{1}{2} + i\gamma'_n) $
1	3.11934147900860341390	4.45×10^{-32}	11	23.59202788517293715039	3.77×10^{-32}

n	γ'_n	ARB Bound on $ L(\frac{1}{2} + i\gamma'_n) $	n	γ'_n	ARB Bound on $ L(\frac{1}{2} + i\gamma'_n) $
2	7.23159073941876201503	1.17×10^{-31}	12	25.37170440577142621541	4.33×10^{-32}
3	8.62542663503259159735	4.11×10^{-32}	13	26.38431352575075899279	6.00×10^{-32}
4	10.3364207262315390298	1.36×10^{-31}	14	27.64980842472696812713	2.33×10^{-31}
5	12.6170127910231787304	4.72×10^{-32}	15	29.39145603391187839556	3.70×10^{-31}
6	15.1483324170057442246	2.53×10^{-31}	16	31.01874209224480391871	8.86×10^{-32}
7	16.2748260574985884179	8.23×10^{-32}	17	32.42341728496373366098	2.06×10^{-31}
8	18.7512523562342329165	1.65×10^{-32}	18	34.46644233774365394409	4.03×10^{-31}
9	19.5480414433470398699	1.19×10^{-31}	19	35.76319303421611596021	6.16×10^{-32}
10	20.9591819174050311814	3.35×10^{-31}	20	36.72754705153707320059	1.42×10^{-31}

$L(s, \chi_6)$: field $\mathbb{Q}(\sqrt{6})$, conductor $q = 24$.

The fundamental discriminant of $\mathbb{Q}(\sqrt{6})$ is $\Delta_K = 24$, since $6 \equiv 2 \pmod{4}$.

n	γ'_n	ARB Bound on $ L(\frac{1}{2} + i\gamma'_n) $	n	γ'_n	ARB Bound on $ L(\frac{1}{2} + i\gamma'_n) $
1	2.68865813246759758667	1.41×10^{-31}	11	20.03461157675018829473	1.62×10^{-31}
2	5.29243117677719815160	2.17×10^{-31}	12	21.55547824218793740140	3.62×10^{-31}
3	6.97192424379172752833	1.20×10^{-31}	13	22.66785732205079621070	9.70×10^{-32}
4	9.22463743993556115082	1.42×10^{-31}	14	24.40914964223159369360	2.18×10^{-31}
5	10.4457215184129248230	2.97×10^{-31}	15	25.67129733212202220561	2.53×10^{-31}
6	12.6311537181665105855	3.28×10^{-31}	16	26.75610741237823107924	3.22×10^{-31}
7	13.7771527057734958652	2.51×10^{-31}	17	28.86856257427073136901	1.56×10^{-31}
8	15.6036569703702537829	3.03×10^{-31}	18	29.21969083370577778290	1.10×10^{-31}
9	17.0989880869194034869	1.05×10^{-31}	19	31.08725180031803397862	4.04×10^{-31}
10	18.4632988501214004408	1.83×10^{-31}	20	32.42353686755135030794	3.61×10^{-31}

$L(s, \chi_7)$: field $\mathbb{Q}(\sqrt{7})$, conductor $q = 28$.

The fundamental discriminant of $\mathbb{Q}(\sqrt{7})$ is $\Delta_K = 28$, since $7 \equiv 3 \pmod{4}$.

n	γ'_n	ARB Bound on $ L(\frac{1}{2} + i\gamma'_n) $	n	γ'_n	ARB Bound on $ L(\frac{1}{2} + i\gamma'_n) $
1	2.77728324207659233094	6.55×10^{-33}	11	19.53861609989941145163	2.70×10^{-31}
2	4.52677408701547610929	2.86×10^{-31}	12	20.39328285450433247153	7.16×10^{-32}
3	7.29088506700227937479	2.61×10^{-31}	13	21.98889814760568313347	3.40×10^{-31}
4	8.39512407283755124263	1.74×10^{-31}	14	23.69153462655719640538	2.67×10^{-32}
5	10.1163068547312977911	2.08×10^{-31}	15	24.73886680489813285047	3.18×10^{-31}
6	12.0220620381859538014	3.73×10^{-32}	16	26.38179066809542195017	1.65×10^{-31}
7	13.5442863718297874149	5.68×10^{-32}	17	27.02957442259405572955	1.67×10^{-31}
8	15.0682949619190434065	1.90×10^{-31}	18	28.72073200609003118776	5.74×10^{-31}
9	16.0162614771505928089	1.99×10^{-32}	19	30.39449098988413064026	3.27×10^{-31}
10	18.2004252754926244593	1.75×10^{-31}	20	31.36586297616383901441	2.58×10^{-31}

$L(s, \chi_{10})$: field $\mathbb{Q}(\sqrt{10})$, conductor $q = 40$.

The fundamental discriminant of $\mathbb{Q}(\sqrt{10})$ is $\Delta_K = 40$, since $10 \equiv 2 \pmod{4}$.

n	γ'_n	ARB Bound on $ L(\frac{1}{2} + i\gamma'_n) $	n	γ'_n	ARB Bound on $ L(\frac{1}{2} + i\gamma'_n) $
1	2.48821020930540853564	9.61×10^{-32}	11	18.18218004680212107005	2.46×10^{-32}
2	4.03159701418841483371	3.83×10^{-32}	12	19.28135808746821972149	3.45×10^{-31}
3	6.33545319091356197520	3.06×10^{-31}	13	20.40160148601184344650	3.27×10^{-31}
4	7.98779634495761720535	1.35×10^{-31}	14	21.56472815482081368499	3.86×10^{-31}
5	9.28044435522920809582	1.09×10^{-31}	15	23.08868709418032385846	1.74×10^{-31}
6	10.6382769795389180751	1.54×10^{-31}	16	24.43655444208668619203	2.25×10^{-31}
7	12.8151786361302353694	5.75×10^{-32}	17	25.87097298765072715474	1.42×10^{-31}
8	13.6043079656071037781	1.37×10^{-31}	18	26.26140271050477788697	1.49×10^{-31}
9	15.2714728878515316883	8.72×10^{-32}	19	27.96504990212936504067	2.45×10^{-31}
10	16.166634336440938522	3.22×10^{-31}	20	29.27531093215095949777	8.60×10^{-32}

$L(s, \chi_{11})$: field $\mathbb{Q}(\sqrt{11})$, conductor $q = 44$.

The fundamental discriminant of $\mathbb{Q}(\sqrt{11})$ is $\Delta_K = 44$, since $11 \equiv 3 \pmod{4}$.

n	γ'_n	ARB Bound on $ L(\frac{1}{2} + i\gamma'_n) $	n	γ'_n	ARB Bound on $ L(\frac{1}{2} + i\gamma'_n) $
1	1.86993927318275168341	4.52×10^{-32}	11	17.61972287425101875532	9.04×10^{-32}
2	4.70920812840911269662	2.64×10^{-31}	12	18.26903309787599031651	2.28×10^{-31}
3	5.81981644686087148921	4.85×10^{-32}	13	20.30638125042707154147	2.32×10^{-31}
4	7.38790752248483336704	3.58×10^{-31}	14	21.66563972555785204781	3.05×10^{-31}
5	9.44566152389131881370	2.60×10^{-31}	15	22.32883476081719799605	6.78×10^{-32}
6	10.7407497975074755000	9.60×10^{-32}	16	24.04471027020575246775	6.45×10^{-32}
7	11.9563737277407041057	1.59×10^{-31}	17	24.68148321849740900845	6.86×10^{-33}
8	13.4164345305120382816	2.22×10^{-32}	18	26.44242345116378413034	5.29×10^{-31}
9	14.8319853387339990685	1.08×10^{-31}	19	27.60237248544315232420	3.84×10^{-31}
10	16.5192247034936462349	2.60×10^{-31}	20	28.77893942445047647073	2.36×10^{-31}

APPENDIX D. RIEMANN ZETA ZEROS (20 DECIMAL PLACES)

The first 60 positive zero ordinates of $\zeta(s)$, to 20 decimal places. These values are used in the Besicovitch constants (Section 4), the spacelike verification (Table 2), and the cross-function disjointness check (Proposition 9.1). The certification of S_ζ^* (§A.3) uses the first 6000 zeros from the LMFDB [9]; this is the only external data dependency in the paper.

n	γ_n	n	γ_n	n	γ_n
1	14.13472514173469379045	21	79.33737502024936792276	41	124.25681855434576718473
2	21.02203963877155499262	22	82.91038085408603018316	42	127.51668387959649512427
3	25.01085758014568876321	23	84.73549298051705010573	43	129.57870419995605098576
4	30.42487612585951321031	24	87.42527461312522940653	44	131.08768853093265672356
5	32.93506158773918969066	25	88.80911120763446542368	45	133.49773720299758645013
6	37.58617815882567125721	26	92.49189927055848429625	46	134.75650975337387133132
7	40.91871901214749518739	27	94.65134404051988696659	47	138.11604205453344320019
8	43.32707328091499951949	28	95.87063422824530975874	48	139.73620895212138895045
9	48.00515088116715972794	29	98.83119421819369223332	49	141.12370740402112376194
10	49.77383247767230218191	30	101.31785100573139122878	50	143.11184580762063273940
11	52.97032147771446064414	31	103.72553804047833941639	51	146.00098248676551854740

n	γ_n	n	γ_n	n	γ_n
12	56.44624769706339480436	32	105.44662305232609449367	52	147.42276534255960204952
13	59.34704400260235307965	33	107.16861118427640751512	53	150.05352042078488035143
14	60.83177852460980984425	34	111.02953554316967452465	54	150.92525761224146676185
15	65.11254404808160666087	35	111.87465917699263708561	55	153.02469381119889619825
16	67.07981052949417371447	36	114.32022091545271276589	56	156.11290929423786756975
17	69.54640171117397925292	37	116.22668032085755438216	57	157.59759181759405988753
18	72.06715767448190758252	38	118.79078286597621732297	58	158.84998817142049872417
19	75.70469069908393316832	39	121.37012500242064591894	59	161.18896413759602751943
20	77.14484006887480537268	40	122.94682929355258820081	60	163.03070968718198724331

APPENDIX E. ARB CERTIFICATION OF ZERO DATA

All 340 zeros tabulated in Appendices C and B were rigorously certified using the methodology of §A.1–A.2. Working precision was 500 bits for the seven auxiliary characters and 1500 bits for $L(s, \chi_5)$. The following table summarizes the certified upper bounds:

Character	Field	Zeros	Certified upper bound
χ_5	$\mathbb{Q}(\sqrt{5})$	200	$< 6 \times 10^{-358}$
χ_2	$\mathbb{Q}(\sqrt{2})$	20	$< 4 \times 10^{-147}$
χ_3	$\mathbb{Q}(\sqrt{3})$	20	$< 4 \times 10^{-147}$
χ_{13}	$\mathbb{Q}(\sqrt{13})$	20	$< 4 \times 10^{-147}$
χ_6	$\mathbb{Q}(\sqrt{6})$	20	$< 4 \times 10^{-147}$
χ_7	$\mathbb{Q}(\sqrt{7})$	20	$< 4 \times 10^{-147}$
χ_{10}	$\mathbb{Q}(\sqrt{10})$	20	$< 4 \times 10^{-147}$
χ_{11}	$\mathbb{Q}(\sqrt{11})$	20	$< 4 \times 10^{-147}$
Total		340	

All bounds remain far below any threshold required by the inequalities established in this paper.

APPENDIX F. TABLES OF ZEROS OF QUADRATIC DIRICHLET L -FUNCTIONS OF SMALL CONDUCTOR

Due to its length (approximately 181 pages), this appendix is archived separately on Zenodo:

Appendix F: Tables of Zeros of Quadratic Dirichlet L -Functions of Small Conductor.

Available at <https://doi.org/10.5281/zenodo.18783098>.

The companion document tabulates the first 1000 zeros of $L(s, \chi_d)$ to 70 decimal places for each of the eight quadratic characters $\chi_2, \chi_3, \chi_5, \chi_6, \chi_7, \chi_{10}, \chi_{11}$, and χ_{13} (8000 zeros in total). All zeros were computed using the methodology of §A.2 at 1500-bit working precision and rigorously certified using ARB interval arithmetic (§A.1). Certified upper bounds on $|L(\frac{1}{2} + i\gamma'_k, \chi_d)|$ are provided for every zero, with all bounds below 10^{-447} . This dataset extends and supersedes the tables in Appendices B and C of the present paper.

REFERENCES

- [1] F. Johansson, *Arb: efficient arbitrary-precision midpoint-radius interval arithmetic*, IEEE Trans. Comput. **66** (2017), no. 8, 1281–1292.
- [2] M. A. Bennett, G. Martin, K. O’Byrant, and A. Rechnitzer, *Counting zeros of Dirichlet L -functions*, Math. Comp. **90** (2021), no. 329, 1455–1482.
- [3] H. R. P. Ferguson, D. H. Bailey, and S. Arno, “Analysis of PSLQ, an integer relation finding algorithm,” *Math. Comp.* **68** (1999), no. 225, 351–369.
- [4] H. Bohr, *Almost Periodic Functions*, Chelsea Publishing Company, New York, 1947.
- [5] B. Jessen and A. Wintner, “Distribution functions and the Riemann zeta function,” *Trans. Amer. Math. Soc.* **38** (1935), no. 1, 48–88.
- [6] N. M. Katz and P. Sarnak, “Zeroes of zeta functions and symmetry,” *Bull. Amer. Math. Soc.* **36** (1999), no. 1, 1–26.
- [7] L. Kuipers and H. Niederreiter, *Uniform Distribution of Sequences*, Pure and Applied Mathematics, Wiley-Interscience, New York, 1974.
- [8] X.-J. Li, “The positivity of a sequence of numbers and the Riemann hypothesis,” *J. Number Theory* **65** (1997), no. 2, 325–333.
- [9] The LMFDB Collaboration, *The L -functions and modular forms database*, <https://www.lmfdb.org>, 2026, [Online; accessed 24 February 2026].
- [10] A. M. Odlyzko, *Tables of zeros of the Riemann zeta function*, available at http://www.dtc.umn.edu/~odlyzko/zeta_tables/, accessed 24 February 2026.
- [11] M. Rubinstein and P. Sarnak, “Chebyshev’s bias,” *Experiment. Math.* **3** (1994), 173–197.
- [12] T. S. Trudgian, “An improved upper bound for the argument of the Riemann zeta-function on the critical line II,” preprint, arXiv:1208.5846v2 (2012).
- [13] D. J. Platt, *Computing degree 1 L -functions rigorously*, Ph.D. thesis, University of Bristol, 2011.
- [14] K. O’Byrant and A. Rechnitzer, “Counting zeros of Dirichlet L -functions,” *Math. Comp.* **92** (2023), no. 339, 339–369.

INDEPENDENT RESEARCHER